



Mathilde Steinmaßl, BSc

Isolation, re-constitution and characterization of a natural redox chain for efficient in-vitro synthesis of 1-alkenes with the bacterial cytochrome P450 decarboxylase OleT

MASTERARBEIT

Zur Erlangung des akademischen Grades

Diplom-Ingenieurin

Masterstudium Biotechnology

eingereicht an der

Technischen Universität Graz

Institut für Biotechnologie und Bioprozesstechnik

Betreuer

Univ.-Prof. Dipl.-Ing. Dr. techn. Bernd Nidetzky

Dipl.-Biol. Dr.rer.nat. Alexander Dennig

Graz, Januar 2019

Eidesstattliche Erklärung

Ich erkläre an Eides statt, dass ich die vorliegende Arbeit selbstständig verfasst, andere als die angegebenen Quellen/Hilfsmittel nicht benutzt, und die den benutzten Quellen wörtlich und inhaltlich entnommenen Stellen als solche kenntlich gemacht habe.

Graz, am

.....

(Unterschrift)

Statutory Declaration

I declare that I have authored this thesis independently, that I have not used other than the declared sources / resources, and that I have explicitly marked all material which has been quoted either literally or by content from the used sources.

Graz,

date

.....

(signature)

Kurzfassung

1-Alkene stellen wichtige Basischemikalien für die Herstellung von Polymeren und Kraftstoffen dar. Auf herkömmliche Weise werden sie in hochenergetischen Prozessen aus nicht-erneuerbaren Quellen wie Erdgas hergestellt. Eine Alternative dazu ist die enzymatische Herstellung von Alkenen aus nachhaltig produzierbaren Fettsäuren. Für diese Anwendung ist das Cytochrom P450 Enzym OleT von großer Bedeutung, da es die Decarboxylierung von Fettsäuren zu 1-Alkenen als Hauptprodukt katalysiert. Das Enzym wird dazu durch das Substrat aktiviert und kann entweder H_2O_2 oder O_2 und externe Elektronenquellen für die Katalyse verwenden. Die bisher erreichten Produkttiter sind mit bis zu 1 g L^{-1} recht niedrig und β -OH- sowie α -OH-Fettsäuren stellen unerwünschte Nebenprodukte dar. Kopplungseffizienzen die bei der Übertragung von Elektronen auf das Enzym mit bisher verwendeten Systemen erreicht wurden sind niedrig (<61%). Aus diesen Gründen wurde in dieser Arbeit ein Elektronentransfersystem aus dem Originalstamm von OleT, dem Bakterium *Jeotgalicoccus sp.* ATCC8456 identifiziert, isoliert und hinsichtlich dessen Effizienz und kinetischer Parameter charakterisiert. Das System, bestehend aus einem Ferredoxin (Fd_x) und einer NADPH-abhängigen Ferredoxin-Reduktase (FdR_j), wurde in *E. coli* heterolog exprimiert und anschließend aufgereinigt um es in *in-vitro* Versuchen zu charakterisieren. Dabei konnten Kopplungseffizienzen von bis zu >95% erreicht werden. Außerdem wurde ein Einfluss der Ferredoxin-Konzentration auf die Effizienz des Elektronentransfers und auf die Selektivität des P450 Enzyms festgestellt. Mit dem neuen optimierten System konnten die höchsten bisher berichteten Gesamtumsatzzahlen (TTN) mit OleT erzielt werden (bis zu 2255). Eine wichtige Beobachtung war außerdem, dass ein sehr großer Anteil an Elektronen aus der Kette entkoppelt um O_2 zu H_2O_2 zu reduzieren.

Neben dem Elektronentransfersystem wurde auch ein zweites Cytochrom P450 Enzym aus *Jeotgalicoccus sp.* ATCC8456 ($\text{P450}_{j\alpha}$) isoliert und sowohl mit H_2O_2 als auch in Kombination mit dem neuen Elektronentransfersystem getestet. Es stellte sich heraus, dass dieses Enzym sehr effizient die α -Hydroxylierung von Fettsäuren katalysiert.

Abstract

1-alkenes are important building blocks for chemical synthesis and can be used also as drop-in fuels. Usually, they are produced in energy-intensive processes from non-renewable sources like crude oil or gas. For a more sustainable production of 1-alkenes, enzymatic decarboxylation of fatty acids has attracted attention recently. The cytochrome P450 OleT (CYP152L1) has promising potential for the production of 1-alkenes. However, low coupling efficiencies and sometimes rather high amounts of β -OH and α -OH fatty acids as side-products are drawbacks that are sought to be overcome. Besides, moderate product titers (up to 1 g L^{-1}) and low stability against H_2O_2 are reasons to search for an efficient electron transfer system that activates O_2 and therefore allows reaction conditions that are favorable for catalyst stability. In this work, an electron transfer system was identified and isolated from the bacterium *Jeotgalicoccus sp.* ATCC8456, the natural host of OleT. Besides, a new cytochrome P450 enzyme which accepts fatty acids as substrates was isolated from the same bacterium. The new electron transfer system is comprised of a ferredoxin-reductase (FdR_{j1}) and a ferredoxin (Fdx_j). After expression of the electron transfer proteins and the P450 enzymes in *E. coli* BL21 (DE3), they were purified by His-Tag affinity chromatography and characterized in *in-vitro* experiments. Kinetic parameters and cofactor preference were determined in various photometric measurements. These and GC-MS analysis of the substrate/products revealed high efficiency of the system. Coupling efficiencies achieved with the new system (up to >95%) were significantly higher than what has been measured before. However, a significant portion of electrons has been shown to uncouple from the chain and reduce oxygen to form H_2O_2 . It has also been shown that the $\text{FdR}_{j1}/\text{Fdx}_j$ ratio has a high influence on the quality of electron transfer. Higher TTN values than reported before (up to 2255) have been determined with the new optimized system. The newly isolated P450 enzyme ($\text{P450}_{j\alpha}$) was shown to be a novel peroxygenase with high potential for application as efficient fatty acid α -hydroxylase.

Acknowledgements

First and foremost, I want to thank Prof. Dr. Bernd Nidetzky for giving me the opportunity to do my Master thesis on this interesting project as a member of his group. Thank you for your support and especially for the weekly talks about the progress of the project.

Further I want to express my sincere gratitude to my supervisor Dr. Alexander Dennig for introducing me into the topic and for his excellent academic support on the way. Thank you for your helpful and inspiring comments on my experimental and written work.

Further I want to thank Dr. Christina Müller, Dr. Henry Müller and Andrea Friedrich from the Institute of Environmental Biotechnology from TU Graz for providing the genomic data and strain.

Next, I want to mention Prof. Dr. Ruth Birner-Grünberger from the Medical University of Graz who provided the opportunity to do external LC-MS/MS analyses of my protein samples.

I thank all colleagues who shared their knowledge and working experience with me during my time at the institute for the inspirational talks. I also want to thank all colleagues who contributed to the great working atmosphere.

I thank all my friends who accompanied me on my way and enriched my life so much during the past years. In particular I want to mention Daniela, Miriam, Beatrice and Bernhard. I am very thankful for our talks and all the experiences together. Big thanks also to Michi for your support and the good times we are having. Also I want to thank Stefanie for the friendship we built during our time at the institute. Besides, I thank my old friends Tabea, Monika, Katharina and Maria. We did not meet often during the past years due to the distances but your friendship is invaluable.

And last but not least, I would like to thank my family: my parents and also my brothers and sisters for every kind of support during the last years.

Contents

Eidesstattliche Erklärung	ii
Statutory Declaration	ii
Kurzfassung	iii
Abstract	iv
Acknowledgements	v
Contents	vi
List of Figures.....	x
List of Tables.....	xiii
Abbreviations	xv
1 Introduction.....	1
1.1 Chemical production and application of 1-alkenes.....	1
1.2 P450 monooxygenases catalyzing 1-alkene formation	3
1.3 Redox systems for P450 monooxygenases	4
1.4 Catalytic cycle of cytochrome P450 enzymes	8
1.5 Reaction mechanism of OleT.....	10
1.6 Cytochrome P450 enzymes – perspectives and limitations.....	11
1.7 Aim of this thesis	11
2 Material and methods.....	13
2.1 Materials.....	13
2.1.1 Chemicals.....	13
2.1.2 DNA extraction and purification kits	13
2.1.3 Enzymes and PCR components	13
2.1.4 Laboratory equipment.....	14
2.1.5 Bacterial strains	15
2.1.6 Growth media and media additives	15
2.2 3-Step purification protocol for OleT and the mediator	17

2.2.1	Culture conditions and cell disruption	17
2.2.2	Precipitation with $(\text{NH}_4)_2\text{SO}_4$	18
2.2.3	Cation exchange chromatography	18
2.3	Isolation of genes from genomic data.....	19
2.4	Cloning and expression of genes from <i>Jeotgalicoccus sp.</i> ATCC8456	21
2.4.1	Vector map of pET-28a(+)	21
2.4.2	Molecular biological methods.....	22
2.4.3	Purification of genomic DNA from <i>Jeotgalicoccus sp.</i> ATCC8456	23
2.4.4	PCR with genomic DNA from <i>Jeotgalicoccus sp.</i> ATCC8456.....	23
2.4.5	Cloning of the genes of interest into the plasmid vector pET-28a(+)	25
2.4.6	Transformation of plasmid DNA into electro competent <i>E. coli</i> TOP10 cells.....	25
2.4.7	Sequencing of successfully cloned genes	26
2.4.8	Transformation of Plasmid DNA into electro competent <i>E. coli</i> BL21(DE3) cells.....	26
2.5	Production of FdR _{J1} , Fdx _J , P450 _{Jα} and OleT.....	27
2.5.1	Expression of FdR _{J1} , Fdx _J , P450 _{Jα} and OleT	27
2.5.2	Cell lysis of <i>E. coli</i> BL21(DE3) for isolation of FdR _{J1} , Fdx _J , P450 _{Jα} and OleT.....	27
2.5.3	Purification of FdR _{J1} , Fdx _J , P450 _{Jα} and OleT	28
2.6	Protein quantification.....	29
2.7	Homology model generation.....	30
2.8	Quantitative determination of product formation with GC-MS analysis.....	30
2.8.1	Two-phase solvent extraction and derivatization of analytes for GC-MS.....	30
2.8.2	GC-MS analysis	31
2.9	Characterization of the FdR _{J1} -Fdx _J -OleT redox chain	32
2.9.1	Hexacyanoferrat assay for characterization of the reductase activity.....	32
2.9.2	Cytochrome <i>c</i> assay for analysis of electron transfer by Fdx _J	32
2.9.3	Determination of NAD(P) oxidation rates with the FdR _{J1} -Fdx _J -OleT system	33
2.9.4	Dependence of catalytic activity and selectivity of OleT on Fdx _J concentration	33
2.9.5	Quantification of enzymatically produced H ₂ O ₂	34

2.9.6	Catalase study.....	36
2.10	Influence of NADPH and substrate concentration	36
2.11	Substrate screening and NAD(P)H oxidation rate determination for the novel peroxygenase P450 _{Jα}	37
2.11.1	Substrate screening.....	37
2.11.2	NAD(P)H oxidation rate determination with new redox transfer chain – comparison OleT and P450 _{Jα}	37
3	Results and Discussion	38
3.1	Purification of OleT and putative electron mediator from <i>Jeotgalicoccus sp.</i> ATCC8456	38
3.1.1	Cloning of the selected genes into pET28a(+) and transformation into <i>E. coli</i> strains .	42
3.1.2	Heterologous expression and purification of FdR _{J1} Fdx _J and P450 _{Jα}	46
3.1.3	Generation homology models for FdR _{J1} and Fdx _J	51
3.2	Catalytic characterization of the FdR _{J1} -Fdx _J -OleT system.....	54
3.2.1	Reductase activity determination with the small electron acceptor potassium ferricyanide.....	54
3.2.2	Cytochrome <i>c</i> reduction assay	55
3.2.3	NADPH oxidation rates of the FdR _{J1} -Fdx _J -OleT system.....	59
3.2.4	Catalytic activity and selectivity of OleT dependent on mediator concentration	62
3.2.5	Quantification of H ₂ O ₂ released by the reconstituted electron transfer chain.....	64
3.2.6	Effect of catalase on catalytic activity of OleT.....	65
3.3	Influence of NADPH and substrate concentration on C14:0 FA conversion	67
3.4	Biochemical characterization of P450 _{Jα}	69
4	Summary and Conclusion	72
5	Additional Data and Information	74
5.1	DNA and protein sequences.....	74
5.2	Positions of all used enzymes in the <i>Jeotgalicoccus sp.</i> ATCC 8456 genome	77
5.3	Supplementary information regarding LC-MS/MS analysis	79
5.4	Cyt <i>c</i> reduction experiment – output SigmaPlot	80
5.5	GC-MS spectra	81

5.6	GC-MS traces of fatty acid conversions.....	84
5.7	Impact of catalase addition on fatty acid conversion	88
6	References.....	90

List of Figures

Figure 1 Production of 1-alkenes from non-renewable fossil sources.....	1
Figure 2 Oil demand and supply balance 2013 – 2017	2
Figure 3 Prosthetic group of cysteinato-heme P450 enzymes.....	3
Figure 4 Schematic representation of a class I electron transfer system	5
Figure 5 Class II electron transfer system of cytochrome P450 systems	5
Figure 6 Self-sufficient BM-3 system.....	5
Figure 7 (A) Catalytic cycle of cytochrome P450 enzymes.....	9
Figure 8 Proposed mechanism for OleT	10
Figure 9 The coomassie-stained SDS-PAGE of the active fraction purified by Rude <i>et al.</i>	17
Figure 10 Vector map of pET-28a(+)	21
Figure 11 Scheme of a Fe ₄ -S ₄ -cluster, coordinated by 4 cysteine-residues	30
Figure 12 (A): GC-MS chromatogram of conversion of C14:0 FA to 1-tridecene.....	31
Figure 13 Quinoneimine formation from guaiacol and 4-aminoantipyrine (4-AAP).....	35
Figure 14 Calibration curve H ₂ O ₂ concentration	35
Figure 15 Elution of fractions containing OleT and the prospective mediator protein	38
Figure 16 SDS-PAGE of eluted fractions	38
Figure 17 GC-MS analysis after conversion of C18:0	39
Figure 18 The P450 _{Jα} gene fragments produced by cPCR.	42
Figure 19 PCR amplification of genes encoding for possible electron transfer proteins.....	43
Figure 20 Vector map of pET-28a(+) containing Fdx _j	44
Figure 21 Vector map of pET-28a(+) containing P450 _{Jα}	44
Figure 22 Control gel of cPCR reactions with <i>E. coli</i> BL21(DE3) transformed with pET28a(+) to identify presence of Fdx _j	45
Figure 23 Control gel of cPCR reactions with <i>E. coli</i> BL21(DE3) transformed with pET28a(+) to identify presence of FdR _{J1}	45

Figure 24 Control gel of cPCR reactions with <i>E. coli</i> BL21(DE3) transformed with pET28a(+) to identify presence of P450 _{Jα}	46
Figure 25 Purification of FdR _{J1}	47
Figure 26 Purification of Fdx _J	48
Figure 27 Purification of P450 _{Jα}	48
Figure 28 The absorbance spectrum of FdR _{J1}	49
Figure 29 Absorbance spectrum of Fdx _J (A)	50
Figure 30 Absorbance spectra of P450 _{Jα} before and after CO gassing.....	51
Figure 31 Model of FdR _{J1}	52
Figure 32 Electron transfer in FAD-containing ferredoxin reductases from NAD(P)H to FAD	53
Figure 33 Models of <i>Jeotgalicoccus sp.</i> ATCC8456 ferredoxin.....	53
Figure 34 Reduction of K ₃ [Fe(CN) ₆] to K ₄ [Fe(CN) ₆] by the NAD(P)H-dependent enzyme FdR _{J1}	54
Figure 35 Cytochrome <i>c</i> from the heart from <i>Bos taurus</i>	55
Figure 36 Scheme of electron transfer from NAD(P)H via FdR _{J1} and Fdx _J to cyt <i>c</i>	56
Figure 37 Cyt <i>c</i> reduction with 15 μM Fdx _J	56
Figure 38 Michaelis-Menten kinetics of one-electron transfer from NADPH to cyt <i>c</i>	58
Figure 39 Scheme of possible electron transfer from NAD(P)H via FdR _{J1} and Fdx _J to OleT	59
Figure 40 Autooxidation of reduced flavin to form H ₂ O ₂	61
Figure 41 NADPH and NADH oxidation rates in comparison	61
Figure 42 C14:0 FA conversion with increasing concentration of Fdx _J	64
Figure 43 Selectivity of OleT at increasing amounts of Fdx _J	64
Figure 44 Influence of catalase concentration on C14:0 FA conversion	67
Figure 45 Influence of NADPH and substrate concentration on conversion (%)	68
Figure 46 Total amount of C14:0 FA substrate converted at different equimolar NADPH/ substrate concentrations.....	68
Figure 47 Conversion of C10:0 FA substrate by P450 _{Jα}	69
Figure 48 Oxidation rates of NADH or NADPH when employing the FdR _{J1} -Fdx _J system and OleT or P450 _{Jα} FA	70

Figure 49 Position of the gene for OleT (BASYS00724 cypC) in the <i>Jeotgalicoccus sp.</i> ATCC8456 genome.....	77
Figure 50 Position of the gene for Fdx _J (BASYS00361) in the <i>Jeotgalicoccus sp.</i> ATCC8456 genome...	78
Figure 51 Position of the gene for FdR _{J1} (BASYS01288 trxB) in the <i>Jeotgalicoccus sp.</i> ATCC8456 genome.....	78
Figure 52 Position of the gene for P450 _{Jα} (BASYS00261) in the <i>Jeotgalicoccus sp.</i> ATCC8456 genome.	79
Figure 53 GC-MS spectrum of myristic acid methyl ester (C14:0 FA substrate).....	81
Figure 54 GC-MS spectrum of 1-tridecene (main product) [35]	81
Figure 55 GC-MS spectrum of β-hydroxy myristic acid methyl ester (side product) [35].....	81
Figure 56 GC-MS spectrum of decanoic acid methyl ester.	82
Figure 57 GC-MS spectrum of α-hydroxy decanoic acid methyl ester.....	82
Figure 58 GC-MS spectrum of β-hydroxy decanoic acid methyl ester.....	83
Figure 59 GC-MS spectrum of stearic acid methyl ester.....	83
Figure 60 GC-MS spectrum of 1-heptadecene.....	83
Figure 61 Conversion of C14:0 FA. Control reaction without NAD(P)H.	84
Figure 62 Conversion of C14:0 FA. Control reaction without FdR _{J1}	84
Figure 63 Conversion of C14:0 FA. Control reaction without Fdx _J	85
Figure 64 Conversion of C14:0 FA. Control reaction without OleT _{Je}	85
Figure 65 Overlay of GC-MS chromatograms of reactions containing different amounts of Fdx _J	86
Figure 66 GC-MS chromatogram of reaction containing 1 μM of Fdx _J	86
Figure 67 GC-MS chromatogram of reaction containing 15 μM of Fdx _J	87
Figure 68 GC-MS chromatogram of reaction containing 30 μM of Fdx _J	87
Figure 69 GC/MS spectra of catalase study reactions.....	88
Figure 70 Catalase study 1-octanol (ISD).....	88
Figure 71 Catalase study substrate peak overlay.....	89
Figure 72 NADPH/ substrate concentration study. 1 mM FA/ NADPH	89

List of Tables

Table 1 Summary of electron transfer and reaction systems tested so far for electron transfer to the cytochrome P450 decarboxylase OleT.	6
Table 2 Chemicals used in this work.	13
Table 3 DNA extraction and purification kits used in this work.	13
Table 4 Enzymes and PCR components used in this work.	13
Table 5 Laboratory equipment used in this work.	14
Table 6 Bacterial strains used in this work.	15
Table 7 Liquid media used in this work and their compositions.	15
Table 8 Composition of lysogeny broth agar.	16
Table 9 Media additives used in this work and their stock concentrations/ compositions.	16
Table 10 Fractions collected during purification.	19
Table 11 Selection of genes annotated as coding for electron transferring proteins.	20
Table 12 Primers for BASYS00361 (ferredoxin Fdx ₁), for BASYS01288 (ferredoxin reductase FdR ₁) and for BASYS00261 (P450 _α)	22
Table 13 Thermocycler program for cPCR with ONETAQ® QUICK-LOAD® 2X Master Mix.	24
Table 14 DNA concentrations after purification of cPCR reactions with the GeneJET PCR Purification Kit (ThermoFisher).....	24
Table 15 Settings for ultra-sonication used for cell disruption (used for all protein isolation steps)...	28
Table 16 Buffers for purification buffers A (loading buffer) and B (elution buffer) and storage buffer C.	29
Table 17 Reactions for hexacyanoferrat assay.....	32
Table 18 Reactions and control reactions for conversion of C14:0 FA substrate by OleT.	34
Table 19 Quinoneimine dye (measured as absorbance at 509 nm) formed in dependence of H ₂ O ₂ concentration.	35
Table 20 Genes isolated from the <i>Jeotgalicoccus sp.</i> ATCC8456 genome and their expression products.....	42
Table 21 Cloning statistics.	43

Table 22 NAD(P)H oxidation rates of FdR _{J1} using the small single electron acceptor K ₃ [Fe(CN) ₆] ³⁻	55
Table 23 Electron transfer activities from FdR _{J1} Fdx _J using cyt c as final electron acceptor and controls	57
Table 24 Electron transfer activities from FdR _{J1} to Fdx _J using the final electron acceptor cyt c. The activities were calculated from data obtained by Michaelis-Menten analysis.....	59
Table 25 Measurement of NAD(P)H oxidation rates.....	60
Table 26 The final electron acceptor and constitution of the transfer chain influence the ratio between NADPH and NADH oxidation rates.....	62
Table 27 Peroxide formation from electrons reducing dissolved O ₂	65
Table 28 NAD(P)H consumption rates [mM h ⁻¹] employing the FdR _{J1} -Fdx _J system and OleT or P450 _{Jα}	70
Table 29 Conversions (%) of FA substrate to α-OH FAs using NADH or NADPH as reductants and the FdR _{J1} -Fdx _J -P450 _{Jα} electron transfer system	71
Table 30 LC-MS/MS protein analysis hits. Heterologous expressed Fdx _J (highlighted in grey) was excised from SDS gel and submitted to LC-MS/MS analysis	80

Abbreviations

Abs	Absorbance
ALA	Δ -aminolevulinic acid
DMSO	Dimethyl sulfoxide
DTT	Dithiothreitol
EtOAc	Ethyl acetate
EtOH	Ethanol
FA	Fatty acid
FAD	Flavin adenine dinucleotide
FDH	Formate dehydrogenase
FdR _{J1}	NADPH-dependent ferredoxin reductase from <i>Jeotgalicoccus sp.</i> ATCC 8456
Fdx _J	Ferredoxin from <i>Jeotgalicoccus sp.</i> ATCC 8456
GC-MS	Gas chromatography coupled to mass spectrometry
HRP	Horse raddish peroxidase
KPi	Phosphate buffer
LB	Lysogeny broth
OleT	Cytochrome P450 fatty acid decarboxylase from <i>Jeotgalicoccus sp.</i> ATCC 8456
ONC	Overnight culture
P450 _{Jα}	Cytochrome P450 fatty acid α -hydroxylase from <i>Jeotgalicoccus sp.</i> ATCC 8456
PCR	Polymerase chain reaction
SDS-PAGE	Sodium dodecyl sulfate polyacrylamide gel electrophoresis
TAE (buffer)	Tris-acetate-EDTA buffer
TB	Terrific broth
TSBYE	tryptic soy broth with yeast extract
α -OH FA	Alpha-hydroxy fatty acid
β -OH FA	Beta-hydroxy fatty acid

1 Introduction

1.1 Chemical production and application of 1-alkenes

Linear α -olefins (1-alkenes) are widely used as platform chemicals for the production of lubricants, detergents, polymers and surfactants [1][2][3][4]. Besides, they can be directly used as drop-in fuels. Especially short chain alkenes are among the most important man-made building blocks in organic synthesis (predicted worldwide capacity in 2020: 200 mio tons of ethylene and 140 mio tons of propylene) [5]. In nature, 1-alkenes are barely found with the exception of cutanic waxes of some kinds of beetles and as antimicrobial volatile agents in bacteria [6][7][8].

Traditionally, 1-alkenes are produced from non-renewable sources (crude oil, gas, coal) in energy-intensive processes (see figure 1). Crude oil is fractionated to obtain naphta which is used as feed material for alkene production. Short- and medium-chain 1-alkenes are obtained via steam cracking processes (450-800 °C, >10 bar) and via the SHOP (shell higher olefin process) (80-120 °C, >70 bar) also longer chain internal alkenes can be produced [9]. Drawbacks are that high temperatures and pressures as well as expensive and toxic catalysts (Cr/Ni) are needed for the production of olefins. Further, the production of odd-numbered α -olefins presents a current synthetic challenge.

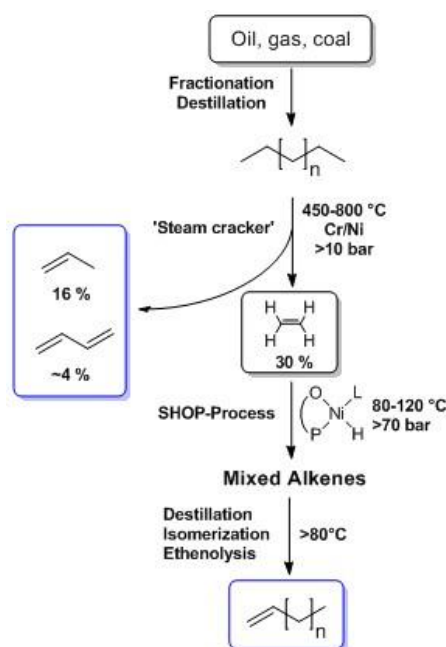


Figure 1 Production of 1-alkenes from non-renewable fossil sources. Via steam-cracking, short-chain alkenes are produced that can be polymerized by shell higher olefin process (SHOP)) to obtain even-numbered medium- and long-chain alkenes. High pressures (>10 bar) and temperatures (450-800 °C) as well as toxic catalysts (Cr/Ni) are applied in the steam cracker. In the SHOP-Process even higher pressures (>70 bar) and fairly high temperatures (80-120 °C) are required. The figure was taken from Dennig *et al.* (2016) [9].

An alternative to the production of alkenes from fossil sources has been described by Liu *et al.* (2014). They showed decarboxylation of fatty acids using a Pd catalyst. Hereby, also odd-numbered olefins can be produced. However, the high price and limited availability of Pd, which constitutes only part of the expensive catalyst, pose a problem. Temperature has to be increased to 132 °C and application of vacuum is necessary to separate formed acetic acid and olefins. A further disadvantage is that carbon monoxide is produced as a side product [10].

To produce 1-alkenes in an environmentally more sustainable way, enzymatic systems exhibit promising potential. Recently, the cytochrome P450 enzyme OleT from *Jeotgalicoccus sp.* ATCC 8456 (CYP152L1) has been found to decarboxylate saturated fatty acids into terminal olefins using H₂O₂ [11] or O₂ as oxidants. Advantages are that enzymatic decarboxylation takes place at mild reaction conditions (room temperature, atmospheric pressure) and no toxic metal catalysts are needed. Enzymes are completely renewable and biodegradable so that there is no problem of waste disposal after production. Intense studies on OleT and other enzymes exhibiting decarboxylation potential are of great interest. It poses a possibility of carbon-neutral production of olefins from abundant renewable sources (optimally from saturated fatty acid waste material). This will be important due to the threatening climate change and the impending shortage of fossil fuels [1].

The world's demand for platform chemicals and fuels is significantly growing, whereas the peak of oil production is foreseeable in the next decades [12]. An important analysis on oil demand/supply balance published by the IEA (International Energy Agency) in 2017 (figure 2) shows that the demand is about to outgrow its supply [13]. Oil prices therefore are increasing and susceptible to many factors (e.g. political and economic stability). Furthermore, many European countries are vastly dependent on the import of fuels. To overcome the impending shortage of available fossil resources, it is unavoidable to further the development towards bio-based production of fuels and key chemicals from renewable sources [14].

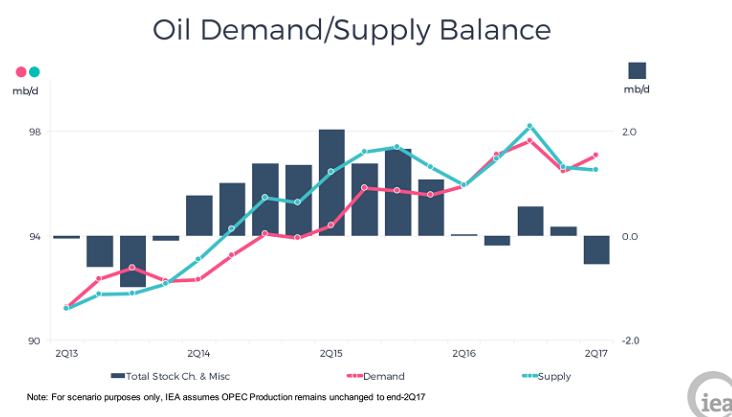


Figure 2 Oil demand and supply balance 2013 – 2017 was published by IEA (International Energy Agency) in 2017 [13].

1.2 P450 monooxygenases catalyzing 1-alkene formation

P450s are a structurally diverse group of enzymes. They mostly act as monooxygenases containing a heme-b prosthetic group (figure 3) that receives electrons from external sources for activation of molecular oxygen. There is a diverse range of reactions they are able to catalyze, such as hydroxylation, demethylation, dealkylation, epoxidation or the oxidative cleavage of C-C bonds [15][16][17][18][19][20]. All P450 enzymes have in common that the fifth ligand to their iron in the heme prosthetic group is a thiolate and that upon binding of CO to the reduced heme iron, their absorption maxima are shifted to 450 nm. The enzymes are named after this phenomenon [20][21].

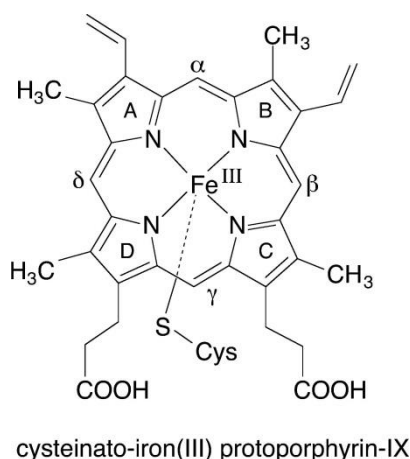


Figure 3 Prosthetic group of cysteinato-heme P450 enzymes: The Fe(III) protoporphyrin-IX is linked with a proximal cysteine ligand. The figure was taken from Meunier *et al.* (2014) [20]. Note that in its ground state there is a water molecule as a sixth ligand coordinated to the iron center.

OleT belongs to the CYP152 family of cytochrome P450 enzymes. Other members of this group are for example CYP152B1 (CYP_{SP α}) and CYP152A1 (CYP_{BS β}), two fatty acid hydroxylating enzymes with 41% and 36% sequence homology to OleT, respectively. OleT is able to decarboxylate fatty acids via oxidative C-C bond cleavage. It has been isolated by Rude *et al.* (2011) in a reverse genetic approach and since then attracted attention of several working groups, as direct decarboxylation of FA into 1-alkenes was shown for the first time by an isolated enzyme. It serves as a model organism for mechanistic as well as application studies [11]. Another enzyme that is able to decarboxylate fatty acids is the peroxygenase CYP152A1 (CYP_{BS β}), which has been shown to have a chemoselectivity of about 10% towards decarboxylation of substrate, whereas other products are α - and β -hydroxy fatty acids [11][22]. In 2017, Xu *et al.* reported two new CYP152 straight-chain saturated fatty acid decarboxylating peroxygenases, namely CYP-Aa162 (5.1 \pm 0.1% chemoselectivity towards 1-alkene production from lauric acid) and CYP-Sm46 Δ 29 (66.1% and 57.4% chemoselectivity towards 1-alkene production from C12:0 and C14:0 fatty acids, respectively). Their overall conversions were 77.3% \pm 1.0% (CYP-Aa162) and 83.5% \pm 3.4% (CYP-Sm46 Δ 29) [23]. In 2014, Rui *et al.* reported a nonheme Fe(II)-containing enzyme that activates O₂ to oxidatively decarboxylate medium-chain fatty

acids, UndA from *Pseudomonas sp.*. UndA has a very narrow substrate scope (C10 – C14 substrates) and low product titers ($< 3 \mu\text{g}\cdot\text{mL}^{-1}$) pose a problem. Besides, the reducing agent is unknown for this enzyme [24].

OleT is in the main research focus when it comes to fatty-acid decarboxylating P450s, mainly because it was the first cytochrome P450 enzyme discovered to catalyze this reaction and because of its high selectivity towards 1-alkenes formation. Product titers of 1-alkenes are still quite low (up to $1 \text{g}\cdot\text{L}^{-1}\cdot\text{h}^{-1}$) and the enzyme is obtained in low soluble amounts (about $20 \text{mg}\cdot\text{L}^{-1}$) [22][25]. Further drawbacks are that the enzyme is not very stable against H_2O_2 and that efficient and economic electron transfer systems that deliver electrons from NAD(P)H to the oxygenase are needed.

1.3 Redox systems for P450 monooxygenases

OleT is able to utilize H_2O_2 or O_2 as oxidants. Molecular oxygen has to be activated with two electrons that are transferred to the heme iron of the enzyme via electron transfer proteins. In table 1, electron transfer systems that have previously been studied in combination with OleT, are summarized. Electrons typically derive from NADH or NADPH and are transferred via proteins that contain prosthetic groups which allow electron transfer (e.g. flavin groups or iron-sulfur-clusters). The most prominent and widely distributed electron transfer system in bacteria is the class I bacterial electron transfer system [18] comprised of a NAD(P)H-dependent ferredoxin reductase and a ferredoxin (figure 4). This system is usually found in bacteria or in mitochondria. In bacteria, all three proteins are soluble, in mitochondria this is only the case for the ferredoxin, whereas the ferredoxin reductase and the cytochrome P450 are membrane-associated. The iron-sulfur cluster found in bacterial ferredoxins is mostly of the [2Fe-2S] type [26]. Besides, [3Fe-4S] and [4Fe-4S] type clusters have been found (e.g. both in *Streptomyces griseus*) [27][28][29][30]. For OleT, the so far best studied system of this type is the CamAB system, derived from *Pseudomonas putida*, which is comprised of a 2Fe-2S-cluster-containing ferredoxin (CamB) and a NAD(P)H-dependent ferredoxin reductase (CamA). This system transfers electrons to CamC (CYP101), a P450 enzyme that catalyzes hydroxylation of camphor. The ferredoxin is able to transfer one electron at a time whilst the reductase receives two electrons simultaneously from NAD(P)H [18][31][32][33].

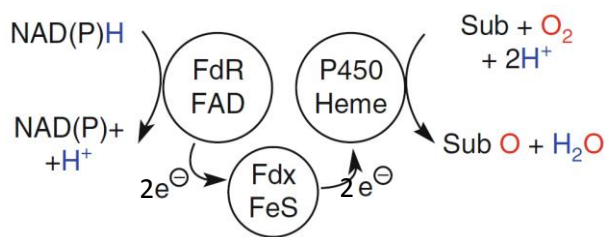


Figure 4 Schematic representation of a class I electron transfer system (bacterial, mitochondrial) of cytochrome P450 systems. Electrons are derived from NAD(P)H and are transferred via FdR (ferredoxin reductase) over Fdx (ferredoxin) to the cytochrome P450 enzyme. FAD = flavin adenine dinucleotide; FeS = iron-sulfur cluster. The figure was taken and adapted from Faber (2011) [33]

Another type of electron transfer system is the microsomal (class II) electron transfer system which is the most widely distributed system found in eukaryotes. It is less complex than the bacterial system and is comprised of a cytochrome P450 reductase (CPR) containing a FAD or FMN cofactor. Via the CPR, electrons can be directly transferred from NAD(P)H to the cytochrome P450 enzyme without the need for an additional transfer protein (figure 5) [18][33].

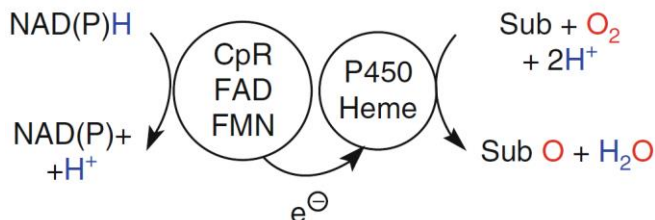


Figure 5 Class II electron transfer system (microsomal) of cytochrome P450 systems. Electrons are derived from NAD(P)H and are transferred via CPR (cytochrome P450 reductase) to the cytochrome P450 enzyme. CPR contains a FAD (flavin adenine dinucleotide) or FMN (flavin mononucleotide) cofactor. The figure was taken from Faber [33].

Besides, there is the possibility of having a self-sufficient system, for example the P450 enzyme BM-3 derived from *Bacillus megaterium* (figure 6). A CPR domain is part of the P450 enzyme so that no separate electron shuttle protein is employed. The CPR domain contains both a FMN cofactor and an iron-sulfur cluster [18][33].

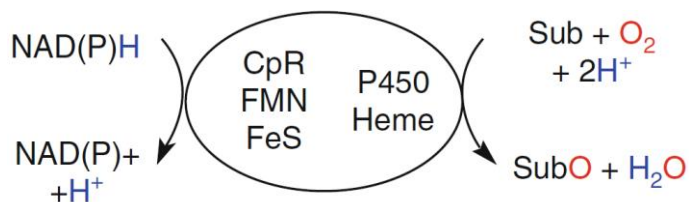


Figure 6 Self-sufficient BM-3 system. The figure was taken from Faber [33].

Table 1 Summary of electron transfer and reaction systems tested so far for electron transfer to the cytochrome P450 decarboxylase OleT.

Entry	Catalyst	Catalyst loading [$\mu\text{M enzyme}/\mu\text{M substrate}$]	Electron transfer proteins	Oxidant	Substrate	Cofactor	$\mu\text{M}_{\text{NAD(P)H}}/\mu\text{M}_{\text{C}_{x:0}}$	Cofactor regeneration system	Coupling [%]	TON [h^{-1}]	TTN	Catalase tested [$\text{U}\cdot\text{ml}^{-1}$]	Reference
1	OleT	0.5/200	---	H_2O_2	C16:0	---		---					Rude <i>et al.</i> (2011) [11]
2	OleT-PhFRED	1/200	PhFRED-fusion (reductase domain)	O_2	C14:0	NADPH	500/200	---	34.9*	87	174 (2h)	20	Liu <i>et al.</i> (2014) [34]
3	OleT	1/200	E. coli Fld/FdR	O_2	C14:0	NADPH	500/200	---	25.1*	63	126 (2 h)	20	Liu <i>et al.</i> (2014) [34]
4	OleT	1/1000	---	H_2O_2	C18:0	---	1000 (H_2O_2)/ 1000	---	85	170	170 (1 h)	---	Dennig <i>et al.</i> (2015) [35]
5	OleT	0.32/1	Spinach FdR/ Fdx	O_2	C18:0	NADPH	1000/1000	---	12.4	---	391 (24 h)	1200	Dennig <i>et al.</i> (2015) [35]
6	OleT	1.5/5000	CamAB	O_2	C18:0	NADH	200/5000	FDH	---	n.d.	2096	1200	Dennig <i>et al.</i> (2015) [35]
7	OleT	1/400	CgFdR-2 /SeFdx-6	O_2	C14:0	NADPH	5000/400	---	7.6*	n.d.	377.6 (16 h)	---	Fang <i>et al.</i> (2017) [36]
8	OleT	2/200	---	H_2O_2	C14:0	---	220 (H_2O_2)/ 200	---	45	n.d.	49.5 (16 h)	---	Fang <i>et al.</i> (2017) [36]
9	OleT-BM3R	1/1000	OleT-BM3R (fusion)	O_2	C18:0	NADPH	1000/1000	---	61.7*	370	617 (12 h)	100	Lu <i>et al.</i> (2018) [4]

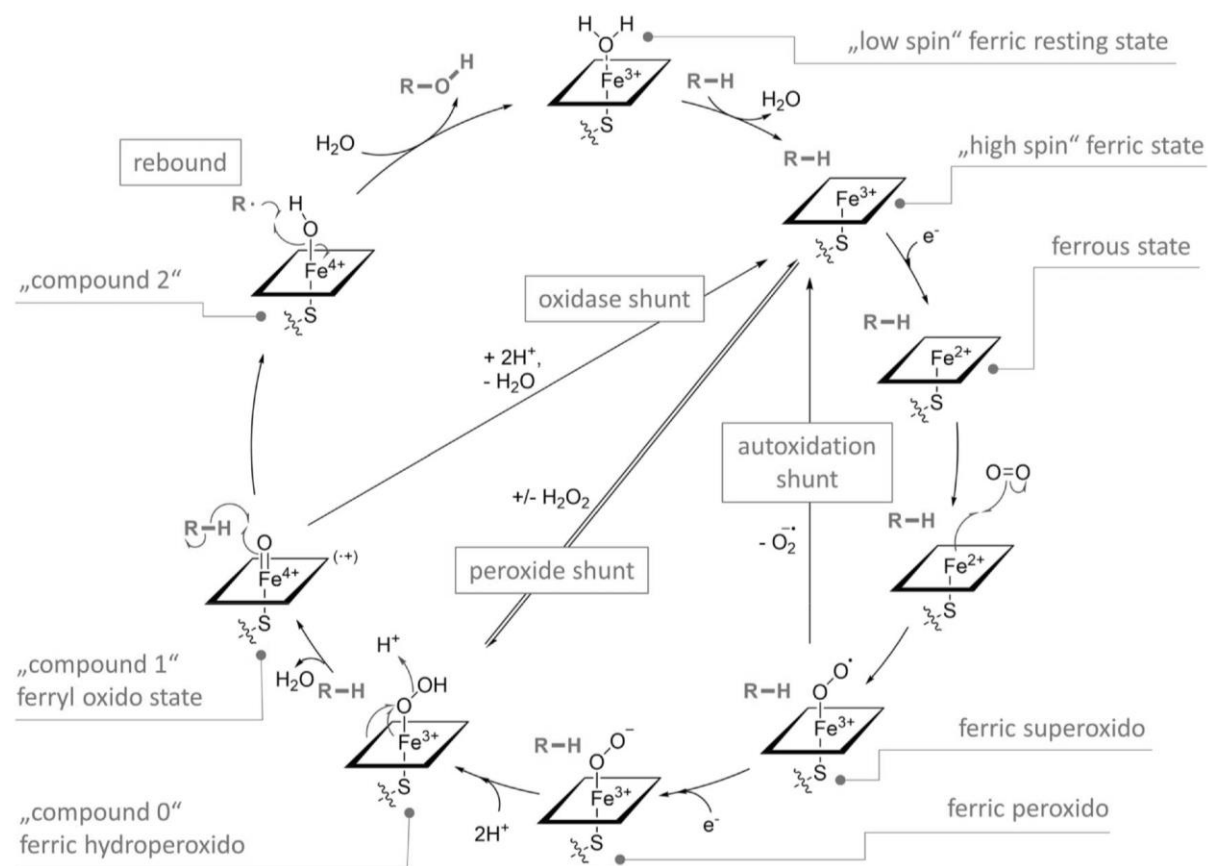
10	OleT-BM3R	1/1000	OleT-BM3R (fusion)	O ₂	C16:0	NADPH	1000/1000	---	32.6*	196	326 (12 h)	100	Lu <i>et al.</i> (2018) [4]
11	OleT-BM3R	3/10000	OleT-BM3R (fusion)	O ₂	C18:0	NADPH	200/10000	PTDH	---	472	1957	100	Lu <i>et al.</i> (2018) [4]
12	OleT	1/500	CamAB	O ₂	C20:0	NADPH	500/500	---	2.58*	12.9	12.9 (1 h)	1000	Wise <i>et al.</i> (2018) [37]
13	OleT	1/500	Fre, FAD	O ₂	C20:0	NADH	500/500	---	2.52*	12.6	12.6 (1 h)	1000	Wise <i>et al.</i> (2018) [37]
14	OleT	1/500	CamAB	O ₂	C20:0	NADH	500/500	---	3.3*	16.5	16.5 (1 h)	1000	Wise <i>et al.</i> (2018) [37]

1.4 Catalytic cycle of cytochrome P450 enzymes

OleT has a moderate sequence homology to CYP_{BSβ} (41%) and to CYP_{SPα} (36%). High sequence homologies between the active sites of OleT and CYP_{BSβ}, a fatty acid β-hydroxylase that uses H₂O₂ as oxidant, led to an initial classification of OleT as peroxygenase [11]. Using O₂ as oxidant, in combination with the reducing agent NAD(P)H, higher conversions were achieved. This observation raised the question whether OleT naturally acts as a monooxygenase and uses O₂ as oxidant [35][34][38].

For oxygen activation, subsequent transport of two electrons to the heme group of OleT is required. When peroxide is used as oxidant the so-called “peroxide shunt” is used to catalyze oxygenase reactions. The catalytic cycle of cytochrome P450 enzymes is shown in figure 7 (A). In figure 7 (B), the OleT active site binding pocket for a fatty acid substrate molecule is shown. The substrate is coordinated by an arginine residue and the heme prosthetic group.

A



B

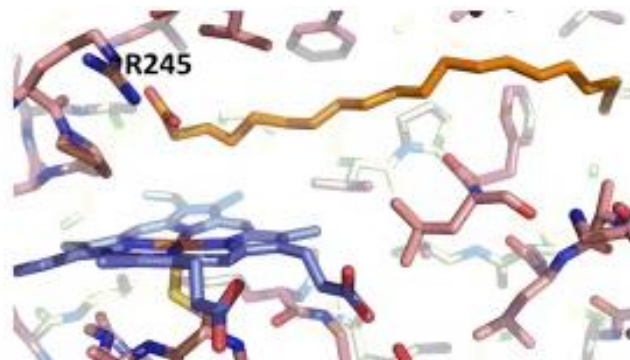


Figure 7 (A) Catalytic cycle of cytochrome P450 enzymes. With sequential supply of two electrons or direct hydrogen peroxide addition (“peroxide shunt”), the heme center gets activated for catalysis. (B) Active site of OleT with bound arachidic acid substrate. Arg245 and heme group (blue) and fatty acid substrate in binding pocket (orange) are shown. (A) was taken from Hammerer *et al.* (2018) [39] and (B) was taken from Matthews *et al.* (2017) [40].

In its ground state, the prosthetic heme - Fe^{III} is axially coordinated by cysteine-thiolate and a water molecule. In absence of a substrate molecule, low-spin (LS) state of the iron is favored [20]. Binding of a substrate molecule perturbs the water molecule coordinated as the sixth ligand of the heme iron and leads the same to shift to high spin (HS) state [41][42]. In HS, Fe^{III} has an increased reduction potential and hence can be much easier reduced.

In the case of monooxygenation, the iron is sequentially reduced by two electrons derived from NAD(P)H and transferred via redox partner proteins. After a first reduction dioxygen binds to the Fe²⁺ containing heme forming an oxy-ferrous complex. After a second reduction, protonation leads to formation of the instable hydroperoxo-ferric intermediate Compound 0 (Fe³⁺-OO(H)⁻), which is rapidly protonated and dehydrated to a Fe⁴⁺-oxo π cation radical (Compound I) [43][44]. This reactive species can abstract an H-atom from a C-H bond in the substrate (C _{α} or C _{β}), forming compound II (Fe⁴⁺-OH) and leading to formation of a substrate radical and therefore high reactivity of the affected C-atom (figure 8). Now, there are two competing reactions, leading to either decarboxylation or to hydroxylation of the substrate: In a rebound mechanism, the -OH group bound to Fe⁴⁺, rebinds to the C-atom leading to hydroxylation. For decarboxylation, the mechanism is not yet fully elucidated. Probably an unstable carbocation (or a biradical) is formed leading to C-C scission and decarboxylation. Both CO₂ and the product then dissociate from the enzyme active site (see 1.5.) [40][44].

In the case of peroxygenases, decarboxylation and hydroxylation are initiated by the peroxide shunt rather than by oxygen activation. Thereby the heme center of the substrate-bound P450 is directly oxidized to Compound 0 (Fe³⁺-OO(H)-) [40].

1.5 Reaction mechanism of OleT

The substrate channel of OleT is highly hydrophobic, as is necessary for binding of a long-chain fatty acid substrate [22]. The residues Arg-245 (figure 7) and Pro-246 are conserved in OleT, CYP_{BSβ} and CYP_{SPα} and are proposed to play an important role for binding and positioning of the substrate. They are essential for bringing the substrate in close proximity to the site where catalysis takes place. The main difference in the active sites of CYP_{BSβ} and OleT is that in CYP_{BSβ} there is a Gln residue in position 85 whereas in OleT there is a His-residue in this position. The glutamine is conserved in most CYP152s. Rude *et al.* (2011) replaced the CYP_{BSβ} Gln-85 with a His residue, which resulted in a higher portion of decarboxylated reaction product in relation to overall hydroxylation products [11]. This mutation experiment confirmed the importance of this residue for the decarboxylation activity of the enzyme. This observation was confirmed by Fang *et al.* (2017) [36]. A possible explanation for this phenomenon is that OleT His-85 donates a proton to compound I during its reduction to compound II by an electron that is abstracted from the fatty acid carboxylate (figure 8). Hsieh *et al.* (2017) complemented this observation with the finding that positioning of the substrate in the active site facilitates formation of compound I and is crucial for the selectivity of the reaction [45]. Terminal alkene and CO₂ are formed by homolytic C-C bond cleavage.

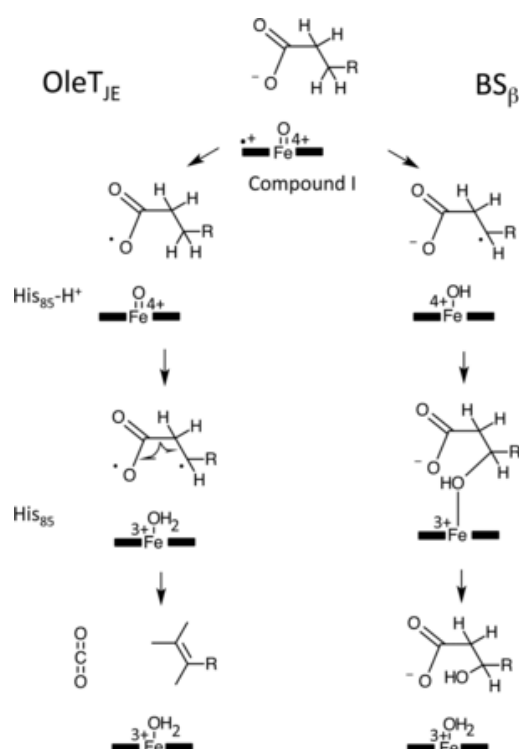


Figure 8 Proposed mechanism for OleT. The cytochrome P450 enzyme OleT catalyzes decarboxylation whereas the related enzyme CYP_{BSβ} forms β-OH fatty acid as its main product. The main difference in the active sites of both enzymes is residue 85 –which is His in OleT and Gln in CYP_{BSβ} [22].

1.6 Cytochrome P450 enzymes – perspectives and limitations

Cytochrome P450 enzymes are capable of catalyzing a broad variety of different reactions, among them for example demethylation, dealkylation, epoxidation [20] and also C-C cleavage as in the case of OleT [11]. Despite the many advantages of P450s (many different reaction types, activation of oxygen, oxidation of inert C-atoms, high regio- and stereoselectivity, broad substrate spectrum), there are many limitations in their use. One limitation is that some cytochrome P450 enzymes have low activities. OleT has been shown to have an activity of 2.8 min^{-1} [35], in comparison, CYP_{SP α} has a much higher activity of 3800 min^{-1} [46]. Another drawback of P450 enzymes is the need for efficient electron transfer partners. If these transfer partners are not optimally interacting with each other and the P450 enzyme, there will be limitations regarding electron transfer rate and electron coupling, which means, electrons that derive from NAD(P)H will get uncoupled from the transfer chain by reducing dissolved oxygen to O_2^- which can be further reduced to H_2O_2 . These electrons can reach the P450 enzyme via the peroxide shunt pathway. The definition of coupling (%) is given by the following equation.

$$\text{Coupling [\%]} = 100 \times \frac{\mu\text{mol product}}{\mu\text{mol NAD(P)H}}$$

The commercially quite expensive cofactor NAD(P)H is often inefficiently used for substrate conversion (due to uncoupling). By applying a cofactor recycling system, the overall costs can be decreased. As an example, the cofactors NADPH and NADH can be regenerated by adding glucose and the enzyme glucose dehydrogenase, or NADH restoration can be achieved with the enzyme formate dehydrogenase and formate [47][48][49]. Another difficulty is given if substrates are hydrophobic and therefore have low solubility. It is common practice to use co-solvents such as EtOH or DMSO, but those can negatively influence enzyme stability and activity [50]. Applications in whole-cell systems are also not easy. In literature difficulties such as substrate-uptake limitations, product toxicity, low product-release rates and NAD(P)H depletion are described [21][26][51][52][53].

1.7 Aim of this thesis

In this project, a redox chain should be isolated from the bacterium *Jeotgalicoccus sp.* ATCC8456, which is the origin of OleT. The isolated electron transfer chain constituents should then be heterologously expressed in *E. coli* and reconstituted *in-vitro* together with OleT. Electron transfer should be characterized in terms of transfer efficiencies and kinetic parameters involving K_M and k_{cat} .

Methods to determine these parameters involve spectrophotometric as well as GC-MS analyses of the reactions. Also the necessity of the single electron transfer chain constituents should to be determined by studying the effect of leaving out single transfer proteins from the reaction. As electron transfer systems used so far (table 1) have low coupling efficiencies (loss of electrons during catalysis), the aim was to find a more efficient system that allows better electron economy. It was expected that a natural system for the enzyme will allow more efficient catalysis with OleT than the artificially reconstituted systems reported before. No electron transfer system has to date been isolated from 1-alkene producing microorganisms with the specific purpose to be used in combination with an olefin forming enzyme.

Another aim of this work was to get an insight if OleT_{Je} naturally acts as monooxygenase or peroxygenase. In many publications, the enzyme is referred to as a peroxygenase. An argument for this is that peroxide stability of OleT is higher compared to other P450s such as BM3, CYP51B1 or CYP121A1. Differences are especially obvious at high H₂O₂ concentrations (at 2 mM H₂O₂, the rate constant for inactivating heme oxidation (*k*) is 8.51 for OleT and 43.25 for BM3 [40]. But as H₂O₂ generally is toxic to cells and inhibits enzyme functions at sufficiently high concentrations, it seems questionable whether this is the way OleT is activated to catalyze the reaction. Only small concentrations of peroxide can be available in cells (in *E. coli* the intracellular concentration is below 10⁻⁷ M) [54]. Peroxide is capable of oxidizing SH-groups that are important to the function of many enzymes [55]. If there are natural redox partners transferring electrons from NAD(P)H, no toxic peroxide would be needed. Studying the efficiency of a natural redox chain should further help getting a deeper insight into the reaction mechanism of OleT [37].

2 Material and methods

2.1 Materials

2.1.1 Chemicals

All chemicals used were purchased from Sigma Aldrich and Carl Roth if not stated otherwise, and used without further purification.

Table 2 Chemicals used in this work.

Aminolevulinic acid	Sigma Aldrich (Steinheim, Germany)
TMSCHN ₂	Sigma Aldrich (Steinheim, Germany)
(Trimethylsilyl)diazomethane in diethyl ether	
Fatty acids	Sigma-Aldrich (Steinheim, Germany)
Kaliumhexacyanoferrat	E. Merck (Darmstadt, Germany)
b-per	Sigma Aldrich (Steinheim, Germany)

2.1.2 DNA extraction and purification kits

Table 3 DNA extraction and purification kits used in this work.

GeneJET PCR Purification Kit	Thermo Fisher Scientific, Inc. (Waltham, Massachusetts, USA)
Nexttec™ Genomic DNA isolation Kit for Bacteria	Biozym Scientific GmbH (Hess. Oldendorf, Germany)
GeneJET Plasmid Miniprep Kit	Thermo Fisher Scientific, Inc. (Waltham, Massachusetts, USA)
GeneJET Gel Extraction Kit	Thermo Fisher Scientific, Inc. (Waltham, Massachusetts, USA)

2.1.3 Enzymes and PCR components

Table 4 Enzymes and PCR components used in this work.

ONETAQ® QUICK-LOAD®	New England Biolabs (Ipswich, Massachusetts, USA)
Restriction enzymes	Thermo Fisher Scientific, Inc. (Waltham, Massachusetts, USA)

100 bp DNA ladder and a 1 kb DNA ladder	New England Biolabs (Ipswich, Massachusetts, USA)
Lysozyme from chicken egg white (> 40000 U mg ⁻¹)	Sigma Aldrich (Steinheim, Germany)

2.1.4 Laboratory equipment

Table 5 Laboratory equipment used in this work.

French® Pressure Cell Press	SLM Aminco (Silver Spring, Maryland, USA)
Varian Cary® 50 UV-Vis spectrophotometer	Varian
DeNovix DS-11 Spectrophotometer	DeNovix Inc. (Wilmington, North Carolina, USA)
Eppendorf Centrifuge 5415 R	Eppendorf AG (Hamburg, Germany)
ÄKTAprime plus	Amershan BioSciences, GE Healthcare (Chicago, IL, USA)
HisTrap HP protein purification column	GE Healthcare Life Sciences (Chicago, Illinois, USA)
HiTrap SP FF column, 5 mL	GE Healthcare Life Sciences (Chicago, Illinois, USA)
DNA gel electrophoresis Model 200/ 2.0 Power Supply	Bio-Rad Laboratories Ges.m.b.H. (Vienna, Austria)
Bio-Rad Gel Doc 2000 Documentation System	Bio-Rad Laboratories Ges.m.b.H. (Vienna, Austria)
Fisher Scientific* Model 705 Sonic Dismembrator	Thermo Fisher Scientific, Inc. (Waltham, Massachusetts, USA)
Rotary shaker CERTOMAT® BS-1	Sartorius AG (Goettingen, Germany)
PCR thermocycler VWR® Doppio	VWR™ (Radnor, Pennsylvania, USA)
Vortex Reax 2000	Heidolph Instruments GmbH & Co. KG, (Schwabach, Germany)
Ultracentrifuge Sorvall® Evolution RC	Thermo Fisher Scientific, Inc. (Waltham, Massachusetts, USA)
GC-MS: 7890B GC – 5977A MSD	Agilent Technologies (Santa Clara, California, USA)
Sterile workbench Bioair Auro 2000 Lamina Flow	EuroClone S.p.A. (Milan, Italy)
Varioklav Dampfsterilisator	HP Medizintechnik GmbH (Oberschleißheim, Germany)

Minisart® Single use filter unit 0.45	Sartorius AG (Goettingen, Germany)
Analytical Balance ENTRIS® 224I-1S	Sartorius AG (Goettingen, Germany)
Balance LE224S	Sartorius AG (Goettingen, Germany)
WPA CO8000 Cell Density Meter	Biochrom WPA (Cambridge, UK)

2.1.5 Bacterial strains

Table 6 Bacterial strains used in this work.

Strain	Strain description
<i>Jeotgalicoccus</i> sp. ATCC8456	Wild-type
<i>E. coli</i> TOP10	F ⁻ mcrA Δ (mrr-hsdRMS-mcrBC) ϕ 80lacZ Δ M15 Δ lacX74 nupG recA1 araD139 Δ (ara-leu)7697 galE15 galK16 rpsL(Str ^R) endA1 λ^- (Invitrogen)
<i>E. coli</i> BL21(DE3)	str. B F ⁻ ompT gal dcm lon hsdS _B (r _B ⁻ m _B ⁻) λ (DE3 [lacI lacUV5-T7p07 ind1 sam7 nin5]) [malB ⁺] _{K-12} (λ^S)

2.1.6 Growth media and media additives

Liquid media:

All media components were dissolved in ddH₂O and autoclaved at 121 °C for 20 min. LB and TB media were stored at RT, SOC medium was aliquoted (1 mL) and stored at -20 °C.

Table 7 Liquid media used in this work and their compositions

Media	Media composition
LB media	10 g L ⁻¹ tryptone, 5 g L ⁻¹ yeast extract, 10 g L ⁻¹ NaCl, pH 7.0
TB media	20 g L ⁻¹ tryptone, 24 g L ⁻¹ yeast extract, 4 mL L ⁻¹ glycerol, 17 mM KH ₂ PO ₄ , 72 mM K ₂ HPO ₄
TSBYE media	17 g L ⁻¹ tryptone, 3 g L ⁻¹ soytone, 5 g L ⁻¹ NaCl, 2.5 g L ⁻¹ , K ₂ HPO ₄ , 2.5 g L ⁻¹ glucose, 5 g L ⁻¹ yeast extract (final pH 7.3)
SOC media	20 g L ⁻¹ tryptone, 5 g L ⁻¹ yeast extract, 10 mM NaCl, 2.5 mM KCl, 10 mM MgCl ₂ , 20 mM glucose, pH 7

Solid media:

Media components were dissolved in ddH₂O and autoclaved at 121 °C for 20 min. Kanamycin was added at a temperature of ~ 60 °C before the liquid LB agar was filled into plastic Petri dishes (~20 ml per plate). Agar plates were then stored at 4 °C until use.

Table 8 Composition of lysogeny broth agar.

Media	Media composition
LB agar	10 g L ⁻¹ tryptone, 5 g L ⁻¹ yeast extract, 10 g L ⁻¹ NaCl, 15 g L ⁻¹ agar agar, pH 7.0

Media additives:

Media additives were prepared as 1000x (1000-fold concentrated) stock solutions. Chemicals were dissolved in ddH₂O and solutions were sterilized by filtration (0.2 µM filter). Trace element solution was stored at 4 °C until use. All other stock solutions were stored as 1 mL aliquots at -20°C.

Table 9 Media additives used in this work and their stock concentrations/ compositions.

Media additive	Stock concentration/ composition
ALA (aminolevulinic acid)	0.5 M
Kanamycin	50 g L ⁻¹
IPTG (isopropyl-β-D thiogalactopyranoside)	0.1 M
Trace element solution	0.5 g L ⁻¹ CaCl ₂ ·2H ₂ O, 0.18 g L ⁻¹ ZnSO ₄ · 7H ₂ O, 0.1 g L ⁻¹ MnSO ₄ ·H ₂ O, 20.1 g L ⁻¹ Na ₂ -EDTA, 16.7 g L ⁻¹ FeCl ₃ ·6H ₂ O, 0.16 g L ⁻¹ CuSO ₄ ·5H ₂ O

2.2 3-Step purification protocol for OleT and the mediator

The first attempt to obtain the mediator molecule for OleT was using a reverse genetic approach. Rude *et al.* were the first to isolate OleT from the Gram-positive coccoid bacterium *Jeotgalicoccus sp.* ATCC8456 in 2010 [11]. In their original protocol, OleT was obtained following a 3-Step purification protocol. The SDS-PAGE that was run after purification showed not only a band for OleT (50 kDa), but also one of much lower molecular mass (15 kDa), which could not be assigned to any protein (figure 9) [11]. The hypothesis was that this could be the wanted mediator, as it could be bound to OleT and and co-elute. Therefore, the original purification protocol was repeated and modified to obtain the band of lower molecular mass. The band was then excised from the gel and prepared for LC-MS/MS analysis.

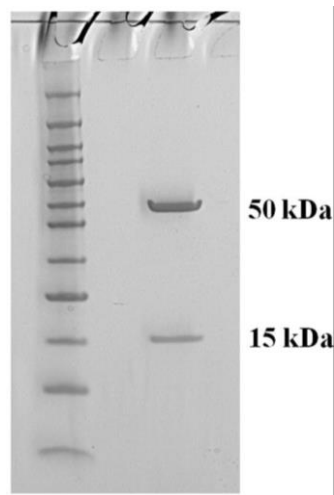


Figure 9 The coomassie-stained SDS-PAGE of the active fraction purified by Rude *et al.* The isolation was done in a three-step purification protocol and contains the 50 kDa OleT band and a 15 kDa band [11].

2.2.1 Culture conditions and cell disruption

Jeotgalicoccus sp. ATCC8456 was grown in 6 x 1 L tryptic soy broth supplemented with 0.5% yeast extract (TSBYE) at 30 °C for 24 h. The cells were recovered by centrifugation (8850 x g, 15 min, 4 °C) and the pooled pellet was resuspended in 100 ml 50 mM Tris (pH 8, 0.1 M NaCl, 2 mM DTT, bacterial protease arrest (5 ml of P-8465 protease inhibitor cocktail, Sigma Aldrich)). Cell disruption was achieved using a French press (2 cycles, 1500 psi) followed by sonication (pulse 2 sec, pause 4 sec, amplitude 60%, total time 5 min). The resulting slurry was transferred to Eppendorf tubes and centrifuged (11000 x g, 60 min, 4 °C) to remove cell debris.

The original 3-step purification protocol (Rude *et al.*) is comprised of a precipitation procedure with ammonium sulfate, a cation exchange chromatography step and an anion exchange chromatography step. It has been adjusted and shortened to a 2-step purification protocol, omitting the final anion

exchange chromatography step, as the 15 kDa band was already obtained in high purity after cation chromatography.

2.2.2 Precipitation with $(\text{NH}_4)_2\text{SO}_4$

After centrifugation of the disrupted cells, all supernatants were collected and ammonium sulfate $(\text{NH}_4)_2\text{SO}_4$ was added to a concentration of 50% saturation. The exact amount of $(\text{NH}_4)_2\text{SO}_4$ was calculated using the EnCor Biotechnology Inc. Ammonium Sulfate Calculator (<http://www.encorbio.com/protocols/AM-SO4.htm>). The mixture was stirred for 60 minutes at 4 °C and white protein precipitate was formed. The mixture was retransferred to fresh Eppendorf tubes and centrifuged (11 000 x g, 30 min, 4 °C) to remove the precipitated protein. After pooling all supernatants, $(\text{NH}_4)_2\text{SO}_4$ concentration was increased to 65% saturation and the mixture was stirred for further 60 min at 4 °C. Thereafter, another centrifugation step was conducted (11000 x g, 30 min, 4 °C). The supernatants were discarded and the protein pellets resuspended in a total of 70 ml 50 mM Tris (pH 8, 2 mM DTT) [11].

2.2.3 Cation exchange chromatography

A 5 ml HiTrap SP FF column was equilibrated with 50 mM Tris buffer (pH 8, 2 mM DTT) before the *Jeotgalicoccus sp.* ATCC8456 protein suspension was loaded (3 ml min⁻¹). The column was then washed with 10 column volumes 50 mM Tris (pH 8, 2 mM DTT, 0.04 M NaCl). In the original protocol, a concentration of 0.4 M NaCl was described, which resulted here in unwanted washout of all proteins [11]. The salt concentration was therefore decreased. A NaCl gradient was then applied (3 ml min⁻¹, 20 min) to reach a final concentration of 1 M (0.04 M NaCl → 1 M NaCl). 5 ml fractions were collected at the outflow.

The third step of the purification protocol from Rude *et al.* (2011) (anion exchange chromatography with 1 ml Resource Q column) was not necessary and would have been pointless, as the protein was already very pure after single cation exchange chromatography (see results section 3.1). Further loss of protein was prevented by leaving out the anion chromatography step.

Fractions were tested for olefin-forming activity by demonstrating conversion of stearic acid to 1-heptadecene. The analyzed fractions were: *Jeotgalicoccus sp.* ATCC8456 cell lysate; cell debris; protein pellet after precipitation with 50% $(\text{NH}_4)_2\text{SO}_4$; supernatant after precipitation with 65 % $(\text{NH}_4)_2\text{SO}_4$; resuspended pellet after precipitation with 65% $(\text{NH}_4)_2\text{SO}_4$; the 4th washing fraction from the 5 ml HiTrap SP FF column and the assumed active fraction from the cation exchange chromatography column (table 10). For activity-testing, 4 µL of DMSO saturated with stearic acid were mixed with 1496 µL 50 mM Tris buffer (pH 8, 2 mM DTT) and 500 µL of the respective (resuspended) fraction. The samples were prepared to have a salt concentration of 0.1 M

(resuspension in or dilution with buffer). An amount of 0.8 mM of H₂O₂ per hour (4x) was added. Reactions were then acidified and extracted according to the protocol for two phase solvent extraction (see 2.8.1).

Fractions containing olefin-forming activity were pooled and dialyzed against 1 L Tris buffer (pH 8, 2 mM DTT, 0.04 M NaCl). The protein was concentrated to 5 ml (40 mM NaCl) and 2.5 µl of the sample were loaded onto the SDS-PAGE gel. The fractions mentioned before were also analyzed by SDS-PAGE (table 10).

Table 10 Fractions collected during purification that were analyzed with SDS-PAGE and tested for olefin-forming activity.

Cell debris
Lysate
Protein pellet 50% (NH ₄) ₂ SO ₄
Pellet after precipitation with 65% (NH ₄) ₂ SO ₄
Supernatant after precipitation with 65% (NH ₄) ₂ SO ₄
Washing fraction
Active fraction (contains FA decarboxylase activity)

As both expected bands were present in the active fraction, the one of 15 kDa was excised, stored in water, and sent to external LC-MS/MS analysis. Protocol and parameters of this analysis can be found in the annex section 5.3.

2.3 Isolation of genes from genomic data

Colleagues from the TU Graz Institute of Environmental Biotechnology sequenced and annotated the whole genome from *Jeotgalicoccus sp.* ATCC8456.

As the reverse genetic approach did not lead to meaningful evidence for an electron transfer protein, search for the mediator was continued by searching the genome for suitable candidates. Identification of potential electron transferring proteins from the genome was done via different approaches.

First, a protein BLAST search was done (leaving default parameters) with sequences of putidaredoxin reductase CamA (UniProt accession nr. P16640) and its 2Fe-2S ferredoxin-type redox partner CamB (Putidaredoxin) (P00259) from *Pseudomonas putida* (bacterial class I P450 electron transfer

system) against the *Jeotgalicoccus sp.* ATCC8456 genome. The CamAB system is comprised of a FAD-containing reductase (CamA) that is able to transfer electrons from NADH or NADPH to a ferredoxin (CamB) [18]. BLAST search was done also against another system of the same type, consisting of *E. coli* flavodoxin/ferredoxin-NADP reductase fpr (UniProt accession nr. P28861) and its 2Fe-2S ferredoxin partner fdx (UniProt accession nr. P0A9R4). Further, BLASTp search was done against the *E. coli* flavodoxin system FldA/fdrA (flavodoxin 1 from *E. coli* K12 (UniProt accession nr. P61949)). This is a class III bacterial electron transfer system, which resembles the class I system but contains a flavodoxin instead of a ferredoxin protein to transfer electrons from a FAD protein.

Then, the genome was manually searched for ferredoxin and flavoprotein genes and respective reductases, and selected candidates that could play a role in electron transfer with cytochrome proteins. The search was done taking in account indications in gene names and/or motifs that are typical for electron transfer proteins, such as flavin binding sites. Selected genes are listed in table 11.

Table 11 Selection of genes annotated as coding for electron transferring proteins. 1 – 5 are potential class I system candidates. 6 – 10 are potential flavodoxin – flavodoxin-reductase system candidates.

Entry	Annotation (No.)	Annotated as
1	BASYS00024	Putative electron transport protein yhbA [H]
2	BASYS00361	Ferredoxin [H]
3	BASYS01288	Ferredoxin-NADP-reductase [H], trxB [C]
4	BASYS02089	Ferredoxin-NADP-reductase 1 [H], trxB [C]
5	BASYS00026	NADPH-dependent nitro/flavinreductase [H] nfrA1
6	BASYS00103	Predicted flavoprotein (similar to ytfP [H])
7	BASYS01648	FMN reductase [H] predicted flavoprotein, msuE
8	BASYS01649	NADPH-dependent FMN reductase

The most promising candidates are the gene for a prospective ferredoxin (entry 2, table 11) and the two genes annotated as ferredoxin-NADP-reductases (entry 3 and 4, table 11), as these molecule types are components of a typical class I bacterial electron transfer system.

2.4 Cloning and expression of genes from *Jeotgalicoccus sp.* ATCC8456

2.4.1 Vector map of pET-28a(+)

Plasmid pET-28a(+) has been chosen as vector for heterologous protein expression, as it reaches high copy numbers within bacterial cells. The gene of interest is under tight control of an inducible T7 expression system. Cells for production of the desired protein contain a DE3 gene coding for T7 polymerase. *E. coli* strain BL21(DE3), in which a lac-inducible promoter is responsible for transcription of the T7 polymerase gene, has been chosen for expression. A vector map of pET-28a(+) is depicted in figure 10.

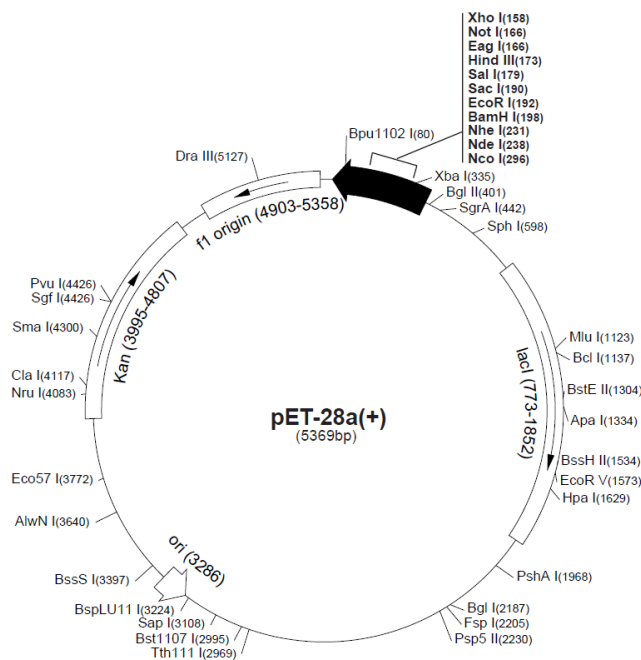


Figure 10 Vector map of pET-28a(+) high-copy expression plasmid with T7 expression from Novagen [56]. Selected genes were cloned into the multiple cloning site using restriction-ligation cloning.

pET-28a(+) was isolated from *E. coli* Top10 cells (50 ml ONC in LB-Kan^R medium) containing the respective plasmid. A volume of 4 ml ONC was treated with the GeneJET Plasmid Miniprep Kit (Thermo Scientific™) according to the user manual instructions and plasmid DNA was eluted with 40 µL pre-warmed MilliQ water.

2.4.2 Molecular biological methods

Primers were designed to have a melting temperature (T_m) of about 60 °C. Short nucleotide extensions consisting of restriction sites and a few further bases (6 bases) to foster restriction enzyme recognition were added at the N-termini of the primers. The SnapGene® software was used for design and selection of suitable restriction sequences that do not occur inside the genes of interest. All oligonucleotides were reviewed with OligoAnalyzer (IDT) to ensure low thermodynamic tendency towards hairpin and/or homo-/heterodimer formation (<https://eu.idtdna.com/calc/analyzer>). Primers were designed to have N-terminal attachment of the 6x His-Tag sequence when ligated into pET-28a(+).

Primers for cloning the Fdx_j gene contained restriction sites for NdeI (forward primer) and XhoI (reverse primer). The same restriction sites were attached to primer sequences for FdR_{j1} . Other electron transfer candidates were also amplified from the genome to have alternatives in case ferredoxin and the primary chosen ferredoxin reductase did not work for any of both P450s (OleT or new P450). A summary of restriction sites and primer sequences is shown in table 12. Full DNA sequences of the Fdx_j and FdR_{j1} genes are given in the annex (5.1). IDT oligoanalyzer predicted homo- and heterodimer formation tendencies to be as low to not constrain PCR reactions.

Apart from the electron transfer candidates, a second P450 enzyme that was annotated as cytochrome enzyme with fatty-acid peroxygenase activity was isolated from *Jeotgalicoccus sp.* ATCC8456. The new enzyme was isolated to see whether it accepts fatty acids as substrate and electrons delivered by a potential electron transfer system. This second P450 enzyme was already identified by Rude *et al.*, but soluble expression of the N-his-tagged protein failed. Therefore, the protein was cloned upstream of a C-terminal his-tag to reduce possible folding problems during expression. Primer sequences were designed by the same criteria as for the electron transfer proteins. As heterodimer formation tendencies were fairly high, a silent mutation was induced to the forward primer (red) to minimize possible challenges during PCR.

Table 12 Primers for BASYS00361 (ferredoxin Fdx_j), for BASYS01288 (ferredoxin reductase FdR_{j1}) and for BASYS00261 ($P450_{j\alpha}$). Restriction sites are marked in grey and a base change (to minimize primer-dimer formation) is highlighted. T_m is the melting temperature in °C.

Gene	Protein	Primer direction	Primer sequence	Restriction site	T_m [°C]
BASYS00361	Fdx_j	Fwd 5' → 3'	GTACCTCATATGTGCGCTAAGAAATA CACA ATCGTTGAC	NdeI	59.3 °C
BASYS00361	Fdx_j	Rev: 5' → 3'	AGTGTACTCGAGCTATTCATACTTCA ATGGATCACCATCAAATGGTTC	XhoI	59 °C

BASYS01288	FdR _{J1}	Fwd 5' → 3'	GTACCCCATATGAAAGATGAAATTAC AGATATAACAATTATTGGCGGTG	NdeI	59 °C
BASYS01288	FdR _{J1}	Rev: 5' → 3'	AGTGTCTCGAGTTAATTTGTTTGA AGACACTTGTAGAGTGTTTTGGTTG	XhoI	59.6 °C
BASYS00261	P450 _{Jα}	Fwd 5' → 3'	GTAATCGCCATGGGCATGAACTCAA ATATGCCAAATGATTCTGGTTTCGAC	NcoI	60.5 °C
BASYS00261	P450 _{Jα}	Rev: 5' → 3'	AGTGTGCTCGAGGGCGGTTTTGATA CGTGTGGCTTAATCTCACTTTGTC	XhoI	59.1 °C

2.4.3 Purification of genomic DNA from *Jeotgalicoccus sp.* ATCC8456

Prior to amplification of the selected genes, genomic DNA was purified from *Jeotgalicoccus sp.* ATCC8456. This was done with 3 different methodologies: 1) Taking one colony and resuspending it in 50 µL lysis buffer containing 20 mM Tris, 3 mM MgCl₂, 0.5 % (v/v) Tween 20, 0.5 % (v/v) TritonX 100 and 60 µg/ml proteinase K). This buffer recipe had been adopted and slightly changed from a protocol for purification of genomic DNA from the Gram-positive *Staphylococcus aureus* (Richardson Lab at UNC Chapel Hill; <http://richardsonlab.web.unc.edu/protocols/colony-pcr-for-s-aureus/>). In this protocol the detergents NP-40 or IGEPAL® CA-630 are used instead of Triton X-100. Resuspended cells were incubated at 55 °C for 1 h and at 95 °C for 10 min and then centrifuged for 10 minutes at 16,100 x g to get rid of cellular debris. 2) Suspending a spatula tip of frozen *Jeotgalicoccus sp.* ATCC8456 cells in 100 µL lysis buffer and performing the purification steps as described for 1). 3) Using the nexttec™ genomic DNA isolation kit. Therefore, cells were taken from a frozen pellet and resuspended in LB medium to a final OD₆₀₀ of 1.5, whereof 2 x 0.5 ml were taken for lysis. All further steps were carried out according to the producer's manual instructions. Eluted DNA was stored at -70 °C overnight.

The genomic DNA that was obtained by following the nexttec™ genomic DNA isolation protocol was used for further work.

2.4.4 PCR with genomic DNA from *Jeotgalicoccus sp.* ATCC8456

In-vitro amplification of the selected genes was achieved by polymerase chain reaction (PCR) using ONETAQ® QUICK-LOAD®, containing a blend of Taq and Deep VentR™ DNA Polymerases. Reaction mixtures of 50 µL contained 25 µL ONETAQ® QUICK-LOAD® 2X Master Mix with standard buffer, 5 µL purified genomic DNA and 0.2 µM forward and reverse primer, respectively. Reaction mixtures were

placed in a thermocycler and the genes were amplified using the temperature program depicted in table 13. As control, one sample without template and one without primer were prepared.

Table 13 Thermocycler program for cPCR with ONETAQ® QUICK-LOAD® 2X Master Mix.

Step	Temperature [°C]	Time [s]
Initial Denaturation	94	60
Denaturation	94	30
Annealing	55	30
Elongation	68	180
Final Elongation	68	300
Storage	10	∞

} 30 cycles

To ensure successful amplification of the desired DNA fragments, 5 µL samples of PCR reaction mixtures, including the two controls, were analyzed on 1% (w/v) agarose gel in 1x TAE buffer (100 V, 0.5 h). Due to different sizes of the genes that were analyzed, two different DNA ladders were run simultaneously (100 bp DNA ladder and a 1 kb DNA ladder).

As all PCR reactions were completed successfully, fragments were purified using the GeneJET PCR purification kit (ThermoFisher). According to the user's manual instructions, 1:1 mixtures of completed PCR reactions and binding buffer were loaded onto the columns. For the shortest fragment (BASYS00361, 252 bp), additionally the same amount of isopropanol was added, to ensure strong binding to the column. Elution of the fragments was done with 30 µL pre-warmed (30 °C) ultrapure ddH₂O. DNA concentrations of the fractions (listed in table 14) were measured with a NanoDrop™ spectrophotometer.

Table 14 DNA concentrations after purification of cPCR reactions with the GeneJET PCR Purification Kit (ThermoFisher)

Entry	Annotation (No.)	Coding for	DNA conc. [ng/µL]
1	BASYS00024	See table 11	131.14
2	BASYS00361	Fdx _j	134.92
3	BASYS01288	FdR _{J1}	109.22
4	BASYS02089	See table 11	97.10
5	BASYS00026	See table 11	117.63
6	BASYS00103	See table 11	94.41
7	BASYS01648	See table 11	122.30
8	BASYS01649	See table 11	114.02

2.4.5 Cloning of the genes of interest into the plasmid vector pET-28a(+)

The purified PCR fragments were restricted to obtain sticky DNA ends that allow ligation into pET-28a(+) vectors that were treated with the same restriction enzyme combinations. Here, only the restriction and ligation steps for the new electron transfer system and for P450_{J_α} are described. The system that was cloned for further characterization is consisting of ferredoxin (Fdx_J) and ferredoxin-NADP-reductase (FdR_{J1}).

Restriction enzymes used for cutting the ferredoxin (Fdx_J) and ferredoxin-NADP-reductase (FdR_{J1}) gene fragments were NdeI and XhoI. Reaction mixtures of a total volume of 50 μL contained 5 μL 10 x FastDigest buffer, 1 μL of each enzyme, 1 μg DNA and ddH₂O. 1 μL of FastDigest enzyme is able to cleave 1 μg of substrate DNA in 5 to 15 minutes under optimal conditions. The reactions were incubated for 4 h at 37 °C and stopped by heating (80 °C, 5 min). The plasmid pET-28a(+) was treated with the same combination of restriction enzymes. Reaction mixtures (20 μL) contained 2 μL 10 x FastDigest buffer, 0.5 μL of each enzyme, 1 μg plasmid DNA and ddH₂O. Reactions were incubated for 2 h at 37 °C. Enzymes were inactivated by heating (80 °C, 5 min).

For cutting the gene of P450_{J_α}, the restriction enzymes XhoI and NcoI were used. The 50 μL reaction mixture contained 1 μg (30 μL) purified PCR product, 1 μL of each restriction enzyme, 5 μL Tango 10x buffer and 13 μL of water. The amount of 2 μg pET-28a(+) was also cut in an 50 μL reaction mixture containing the same restriction enzymes and buffer. The reactions were stopped according to the procedure described above for the FdR_{J1} and Fdx_J gene fragments.

For each of the fragments, a 20 μL ligation reaction was set up containing 2 μL 10 x T4 DNA ligase buffer, 50 ng cut vector DNA, insert DNA in a 3:1 ratio to vector DNA and 1 μL T4 DNA ligase. Additionally, religation control reactions without insert DNA were prepared. The reactions proceeded for 1 h at room temperature before they were stopped by thermal inactivation at 65 °C for 10 min. The ligation products were purified using the GeneJet PCR purification kit. Elution of the ligation products was done with 20 μL pre-warmed ultrapure water.

2.4.6 Transformation of plasmid DNA into electro competent *E. coli* TOP10 cells

For transformation, 3 μL of ligated plasmid DNA (50 ng) were added to 100 μL of electro competent *E. coli* TOP10 cells [57]. Both purified ligations with or without gene of interest were transformed into the cells. The cells were thawed on ice and subsequently transferred into an electroporation cuvette, which was then placed in an electroporator. Cells were pulsed in EC2 mode before 350 μL of pre-warmed SOC medium (37 °C) were added to regenerate the cells for 1 h at 37 °C and 350 rpm. The

regenerated cells were then plated on LB-Kan^R plates. The plates were incubated overnight at 37 °C and the grown colonies were counted for statistical evaluation.

The competent cell's ability to take up DNA was confirmed by transforming them with empty pET-28a(+) (8 µL of 129.08 ng/µL vector). The transformed and recovered cells were plated (dilution 1 : 100) on LB-Kan^R plates and incubated overnight at 37 °C.

To analyze cloning success, ten *E. coli* TOP10 colonies that were transformed with pET-28a(+) containing Fdx_j and FdR1_j gene fragments were picked from the plates for colony PCR, respectively. For colonies transformed with plasmids containing the P450_{Jα} gene, 20 colonies were picked. The colonies were picked with a sterile pipette tip to suspend them in cPCR reaction mixtures and to streak them out on fresh LB-Kan^R plates, respectively. The plates were then incubated at 37 °C overnight. Colony PCR was done as described under 1.5.3 using a total reaction volume of 25 µL and 26 PCR cycles. Fdx_j PCR fragments were run on the gel together with the Thermo Scientific™ GeneRuler DNA Ladder Mix, FdR1_j PCR fragments together with the Invitrogen™ 100 bp DNA Ladder (6 µL of standard, respectively). The completed 10 cPCR reactions per gene were loaded onto a 1% agarose gel with a volume of 8 µL, respectively.

For each of the cloned fragments at least one picked clone showed a clear band at the expected sizes of 300 bp (Fdx_j) and 1000 bp (FdR1_j) on the gel. For the P450_{Jα} gene, 5 positive clones were picked.

2.4.7 Sequencing of successfully cloned genes

The clones that showed bands of the correct size on the agarose gel were taken from the LB-Kan^R plates to isolate the plasmids with Thermo Scientific™ GeneJET Plasmid Miniprep Kit according to the user manual instructions. The plasmids were eluted with 30 µL MilliQ water and 13 µL (2000 ng DNA) were sent for sequencing to a sequencing service (the company LGC genomics). Standard T7 primers that bind to the pET-28a(+) plasmid up- and downstream regions of the genes of interest were applied for sequencing (bidirectional).

The DNA sequence for the subcloned Fdx_j was correct and the one for FdR1_j contained one base change at position 48 which was a silent mutation of the base triplet ACA to ACG. Both base triplets are coding for the same amino acid, threonine, and therefore the Fdx_j sequence was suitable for further work. Also for the P450_{Jα} gene a clone containing the correct sequence was found.

2.4.8 Transformation of Plasmid DNA into electro competent *E. coli* BL21(DE3) cells

For transformation into the final expression host *E. coli* BL21(DE3), 2 µL of plasmid DNA (containing 280 – 380 ng DNA) were added to 100 µL of electrocompetent *E. coli* BL21(DE3) cells. Further steps

proceeded according to 2.4.6. Colonies grew very dense on the LB-Kan^R plates, so that cells were picked and streaked out to obtain single colonies.

2.5 Production of FdR_{J1}, Fdx_J, P450_{Jα} and OleT

After transformation of *E. coli* BL21(DE3) with plasmids containing genes of interest, the proteins and enzymes were produced in liquid media.

2.5.1 Expression of FdR_{J1}, Fdx_J, P450_{Jα} and OleT

Expression was done for all proteins in *E. coli* BL21(DE3) cells. Pre-cultures were prepared by inoculating sterile 50 ml Sarstedt tubes containing 15 mL TB-Kan^R medium with cells from a glycerol stock using a sterile inoculation loop. Pre-cultures were grown over night (37 °C, 150 rpm). From the pre-cultures, 2 ml were transferred into sterile Erlenmeyer flasks (1000 mL) containing 200 mL TB medium and 50 µg mL⁻¹ kanamycin (5 flasks per protein). Cells were grown to an OD₆₀₀ of 1.0 (37 °C, 150 rpm) before expression was induced by adding IPTG in a final concentration of 1 mM. Media for both P450 enzymes and Fdx_J additionally contained trace element solution (see table 9) and expression required the heme precursor molecule 5-aminolevulinic acid (5-Ala) which was added in a final concentration of 0.5 mM. After adding all components cells were grown for 20 h at 25 °C and cells were harvested (8850 x g, 15 min, 4 °C). Remaining medium was discarded and the pellets containing FdR_{J1}, Fdx_J, P450_{Jα} or OleT were stored at -20 °C.

2.5.2 Cell lysis of *E. coli* BL21(DE3) for isolation of FdR_{J1}, Fdx_J, P450_{Jα} and OleT

For fast control of expression success, cell lyses were done with 3 ml B-Per, according to the user manual instructions. 10 µL samples, consisting of 5 µL B-Per treated cell slurry, 2.5 µL NuPAGE[®] LDS Sample Buffer (4x), 1 µL NuPAGE[®] Reducing Agent (10x) and 1.5 µL H₂O were loaded on a SDS gel to see whether expression worked and if yes, to estimate the amounts of the proteins that were expressed.

For production of the proteins for *in-vitro* activity tests, cells were lysed with lysozyme. Therefore, the cell pellets were thawed on ice and resuspended in 50 mL Buffer C (KPi 100 mM, pH 7.5, 20% glycerol, 300 mM KCl) containing 1 mg/ml lysozyme, respectively. The resuspended cells were incubated for 45 min at 37 °C and the cell slurry was transferred to a beaker containing a magnetic stirring bar, the beaker was placed into another beaker containing iced water and the whole appliance was put on a magnetic stirrer. Cells were disrupted further by sonication, which was conducted according to the settings described in table 15.

Table 15 Settings for ultra-sonication used for cell disruption (used for all protein isolation steps).

Amplitude	70%
Total time	5 min
Pulse time	2 sec
Pause	4 sec

After transferring the slightly viscous slurry into Eppendorf tubes, the cell debris was removed by ultracentrifugation (16000 x g, 15 min, 4 °C). Supernatants were pooled in a Sarstedt tube and filtered through a 0.45 µM PTFE filter. The supernatant was stored on ice until loading onto a GE Healthcare HisTrap HP 5 ml column.

2.5.3 Purification of FdR_{J1}, Fdx_J, P450_{Jα} and OleT

His-tagged redox proteins and P450 enzymes from the previously produced cell lysates were purified performing affinity chromatography [58]. For each of the proteins the following solutions were prepared and filtered to proceed with the purification: 1000 mL buffer A (KPi 100 mM, pH 7.5, 20% (v/v) glycerol, 300 mM KCl, 0 mM imidazole for FdR_{J1} and Fdx_J, 50 mM imidazole for P450_{Jα} and OleT), 1000 mL buffer B (KPi 100 mM, pH 7.5, 20% glycerol, 300 mM KCl, 500 mM imidazole), 1000 mL buffer C (dialysis buffer; KPi 100 mM, pH 7.5, 20% glycerol, 300 mM KCl). Compositions of all buffers are described in table 16. A HisTrap HP 5 ml column, packed with nickel sepharose high performance (HP) affinity resin was connected to an Äkta flow system with UV detection. The flow rate was set to 4 ml min⁻¹ and kept constant during all purification steps. Relevant parameters were recorded and controlled by the Äkta system (pressure, temperature, UV absorbance at 280 nm, conductivity, flow rate). The following steps were conducted for selectively purifying the His-tagged proteins: 1. Flushing of the system with 50 mL filtered ddH₂O (10 column volumes) to remove 20% (v/v) EtOH which was used as storage solvent. 2. Equilibration of the column by flushing it with 50 ml Buffer A. 3. Loading of the filtered protein solution via a 10 mL loop (3 x 10 mL). 4. Washing of the column with 50 mL buffer A to remove unbound proteins. 5. Elution of the protein of interest by application of an imidazole gradient from 0 to 100 % buffer B in a total volume of 50 ml. During the experiment, 5 ml fractions were collected at the outflow by the Äkta purification system. The following fractions were taken for SDS-PAGE analyses: Cell-free lysate, a fraction collected during loading, washing fractions, fractions containing eluted protein. Samples were prepared as follows: 10 µL of protein sample, 15.5 µL NuPAGE® LDS Sample Buffer (4x), 5 µL NuPAGE® Reducing Agent (10x) and 19.5 µL ddH₂O were mixed and heated at 70°C for 10 minutes. 5 µL of a Thermo Scientific PageRuler™ protein ladder and 12 µL of each sample were loaded onto the NuPAGE® Bis-Tris Mini Gel 4-12% (novex). The gel was

placed in MOPS buffer and samples were run for 40 minutes. Fractions where the protein of interest was detected were pooled and dialyzed against 1 L of buffer C.

Table 16 Buffers for purification buffers A (loading buffer) and B (elution buffer) and storage buffer C.

	For purification of FdR _{J1} and Fdx _J	For purification of P450 _{Jα} and OleT
Buffer A	KPi 0.1 M, pH 7.5, 20 % glycerol, 300 mM KCl, 0 mM imidazole	KPi 100 mM, pH 7.5, 20 % glycerol, 300 mM KCl, 50 mM imidazole
Buffer B	KPi 0.1 M, pH 7.5, 20 % glycerol, 300 mM KCl, 500 mM imidazole	
Buffer C (dialysis buffer)	KPi 0.1 M, pH 7.5, 20 % glycerol, 300 mM KCl	

2.6 Protein quantification

Quantification of P450s (OleT, P450_{Jα}) was done via carbon monoxide titration [59]. A spatula tip of sodium dithionite (Na₂S₂O₄) was added to the enzyme solution (diluted 1:10) for reduction of Fe³⁺ to Fe²⁺. A photometric spectrum was recorded (400-600 nm) after blanking with dialysis buffer. Thereafter, the enzyme solution was gassed for 30 seconds with CO and then the absorbance spectrum was measured again (figure 30 in section 3.1.2). CO binds to the reduced iron in the center of the heme group and shifts the absorption maximum from 420 to 450 nm. As oxygen binds to the heme group a similar way (but with lower affinity), the binding of CO allows quantification of active enzyme. The differential spectrum between the scan measurements before and after CO gassing was taken to calculate the concentration of active enzyme in the solution (equation below) based on the law of Lambert-Beer. The OleT and P450_{Jα} solutions were stored at 4 °C until further use.

$$c(P450x) = \frac{\Delta E(450 \text{ nm}) - \Delta E(500 \text{ nm})}{\epsilon(91)} \times D(10) \times 1000$$

ΔE (450) = differential absorbance at a wavelength of 450 nm

ΔE (500) = differential absorbance at a wavelength of 500 nm

c = concentration [μmol L⁻¹]

ε = extinction coefficient of ferrous P450 bound to CO [cm⁻¹ mM⁻¹] = 91

D = dilution factor (10)

FdR_{J1} and Fdx_J were quantified with a NanoDropTM spectrophotometer. Extinction coefficients (ε) calculated by the ExPASy ProtParam tool (<https://web.expasy.org/protparam/>) were 25900 M⁻¹ cm⁻¹ for FdR_{J1} and 7450 M⁻¹ cm⁻¹ for Fdx_J. These values were calculated based on the amino acid compositions of the proteins [60]. Calculated molecular masses were 37224 Da for FdR_{J1} and 10200

Da for Fdx_{J1} (with 6xHis-tag). The proteins were frozen in liquid nitrogen and stored at -20 °C until further use.

2.7 Homology model generation

Homology models of Fdx_J, FdR_{J1} and P450_{Jα} were generated using the SWISS-MODEL bioinformatics web-server tool (<https://swissmodel.expasy.org/interactive>).

For the FdR_{J1} and P450_{Jα} models, the protein sequences were uploaded to the web-server as target sequence files in FASTA format. The same was done with Fdx_J sequence. Templates with highest similarities were provided with the resulting model. The template with highest sequence identity/homology generated for Fdx_J was *Bacillus thermoproteolyticus* ferredoxin (PDB ID 1WTF; UniProt accession nr. P10245) (79% sequence identity), containing a Fe₃S₄-cluster. As this was unexpected from the sequence pattern containing a prototypical Cys-triplet run Cys-XX-Cys-X-X-Cys close to the N terminus of the polypeptide chain and a fourth Cys residue near the C terminus (part of Cys-Pro-Tyr fragment)(figure 11), a new modeling strategy was followed [61]. A PDB file of the same *Bacillus thermoproteolyticus* ferredoxin containing a Fe₄S₄-cluster (PDB ID 1IQZ) was uploaded as a template for the model generated using the target sequence. The outcome was a PDB file of a model structure containing a Fe₄S₄-cluster.

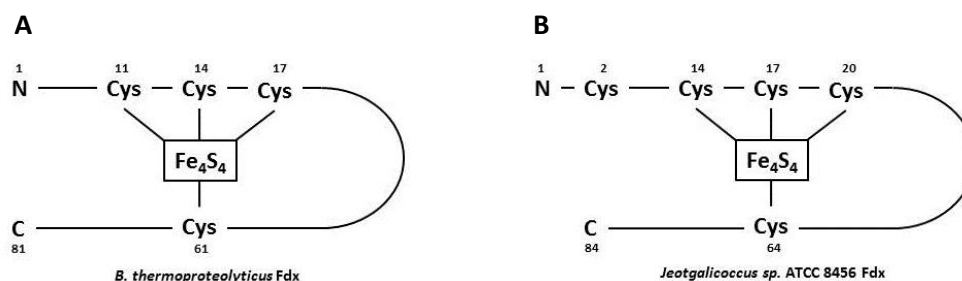


Figure 11 Scheme of the Fe₄-S₄-cluster, coordinated by 4 cysteine-residues, in *Bacillus thermoproteolyticus* ferredoxin (A) [61] and in *Jeotgalicoccus* sp. ATCC8456 (B). Figure A was redrawn from Holm *et al.* and modified. It shows a possible constellation of the Fe-S cluster in *Jeotgalicoccus* sp. ATCC8456.

2.8 Quantitative determination of product formation with GC-MS analysis

2.8.1 Two-phase solvent extraction and derivatization of analytes for GC-MS

Reaction products from the conversions of fatty acid substrates with both P450s were analyzed by gas chromatography coupled with a mass spectrometer (GC-MS) for product identification. Therefore, reactions were acidified by adding 0.1% (v/v) of 5 M HCl. Then, a two-phase solvent

extraction was performed using ethylacetate as the extractant. This solvent was applied due to easy handling and environmental preferableness [62]. A defined amount (0.1% (v/v)) of an internal standard (1-octanol) was added to the extractant and was later used to normalize the quantity of the products and remaining substrate. The organic solvent was given to the reaction mixture in a ratio of 0.3/1 and after thoroughly shaking the mixtures (2 min, RT), the samples were centrifuged (2 min at 4°C and 16.1 x 1000 g) and the supernatant dried over Na₂SO₄ (anhydrous) to eliminate any residual water from the organic phase. Another centrifugation step (1 min) followed to settle Na₂SO₄.

Trimethylsilyl-diazomethane is a reagent with which one can prepare methylated fatty acids in a simple and fast manner at room temperature [63]. Reaction samples were methylated to volatilize remaining substrate and reaction products (hydroxyl fatty acids) for GC-MS analysis. Extracted samples (120 µL) and MeOH (60 µL) were pipetted into glass vials containing 200 µL inlets. Then 10 µL of trimethylsilyl-diazomethane (6 M in hexane) were added, mixed by pipetting, and the vials were closed rapidly.

2.8.2 GC-MS analysis

To analyze substrate depletion and product formation, derivatized samples were analyzed with GC-MS, using liquid injection (injection volume 1 µL, split 50:1, injection temperature 250 °C). The GC-system used was an Agilent Technologies 7890B GC System and analytes were detected with a 5977A mass spectrometer detector. An Agilent HP-5MS column (30 m x 320 µm, 0.25 µm film) and helium as carrier gas were used as stationary and mobile phase, respectively. Heating rate was set to 20 °C/min to reach a final temperature of 320 °C (holding time 5 min). Solvent cut-off was at 3 min. The peaks were analyzed qualitatively with the provided database (NIST) and compared to analytical standards. Quantification was done for 1-tridecene, based on a calibration with the commercial standard. An exemplary gas chromatogram of a C14:0 FA conversion to 1-tridecene and a decay spectrum of this 1-alkene are shown in figure 12.

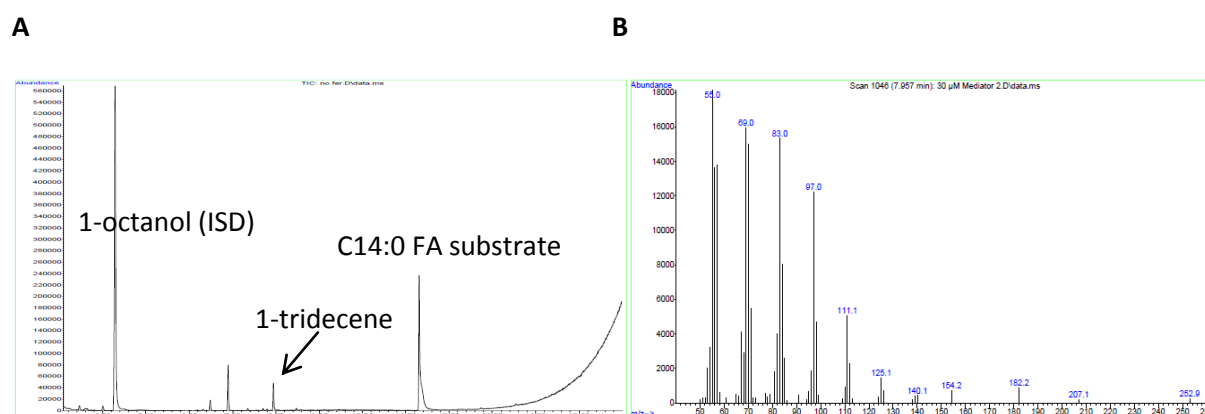


Figure 12 (A): GC-MS chromatogram of conversion of C14:0 FA to 1-tridecene. Internal standard (ISD): 0.1% (v/v) 1-octanol. (B): Decay spectrum of 1-tridecene.

2.9 Characterization of the FdR_{J1}-Fdx_J-OleT redox chain

2.9.1 Hexacyanoferrat assay for characterization of the reductase activity

The ability of the ferredoxin reductase to oxidize NADPH and NADH was examined by analyzing electron transfer to the small electron acceptor molecule Fe(CN)₆³⁻ (the potassium salt of the ferricyanide was used) [64][65]. Another aim of this experiment was to evaluate the cofactor preference of FdR_{J1}. Therefore, mixtures of 1 mL KPi (100 mM, pH 7.5, 300 mM KCl) containing glycerol (20% v/v), K₃[Fe(CN)₆] (1 mM), FdR_{J1} (1 μM for NADPH oxidation or 5 μM for NADH oxidation) and NAD(P)H (400 μM) were assembled. Reactions were done in triplicates and once for each cofactor without FdR_{J1} for control. Detailed reaction assembly compositions are described in table 17.

The reactions were blanked before adding NAD(P)H and decrease in absorbance was monitored spectrophotometrically over time ($E_{420} = 1.04 \text{ mM}^{-1} \text{ cm}^{-1}$).

Table 17 Reactions for hexacyanoferrat assay. Reactions were prepared for both cofactors (NADPH and NADH) in triplicates and controls were prepared as single reactions, omitting the reductase.

Dialysis buffer [μL]	FdR _{J1} (0.598 mM stock) [μL]	K ₃ [Fe(CN) ₆] (20 mM stock) [μL]	NADPH (20 mM stock) [μL]	NADH (20 mM stock) [μL]
930	1.7	50	20	-
930	-	50	20	-
930	8.5	50	-	20
930	-	50	-	20

2.9.2 Cytochrome *c* assay for analysis of electron transfer by Fdx_J

Cytochrome *c* (cyt *c*) reduction was measured to examine electron transfer from NADH or NADPH via FdR_{J1} and Fdx_J to cyt *c* (containing a heme-prosthetic group). This method was described before by Lacour *et al.* and Schallmeyer *et al.* [66][67]. Electrons can be transferred to cyt *c* from the reductase via the ferredoxin [67]. Varying amounts of Fdx_J were applied to determine kinetic parameters (K_M and v_{max}) for reduction of Fdx_J by FdR_{J1}. Enzymatic activity was determined by increase of absorption at 550 nm as reduced cyt *c* absorbs this wavelength. Reaction mixtures were assembled with a final reaction volume of 1 mL (KPi 100 mM, pH 7.5, 300 mM KCl). The reactions contained glycerol (20% v/v), FdR_{J1} (1 μM), Fdx_J (in varying amounts from 0.25 – 130 μM), cyt *c* (20.3 μM or 40.6 μM) and NAD(P)H (200 μM). All reactions were done in duplicates (for 100 μM and 130 μM Fdx_J in triplicates) at room temperature without shaking. All constituents of the reaction mixtures were mixed thoroughly by pipetting and the cofactor was added as last component of the mixtures.

To obtain evidence that all constituents of the electron transfer chain are essential for its functionality and that the transfer works as proposed, control reactions were prepared. Therefore, each component of the electron transfer chain was left out in one of the reactions: (NAD(P)H), FdR₁₁, Fdx_j and cyt *c*. One reaction was prepared with NADH instead of NADPH, to see the difference in cyt *c* reduction velocity between both cofactors.

Time-dependent increase of absorbance caused by reduction of cyt *c* was measured spectrophotometrically (ϵ_{550} of reduced cyt *c* = 28.0 mM⁻¹ cm⁻¹). Reactions were blanked before adding NAD(P)H.

2.9.3 Determination of NAD(P) oxidation rates with the FdR₁₁-Fdx_j-OleT system

Cofactor oxidation was measured when the FdR₁₁-Fdx_j-OleT system was used to convert C14:0 FA.

Mixtures of 1 mL total volume were therefore assembled in KPi 100 mM pH 7.5, containing 300 mM KCl and 20% glycerol, 200 μ M NAD(P)H, 400 μ M C14:0 FA (final 2.5 % (v/v) EtOH in the reaction), 1 μ M OleT and 15 μ M Fdx_j. Reactions were done in triplicates for each cofactor and once for each control. Controls were prepared, leaving out each component of the electron transfer chain in one reaction: NAD(P)H, FdR₁₁, Fdx_j, OleT, substrate and substrate in EtOH. One reaction with 100 μ M ferredoxin was prepared as well. The cofactor oxidation was measured spectrophotometrically as absorbance decrease at 340 nm.

2.9.4 Dependence of catalytic activity and selectivity of OleT on Fdx_j concentration

The influence of Fdx_j concentration on catalytic activity and selectivity of the electron transfer chain was examined. All electron transfer chain components, NAD(P)H, OleT and C14:0 FA substrate were assembled. After 24 h all NAD(P)H was depleted, also in absence of the transfer chain, according to a previous experiment in which extinction decrease at 340 nm was measured. A certain amount of electrons is uncoupled from the proposed transfer pathway by reducing dissolved oxygen to O₂⁻ which can then be further reduced to H₂O₂ which has a limited stability in water. Because of this loss of electrons they will not be transferred via the chain to OleT. This explains why the amount of product that is formed will be lower than the amount of NAD(P)H that is oxidized. To see how the concentration of Fdx_j influences the quality of electron transfer and product formation by OleT, this experiment was conducted. Reactions were assembled in a final reaction volume of 1 mL (KPi 100 mM, pH 7.5, 300 mM KCl, glycerol (20% v/v)). The reactions contained FdR₁₁ (1 μ M), Fdx_j (in varying amounts from 0.25 to 130 μ M), OleT (1 μ M), NAD(P)H (400 μ M) and C14:0 FA (400 μ M in a final 2.5 % (v/v) EtOH concentration). All reactions were done in duplicates at room temperature. Control reactions omitting each component of the transfer chain were prepared as well to see how much electrons are not coupled to product formation by OleT. Controls contained 15 μ M Fdx_j. Reactions

with NADPH and NADH and all chain components were prepared in triplicate, all other controls in single reactions (without cofactor, FdR_{J1}, Fdx_J, OleT or substrate). An overview of the reactions is shown in table 18.

Table 18 Reactions and control reactions for conversion of C14:0 FA substrate by OleT.

	NAD(P)H [μM]	FdR _{J1} [μM]	Fdx _J [μM]	OleT [μM]	C14:0 FA [μM]
NADPH	400	1	15	1	400
NADH	400	1	15	1	400
No Cofactor	0	1	15	1	400
No FdR	400	0	15	1	400
no Fdx	400	1	0	1	400
No OleT	400	1	15	0	400
No FA	400	1	15	1	0

2.9.5 Quantification of enzymatically produced H₂O₂

H₂O₂ formation had to be determined to detect the amount of electrons that leave the electron transfer chain to form H₂O₂ by reduction of oxygen to O₂⁻. Except for recognizing that addition of catalase to reactions has some effect on substrate conversion, this phenomenon has not been shown in detail for any of the systems characterized so far (table 1) and origin of the oxidant will have to be investigated in more detail. H₂O₂ can either decompose in the reaction solution or it can return and activate OleT via the peroxide shunt pathway.

For quantification of H₂O₂, a calibration curve was prepared using defined concentrations of peroxide that range from 20 to 200 μM in the coupling assay. Therefore, a standard 1 ml reaction mixture containing 900 μL of buffer (KPi 100 mM, pH 7.5, 300 mM KCl, 20% (v/v) glycerol), 50 μL of 15 mM 4-AAP (4-aminoantipyrine), 25 μL HRP (horseradish peroxidase) from a 600 U mL⁻¹ stock and 25 μL guaiacol from a 900 μM stock, was assembled in a cuvette. The mixture was blanked at 509 nm and H₂O₂ was added to a concentration of 20 μM in 0.5 ml from a 16 mM stock. After an incubation time of 2 min, the absorbance at 509 nm was noted and the amount of H₂O₂ increased stepwise (see table 19). The formation of the reaction product (quinoneimine dye) was measured at 509 nm and a calibration curve was established by applying absorbance values against H₂O₂ concentrations (figure 14).

Guaiacol is enzymatically oxidized in the presence of hydrogen peroxide by HRP, so that a phenyl radical is produced. The radical reacts with 4-aminoantipyrine (4-AAP) to form a red quinoneimine-dye that has a strong absorbance at 509 nm [68][69]. A scheme of this reaction is shown in figure 13.

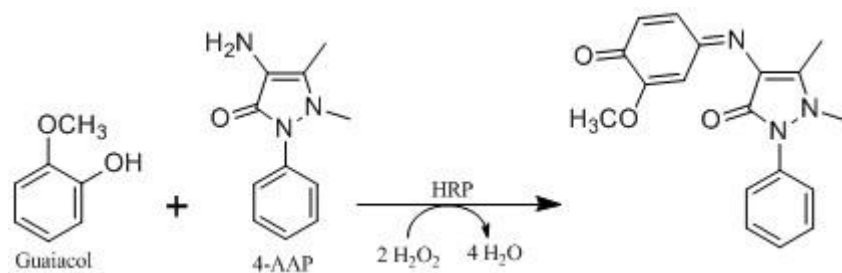


Figure 13 Quinoneimine formation from guaiacol and 4-aminoantipyrine (4-AAP). The figure was redrawn and adapted from Córdoba *et al.* (2015) [70].

Table 19 Quinoneimine dye (measured as absorbance at 509 nm) formed in dependence of H₂O₂ concentration.

$\mu\text{M H}_2\text{O}_2$	Abs [509 nm]
20	0.15
40	0.26
60	0.41
80	0.68
100	0.87
120	1.01
160	1.23
200	1.48

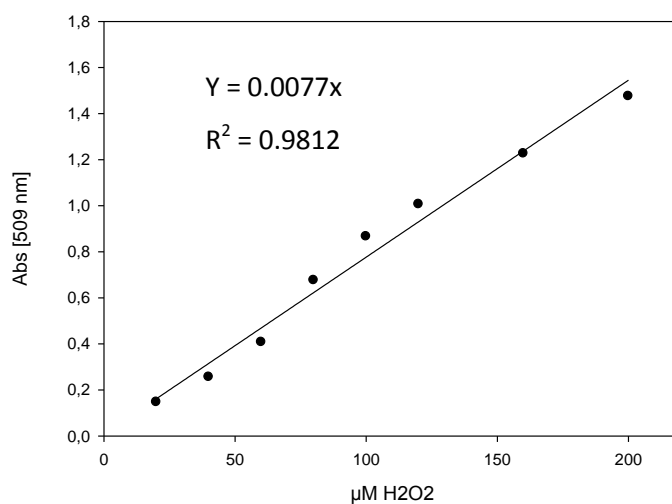


Figure 14 Calibration curve H₂O₂ concentration. Absorbance of the formed quinone-imine dye at 509 nm is applied against the employed peroxide concentration.

After establishing a linear calibration for quantification of H_2O_2 , H_2O_2 released by the FdR_{11} - Fdx_j - OleT system was determined with end-point measurements using the HRP-assay setup described above. Standard 1ml reactions (KPi 100 mM, pH 7.5, 300 mM KCl, 20 % glycerol) containing 2 μM FdR_{11} , 30 μM Fdx_j or 0 μM Fdx_j and 400 μM NADPH were assembled in cuvettes. NADPH depletion was measured at 340 nm on a spectrophotometer. Both reactions ran for the same period of time, until all NADPH was consumed. Then, 500 μL of each reaction were mixed with 400 μL buffer, 50 μL 4-AAP, 25 μL of 600 U/mL HRP and 25 μL of 900 μM guaiacol. After short incubation time, quinoneimine dye concentrations were measured at 509 nm. The measured absorbance was used to calculate H_2O_2 concentration in the reaction samples.

2.9.6 Catalase study

Reactions containing varying amounts of catalase were assembled to see if and at which positions during the electron transfer H_2O_2 is formed. H_2O_2 formation occurs due to electrons leaving the electron transport chain. Catalase oxidizes H_2O_2 and thereby scavenges leaving electrons to prevent them from being retrieved into the enzyme catalytic cycle via the peroxide shunt pathway. As the electrons that are uncoupled cannot reach the P450 enzyme to activate oxygen, product formation will be decreased due to this phenomenon. H_2O_2 formation was determined based on the amount of product (1-tridecene) that was analyzed in GC-MS analysis of the reactions containing varying amounts of catalase.

For this study, 500 μl reactions (KPi 100 mM, pH 7.5, 300 mM KCl, 20 % glycerol) containing 1 μM FdR , 30 μM Fdx , 1 μM OleT , 400 μM NADPH and 400 μM C14:0 FA were assembled. Catalase was added in amounts of 0 to 5000 U mL^{-1} to the reactions that were prepared in triplicates. In a further reaction, chicken egg white serum albumin (0.025 mg) was added to exclude the possibility that the high catalase protein load interferes with the electron transfer and to see that the catalytic activity of the catalase removes the H_2O_2 . Reactions were run at room temperature overnight. Substrate conversion and product formation was determined by GC-MS analysis.

2.10 Influence of NADPH and substrate concentration on conversion

In this experiment the influence of NADPH and C14:0 FA concentration on conversion with the FdR_{11} - Fdx_j - OleT system was examined. Therefore, concentrations of NADPH and C14:0 FA substrate were varied from 200 to 10000 μM and thereby always kept at equimolar ratio. The reactions contained 1 μM FdR_{11} , 30 μM Fdx_j , 1 μM OleT and the respective amount of FA and NADPH. Reaction time was calculated based on NADPH oxidation rates at a C14:0 FA concentration of 400 μM (0.225 μmol μmol^{-1} min^{-1}). Therefore, assuming a linear and full oxidation of 10 mM FA/NADPH, the applied reaction time was 37.5 h. Reactions were run at 37 °C.

2.11 Substrate screening and NAD(P)H oxidation rate determination for the novel peroxygenase P450_{Jα}

2.11.1 Substrate screening

To see whether P450_{Jα} accepts fatty acids as substrate and peroxide as oxidant and if so, to see which products are formed, the following experiment was conducted. Selected FA substrates were investigated for conversion, namely C10:0, C12:0, C13:0, C15:0, C16:0 and C18:0. 1 mL reaction mixtures were assembled, containing P450_{Jα} (3 μM), H₂O₂ (1 mM added in portions of 0.2 mM H₂O₂ 30 min⁻¹) and FA (1 mM) in reaction buffer (KPi pH 7.25 with 20% (v/v) glycerol). Fatty acids were prepared in 100 mM stocks to have a final EtOH concentration of 1% (v/v) in the reaction vial. Reactions were run at 20°C and 650 rpm for 2.5 h. As controls reactions without FA and a reaction without H₂O₂ were prepared. Products and substrate conversion were determined with GC-MS as described above.

2.11.2 NAD(P)H oxidation rate determination with new redox transfer chain – comparison OleT and P450_{Jα}

To see whether the FdR_{J1}-Fdx_J system transfers electrons from the cofactor NAD(P)H to OleT and/or P450_{Jα}, the following experiment was conducted. Oxidation of NAD(P)H was measured with FdR_{J1} and Fdx_J coupled with the two P450s (P450_{Jα} or OleT), respectively. 1 mL reactions contained 200 μM NAD(P)H, 1 μM reductase, 2 μM ferredoxin, 1 μM P450 (OleT or P450_{Jα}) and 200 μM C12:0 FA substrate in buffer C. Cofactor oxidation was measured spectrophotometrically over time by measuring absorbance decrease at 340 nm.

3 Results and Discussion

3.1 Purification of OleT and putative electron mediator from *Jeotgalicoccus sp.* ATCC8456

After ammonium sulfate precipitation of the proteins obtained from the original host *Jeotgalicoccus sp.* ATCC 8456, OleT and co-eluting proteins were purified by cation exchange chromatography. A purification profile (UV, conductivity, pH, pressure, temperature, concentration Buffer B (NaCl)) was recorded using the Äkta system. UV-measurement (254 and 280 nm) was used to detect proteins at the outflow. A small elution peak was obtained, as described before by Rude *et al.*, between 600 and 750 mM NaCl [11]. The peak is depicted in figure 15. The SDS-gel of eluted, pooled and dialyzed fractions is shown in figure 16. Bands corresponding to the molecular mass of 55 kDa (OleT has ~50 kDa) and to the band co-isolated also by Rude *et al.* (2010) could be found in the putative active fractions.

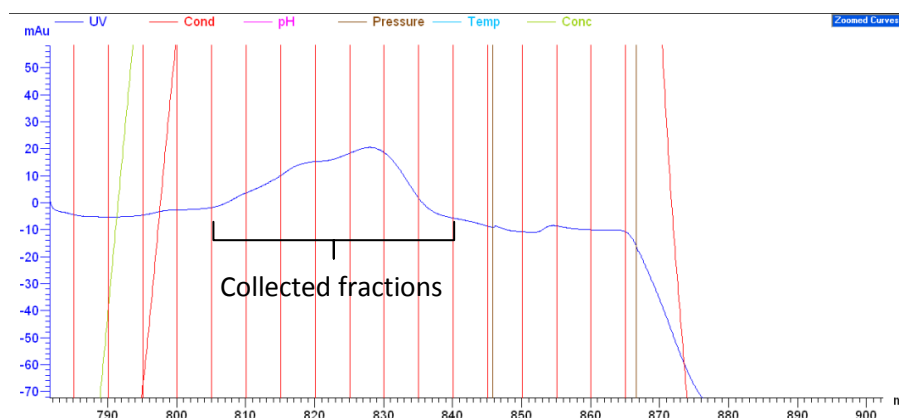


Figure 15 Elution of fractions containing OleT and the prospective mediator protein at [NaCl] = 600-750 mM.

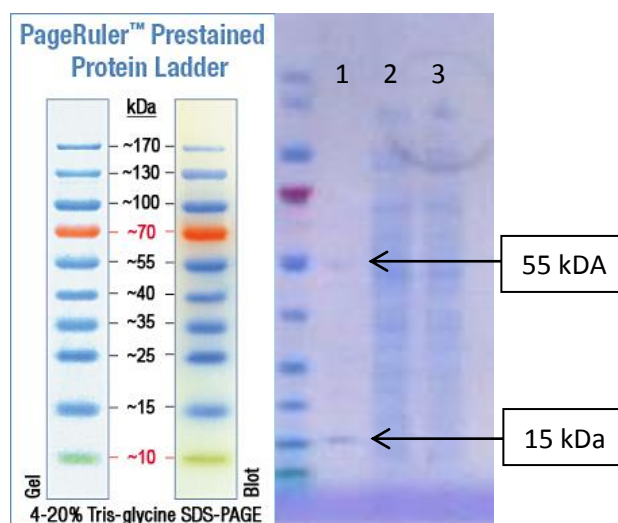


Figure 16 SDS-PAGE of fractions indicated in Figure 17. 0,05% of the active fractions have been loaded in lane 1, 2 and 3. A 55 kDa band (probably OleT) and the putative electron mediator (~15 kDa) are highlighted by arrows.

Fatty acid decarboxylase activity was analyzed after protein purification. Reactions with partially purified proteins were supplemented with H_2O_2 and stearic acid. The only fraction revealing decarboxylation activity corresponds to the one containing OleT according to SDS-PAGE (see figure 16, lane 1). All other fractions did not show any traces of the respective olefin. GC-MS chromatograms of the fraction that potentially contains OleT and putative electron mediator are shown in figure 17.

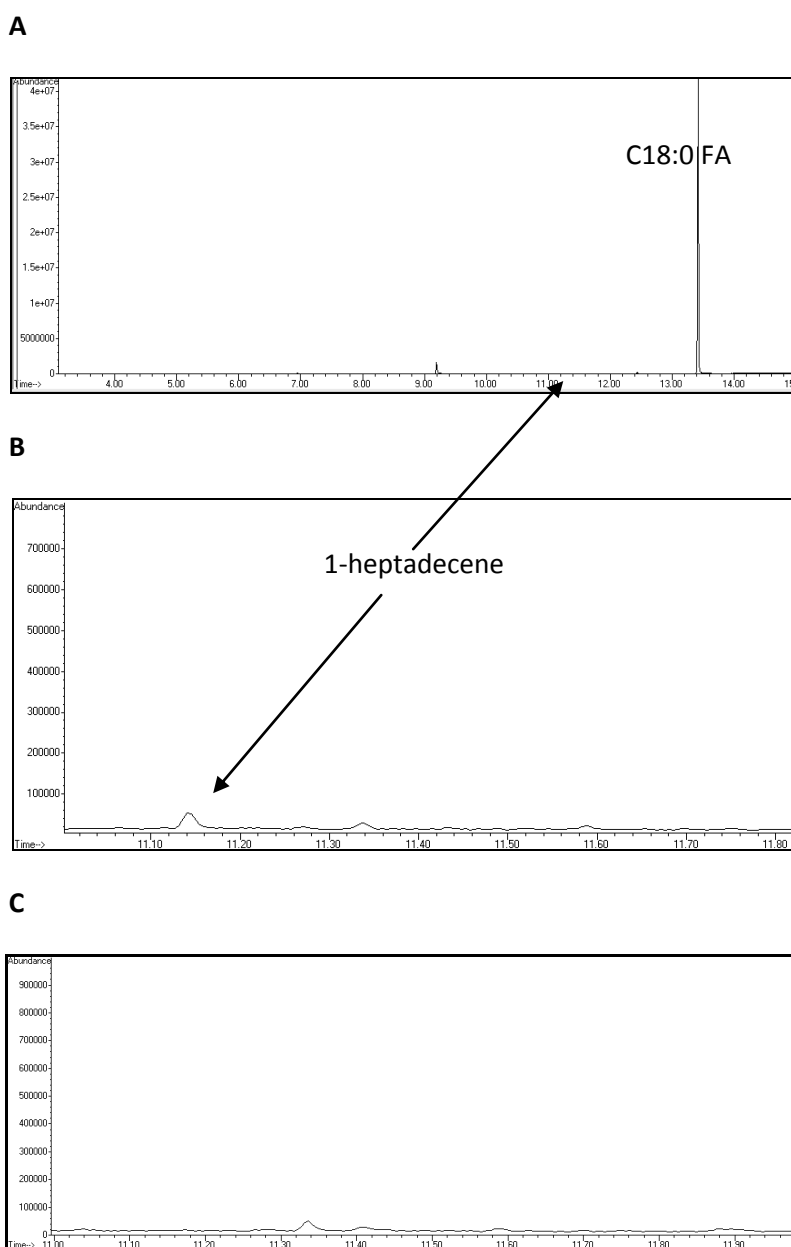


Figure 17 GC-MS analysis after conversion of C18:0 with a fraction containing partially purified OleT and the putative mediator-containing (cation exchanger purified protein). The entire chromatogram (A) and a close-up of the product peak (1-heptadecene) (B) are shown. The GC-MS spectrum of 1-heptadecene is shown in section 5.5 (figure 60). The supernatant after precipitation with 65% $(NH_4)_2SO_4$ (C) showed no decarboxylation activity on C18:0 FA substrate.

The ability to catalyze decarboxylation of stearic acid (C18:0) to 1-heptadecene confirmed the presence of OleT. Since only this fraction revealed decarboxylation activity, it can be assumed that none or only negligible amounts of enzyme were lost during all purification steps or catalases inhibited activity of OleT in other fractions.

The 15 kDa band from the fraction that contains OleT was excised from the SDS gel and subjected to LC-MS/MS analysis. The analysis of the 15 kDa band resulted in 72 hits to proteins encoded in the *Jeotgalicoccus* ATCC8456 genome. Among the top-hits also serum albumin and keratins can be found. Several proteins of about 15 kDa were reported, none which was assigned to a protein with electron transfer function. Therefore, it was concluded that a possible electron mediator does not co-elutes with OleT during purification. Peptide spectrum matches (PSMs) were especially high for some of the human proteins and for prokaryotic ribosomal proteins (high PSM values = high number of detected MS2 spectra). PSM are the total number of identified sequences for a respective protein, including those sequences that are redundantly identified. 50 proteins scored a PMS below 100, 42 candidates were 10 and lower.

The percent coverage is calculated by dividing the number of amino acids in the respective protein by the number of all single amino acids that were found in the whole sample (the higher, the better is the coverage). Even though there are several sequences with coverages as high as 30% or even higher, none of the annotations indicated presence of a potential electron mediator (Fdx, FdR, flavodoxin) [71] for a cytochrome P450 enzyme. The reverse genetic approach to isolate a potential mediator via co-elution was therefore not successful. The purification protocol by Rude *et al.* for the isolation of OleT might require some revision as stated in material methods section. Isolation of electron transfer proteins based on genomic data search was the next step to find a natural electron transfer chain for OleT. Therefore, the *Jeotgalicoccus sp.* ATCC8456 genome was sequenced and the contained open reading frames (ORFs) were annotated.

The TU Graz Institute of Environmental Biotechnology was responsible for sequencing and annotating the genome from *Jeotgalicoccus sp.* ATCC8456. Several known electron mediators were chosen for a protein BLAST search in the genome. Proteins selected for protein BLAST were the flavoprotein putidaredoxin reductase CamA (UniProt accession nr. P16640) from *Pseudomonas putida* and its redox partner, the 2Fe-2S ferredoxin-type CamB (P00259). Further, the flavodoxin- and ferredoxin-NADP reductase (fpr) (P28861) from *E. coli* (strain K12) and its 2Fe-2S ferredoxin partner (P0A9R4) were used for BLAST search. Besides class-I bacterial electron transfer system templates for protein BLAST, also the low-potential flavodoxin 1 (fldA) from *E. coli* K1 (P61949) was used (class III bacterial system). These systems were chosen as they are typical and well described bacterial electron transport systems. They are easily accessible and have been successfully used with

OleT beforehand. The CamAB as well as the *E. coli* Fld/FdR systems have been successfully tested in combination with OleT before [35][34][37].

Resulting alignments were also given as HSPs (high-scoring segment pairs), displaying not the whole sequence but only sections of high similarity in a heuristic alignment approach. CamA scored an identity of 24% to HSP 1 from a gene annotated as Ferredoxin-NADP reductase (BASYS01288). Further, it scored an identity of 23% to HSP 1 from a second gene annotated as Ferredoxin-NADP reductase (BASYS02089). Identity (%) corresponds to the number of identical residues in the query and subject sequences. These two hits show that the two genes in the genome that are annotated as ferredoxin reductases have some similarity to the already known ferredoxin-NADP reductase CamA (P16640) that transfers electrons to the ferredoxin CamB. CamA from *Pseudomonas putida* is a NAD(P)H-dependent FAD-containing reductase which is able to transfer electrons to the [2Fe-2S]-containing ferredoxin CamB. CamB in turn supplies the electrons to CamC, a P450 monooxygenase that is able to hydroxylate camphor [72][73]. The fact that CamA is NADH-dependent affirms its function in D-camphor metabolism (catabolic pathway) [74]. In contrast, NADPH-dependent reactions typically are involved in anabolic pathways [75]. In case NADPH-dependency of the reductase being involved in electron transfer to OleT will be confirmed, this will support the idea that 1-alkenes could function as secondary metabolites and that fatty acid decarboxylation might not be involved in degradation processes. All other BLAST searches did not lead to results obviously giving hints to possible electron transport proteins.

In a second approach the genome was manually searched for possible class I and class III electron transfer candidates. One single ferredoxin gene (BASYS00361) that could complement the two ferredoxin reductase genes was found by protein BLAST. Overall, the combination of the identified proteins would resemble a class I bacterial electron transfer system [18]. Having those three highly promising candidates identified, search was continued to see whether further electron transfer proteins can be found in the genome. Altogether 8 candidates were identified according to electron transfer motifs such as Fe-S clusters or flavodoxins. Of these 10 candidates, we initially focused on the three aforementioned (Fdx₁, FdR₁₁ and FdR₁₂). Besides electron transfer proteins, a second gene annotated as cytochrome P450 fatty-acid peroxygenase (cypC) was identified in the *Jeotgalicoccus* sp. ATCC8456 genome. This gene was also isolated to serve as a second enzyme to test in combination with electron transfer proteins. In table 20, all genes, that were identified for their isolation are listed and described.

Table 20 Genes isolated from the *Jeotgalicoccus sp.* ATCC8456 genome and their expression products.

Entry	Name	Annotation (ORF)	Automatically Annotated as:	Number of amino acids [aa]	Size [kDA]	Closest characterized homologue [%] (with uniprot accession numbers)	Family specific structural motifs
1	Fdx ₁	BASYS00361	Ferredoxin [H]	84	9.1	Bacillus thermoproteolyticus Fdx (P10245) [76]; 79% identity	[Fe4-S4] cluster
2	FdR ₁₁	BASYS01288	Ferredoxin-NADP-reductase [H], trxB [C]	329	36.2	Ferredoxin/flavodoxin NADP+ oxidoreductase 2 (FNR2) from Bacillus cereus (Q816D9) [77]; 49% identity	Flavin
3	FdR ₁₂	BASYS02089	Ferredoxin-NADP-reductase 1 [H], trxB [C]	344	37.7	ferredoxin/flavodoxin NADP+ oxidoreductase 1 (FNR1) from Bacillus cereus (Q81IK1) [77]; 44% identity	Flavin
4	P450 _{1α}	BASYS00261	Fatty-acid peroxygenase [H]	416	48.3	CYP152N1 (C4L2G9) [78]; 48% identity	Heme thiolate

3.1.1 Cloning of the selected genes into pET28a(+) and transformation into *E. coli* strains

Jeotgalicoccus sp. ATCC8456 is a Gram-positive bacterium with a cell wall containing a thick peptidoglycan layer that requires efficient cell disruption to access the genomic DNA before cPCR. Three approaches have been tried for isolation of genomic DNA. They are described under 2.4.3 and with each of the three applied protocols the genomic DNA could be isolated from the bacterial cells in sufficient amount (10-200 ng/μL) and purity. The genomic DNA isolated by the nexttec kit (recommended isolation protocol) was used for further work. In figure 18, PCR of the new P450_{1α} is shown.

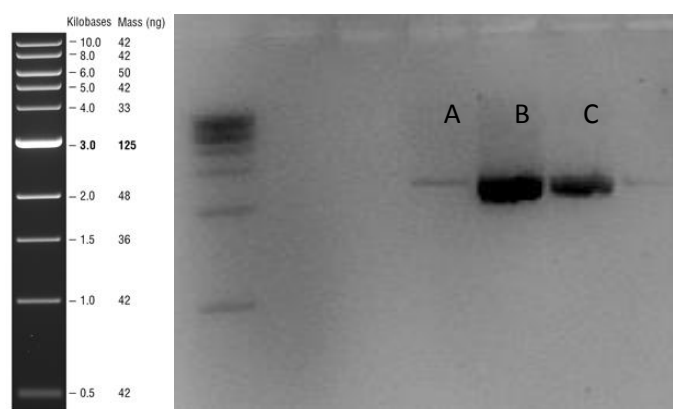


Figure 18 The P450_{1α} gene fragments (expected size was 1.25 kb) produced by cPCR were run on a 1% agarose gel. Genomic DNA templates were isolated from *Jeotgalicoccus sp.* ATCC8456 cells in three different ways, resulting in different amounts of cPCR products. Templates for cPCRs were obtained by three different methods described in the material and methods section (2.4.3) The applied strategies were A) a single colony breakup. B) frozen cell pellet dispersion and cell break up. C) treating a frozen cell pellet with nexttec™ genomic DNA isolation kit. As standard, the GeneRuler™ NEB 1 kb DNA ladder was run on the agarose gel.

The cPCR control gel for the amplification of the 10 selected genes for possible electron transfer proteins (figure 19) shows, that all genes were amplified successfully and could be obtained in sufficient amount to continue with cloning.

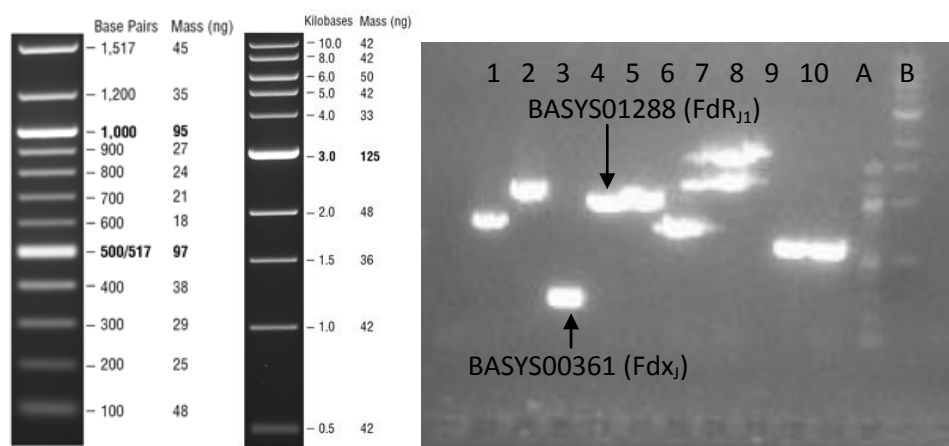


Figure 19 PCR amplification of genes encoding for possible electron transfer proteins was confirmed with agarose gel electrophoresis. The electrophoresis was done in 1% agarose gel (lane 3: Fdx_j, lane 4: FdR_{j1}, lane 5: FdR_{j2}). As standards, the GeneRuler™ NEB 100 bp DNA Ladder (A, left), and the GeneRuler™ NEB 10 kb DNA Ladder (B, right) were used.

As only the proteins Fdx_j, FdR_{j1} and P450_{jα} were tested in the further course of the project, cloning work will be described only for their corresponding genes. After restriction of PCR products, DNA was eluted with 30 μL H₂O from the GeneJet PCR purification column in concentrations of 23.2 ng/μL (Fdx_j), 23.5 ng/μL (FdR_{j1}) and 6.65 ng/μL (P450_{jα}). Digested vectors were obtained in concentrations of 23.9 ng/μL for the redox proteins (pET28a cut with NdeI and XhoI) and 3.36 ng/μL for cloning of the new cytochrome P450 gene (pET28a cut with XhoI and NcoI). After ligation and another purification with the GeneJet PCR purification kit (elution with 20 μL H₂O), concentrations of 16.2 ng/μL (Fdx_j), 12.1 ng/μL (FdR_{j1}) and 6.62 ng/μL (P450_{jα}) were recovered. Empty vectors for religation control were obtained in concentrations of 11 ng/μL (pET28a cut with NdeI and XhoI) and 7.4 ng/μL (pET28a cut with XhoI and NcoI). After ligation, the constructs were transformed into *E. coli* TOP10 cells. Cells were recovered in SOC medium, plated on agar plates containing kanamycin and incubated overnight. Counting of the colonies gave the numbers shown in table 21. The possibly re-ligated vectors were also transformed and gave 24 colonies.

Table 21 Cloning statistics.

Clone	Number of clones on "ligation" plate	Number of clones on "religation" control plate
Fdx _j	76	24
FdR _{j1}	115	24
P450 _{jα}	195	142

Maps of the vector with in-frame cloned protein sequences of Fdx_γ and P450_α are shown in figures 20 and 21.

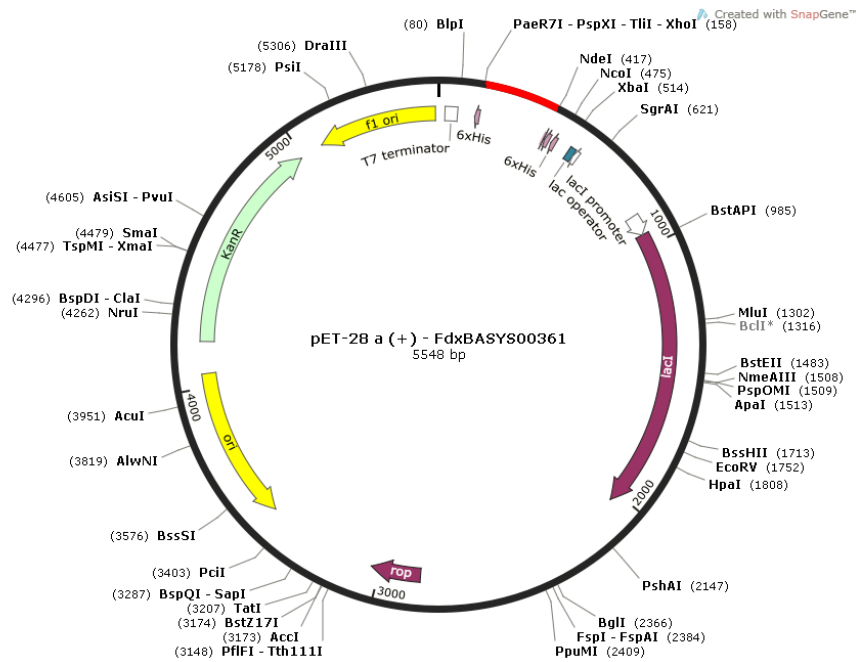


Figure 20 Vector map of pET-28a(+) containing Fdx_γ (shown in red) cloned into the multiple-cloning site (MCS) in-frame of an N-terminal His-tag . Restriction sites for NdeI and XhoI were used for cloning. The vector map was created with the SnapGene® software.

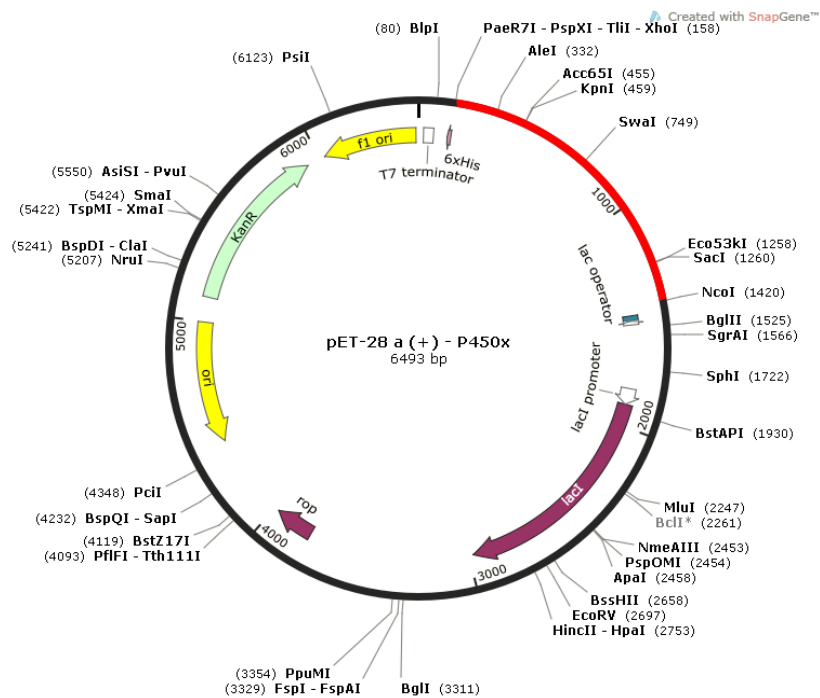


Figure 21 Vector map of pET-28a(+) containing P450_α (shown in red) cloned into the multiple-cloning site (MCS) in-frame of an N-terminal His-tag . Restriction sites for XhoI and NcoI were used for cloning. The vector map was created with the SnapGene® software.

Ten clones were picked, respectively, and cPCR was done using “T7 primer pairs” (T7prom: TAATACGACTCACTATAGG; T7term: GCTAGTTATTGCTCAGCGG). After cPCR, an agarose gel electrophoresis was performed for control of cloning success. The figures 22 and 23 show that amplification of Fdx_j and FdR_{j1} was successful for one of the ten picked clones, respectively. For clone 8 of the ones that should contain the gene fragment for FdR_{j1} and clone 2 of those that should contain the gene fragment for Fdx_j , bands of the correct size were present. The positive result in this case implies positive cloning and cPCR. Previous statistical analysis shows that restriction with both enzymes was not complete. A relatively high portion of vectors were able to re-ligate, which means that only one or no restriction enzyme has cut the original plasmids and that the religation was successful. For most of the clones that were picked, control cPCR was not successful, which can be seen on the agarose gel as no amplified fragment can be detected in this case. For $P450_{J\alpha}$, 20 clones were picked whereof 5 showed a positive band on the gel (figure 24).

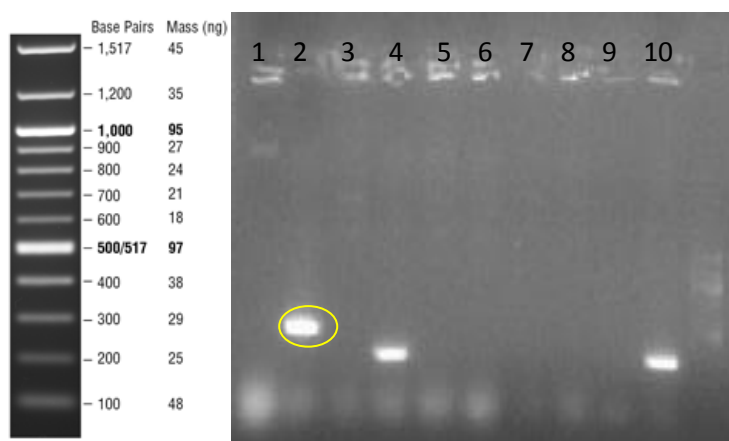


Figure 22 Control gel of cPCR reactions with *E. coli* BL21(DE3) transformed with pET28a(+) to identify presence of Fdx_j . In clone 2, presence of Fdx_j was confirmed by its successful amplification.

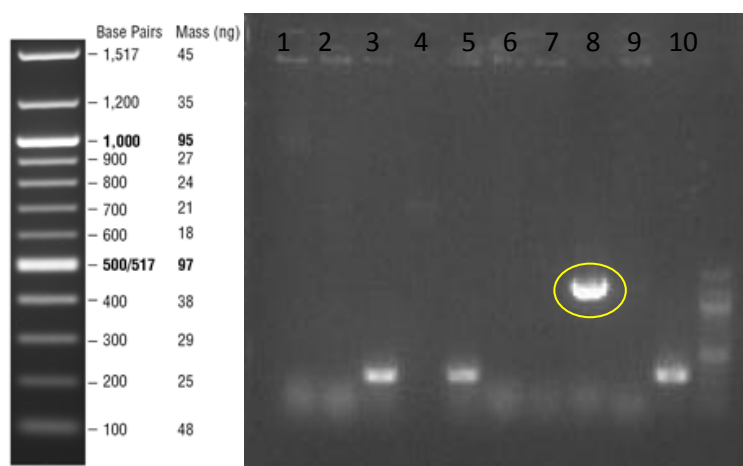


Figure 23 Control gel of cPCR reactions with *E. coli* BL21(DE3) transformed with pET28a(+) to identify presence of FdR_{j1} . In clone 8, presence of FdR_{j1} was confirmed by its successful amplification.

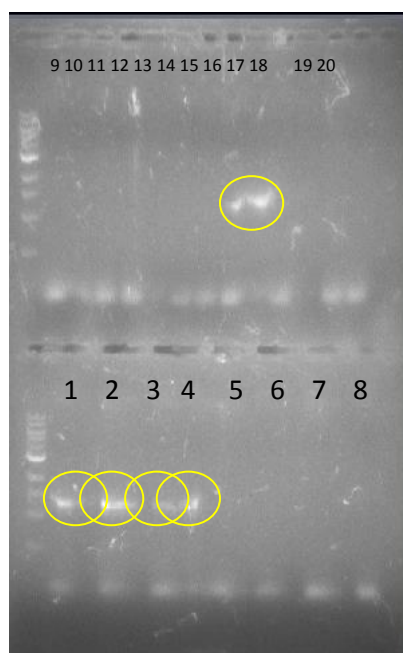


Figure 24 Control gel of cPCR reactions with *E. coli* BL21(DE3) transformed with pET28a(+) to identify presence of P450_{Jα}. In clones 1, 2, 3, 4 and 17, presence of P450_{Jα} was confirmed by their successful amplification. Clone 17 was used for further work.

The Fdx_J gene was cloned successfully and sequencing showed that the cloned fragment did not contain any mutation. The FdR_{J1} gene fragment contained one silent mutation of an adenosine base into a guanine base. The threonine amino acid in position 48 remained unchanged (ACA → ACG). P450_{Jα} was also cloned successfully into pET-28a(+).

Transformation of the previously constructed vectors into *E. coli* BL21(DE3) was successful and cells grew in a dense bacterial lawn as the transformed bacteria were not diluted before plating. Cells from a single colony were picked and streaked on an agar plate to prepare glycerol stocks. This was done to ensure to continue the further work with a single and clean *E. coli* strain.

3.1.2 Heterologous expression and purification of FdR_{J1} Fdx_J and P450_{Jα}

OleT was expressed and purified according to the protocol described by Dennig *et al.* (2015) [35]. For production of the electron transfer proteins Fdx_J and FdR_{J1} and the new enzyme P450_{Jα}, *E. coli* BL21(DE3) cells containing pET28a(+) plasmids with the respective gene fragments were grown in TB medium. Expression of all proteins was induced at an OD₆₀₀ of 1. After expression for 20 h cell densities reached an OD₆₀₀ of 2.6 for Fdx_J, 5.0 for FdR_{J1} and 5.6 for P450_{Jα}. Cell growth is in general affected by energy consumption of the expression machinery [79]. Reason for the difference in cell densities could be interference of the protein activities with cellular functions of the expression host or disturb the energy balance of the expression host. Fdx_J is a rather small protein which might

interfere with transfer of electrons in the *E. coli* host cells. Besides, electrons from Fdx_J can uncouple and lead to the formation of O₂⁻ and H₂O₂ from oxygen, which might influence cell growth as formation of ROS leads to oxidative stress in the cells. Also, flavoproteins like FdR_{J1} have the ability to form the mentioned ROS from O₂. Another reason for the slower growth of *E. coli* during Fdx_J expression might be that high amounts of iron and sulfur respectively cystein that are needed to form the Fe-S clusters [80][81].

After expression, the proteins were purified . Therefore, cellular proteins were extracted from *E. coli* BL21(DE3) cells with lysozyme treatment and sonication. Then, the proteins were applied on a 5 ml HisTrap column and the respective His-tagged target proteins were finally eluted by applying imidazole gradients. Samples of cell-free lysate, washing fractions and fractions collected during elution were analyzed by SDS-PAGE. The gels are shown in figures 25, 26 and 27.

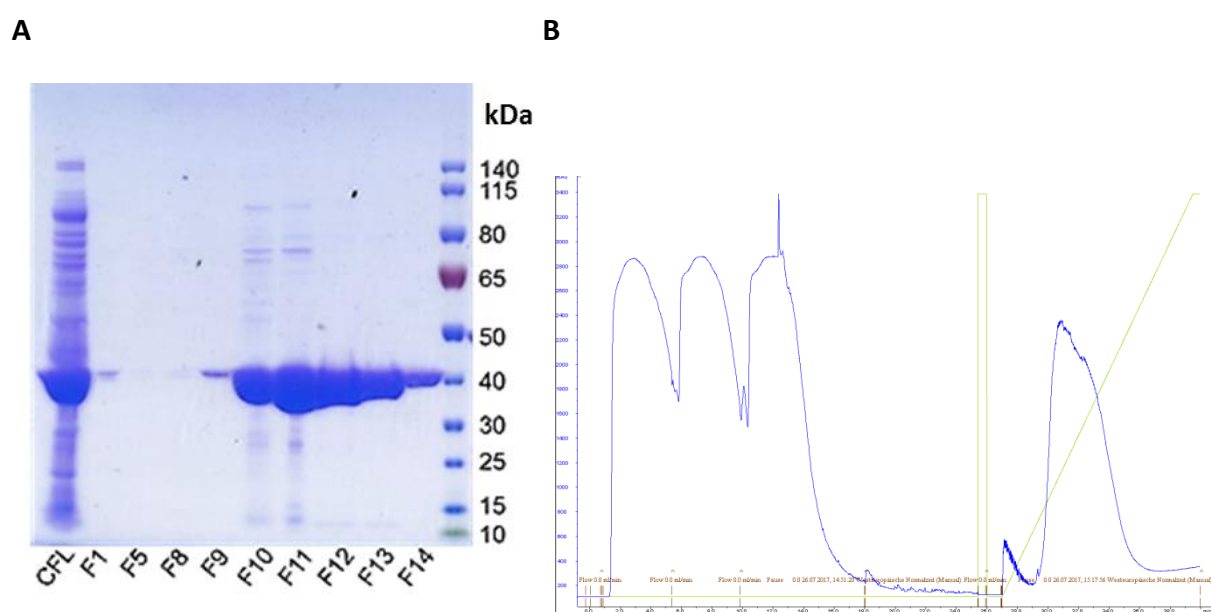


Figure 25 Purification of FdR_{J1}. **A)** SDS-PAGE of the purified fractions, CFL = cell free lysate. F1-F14 are fractions obtained during the purification procedure. **B)** Purification profile obtained from measurements at the outflow of the 5 mL HisTrap column. Blue lane: UV detector signal. Green line = applied imidazole gradient.

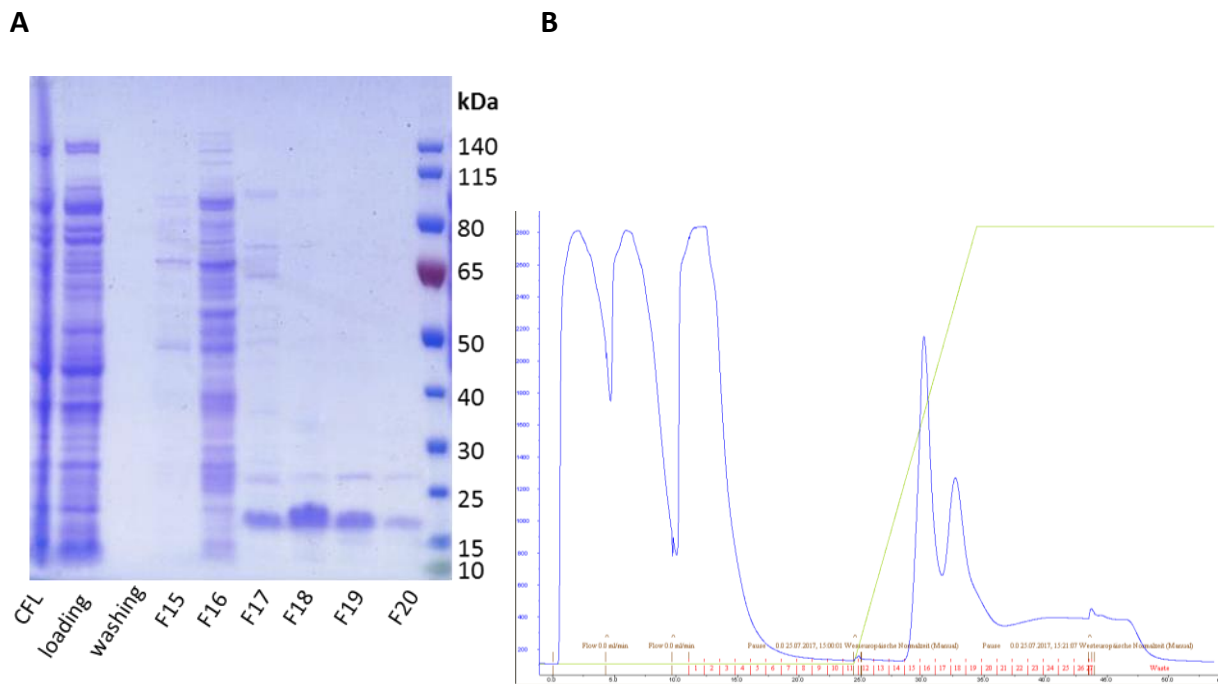


Figure 26 Purification of Fdx. A) SDS-PAGE gel of the purified fractions, CFL = cell free lysate. B) Purification profile obtained from measurements at the outflow of the 5 mL HisTrap column. Blue lane: UV detector signal. Green line = applied imidazole gradient.

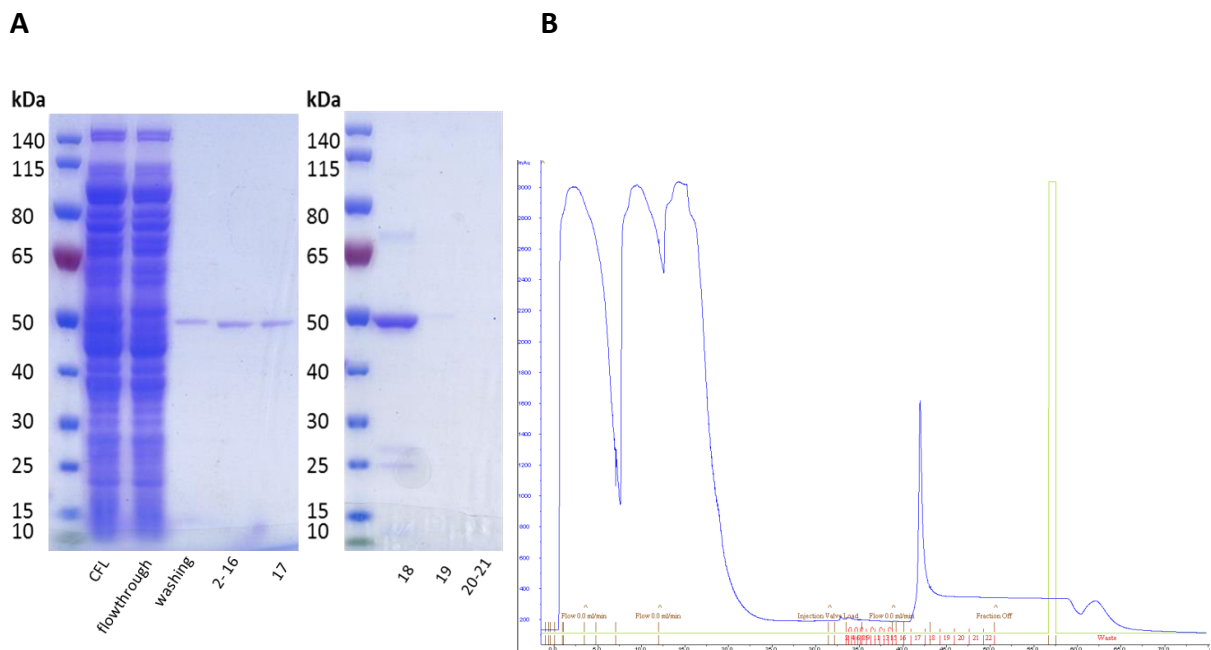


Figure 27 Purification of P450 $_{\alpha}$. A) SDS-PAGE gel of the purified fractions, CFL = cell free lysate. B) Purification profile obtained from measurements at the outflow of the 5 mL HisTrap column. Blue lane: UV detector signal. Green line = applied imidazole gradient.

As the band height of the ferredoxin protein did not match the expected 10 kDa but indicated double size (20 kDa), it was reasoned that the dimeric form of the protein does not monomerize even under

the strong denaturing conditions used (SDS, DTT, 95 °C). The phenomenon that a ferredoxin did not monomerize under denaturing conditions was observed before by Hasan *et al.* with a ferredoxin from *Pyrococcus furiosus* (2002) [82]. To verify the presence of the ferredoxin protein, the 20 kDa band in the SDS-lane was analyzed by LC-MS/MS mass analysis. The band was excised, stored in H₂O and sent for analysis to the Medical University of Graz. The excised protein band was treated with a standardized protocol that involves digestion with chymotrypsin for 3 h, followed by LC-MS/MS analysis of peptide fragments. Analysis results unambiguously showed presence of Fdx_J in the excised band (76% coverage). Definitive evidence whether the protein is dimeric would require further analysis (e.g. native PAGE).

To quantify FdR_{J1} and Fdx_J, their extinction coefficients were calculated with the ExpASY ProtParam online tool. Concentrations of the proteins were calculated from absorbance values at 280 nm. FdR_{J1} was obtained in very high yields after purification (660 mg L⁻¹ shake flask culture) ($\epsilon(\text{FdR}_{J1}) = 25900 \text{ M}^{-1} \text{ cm}^{-1}$). Soluble Fdx_J was recovered in less but still good yields after purification (35 mg L⁻¹ shake flask culture) ($\epsilon(\text{Fdx}_J) = 7450 \text{ M}^{-1} \text{ cm}^{-1}$) owing also to the low molecular mass. Huang *et al.* heterologously expressed a bacterial ferredoxin from *Clostridium pasteurianum* in a comparable amount of up to 40 mg L⁻¹ culture [83].

Absorbance spectra of FdR_{J1} and Fdx_J were recorded to classify the proteins based on comparison with previously recorded spectra of the same protein families. The absorbance spectrum for FdR_{J1} is depicted in figure 28. The blank contained 1 mg/ml BSA to mask absorbance of the peptide chain as it interferes with the specific absorbance for the ferredoxin reductase. The maxima (absorption maxima at 383, 455 and 482 nm) are comparable to those of HaPuR, a flavin-dependent ferredoxin-reductase from *Rhodopseudomonas palustris* (Bell *et al.*).

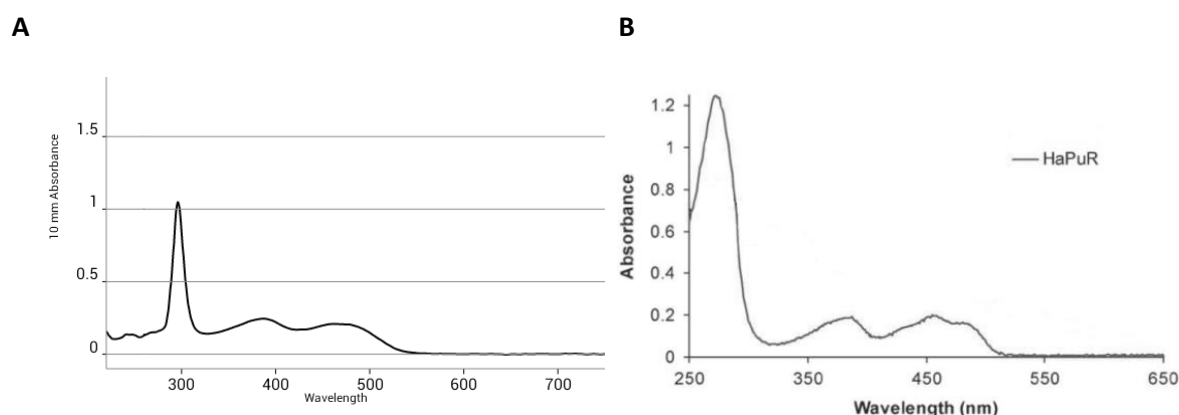


Figure 28 The absorbance spectrum of FdR_{J1} (A) is shown in comparison to the absorbance spectrum of HaPuR from *Rhodopseudomonas phalustris* (B) [65]. PuR has maxima at 383, 455 and 482 nm which are comparable to the maxima observed in FdR_{J1}.

In figure 29 the absorbance spectrum of Fdx_j is shown in comparison to the spectrum of StrB, a peptide that contains a [4Fe-4S]-cluster with a characteristic absorption maximum at 395 nm (Schramma *et al.*). Another comparable spectrum for a ferredoxin containing a [4Fe-4S]-cluster can be found in a publication by Huang *et al.* [83] Fdx_j contains four cysteine residues in an arrangement typical for [4Fe-4S]-clusters. It cannot be excluded from this amino acid sequence pattern nor from the spectrum, that Fdx_j might contain a [3Fe-4S]-cluster or a mixture of both [76]. An EPR (electron paramagnetic resonance) spectrum would be necessary to definitely determine the type of Fe-S cluster.

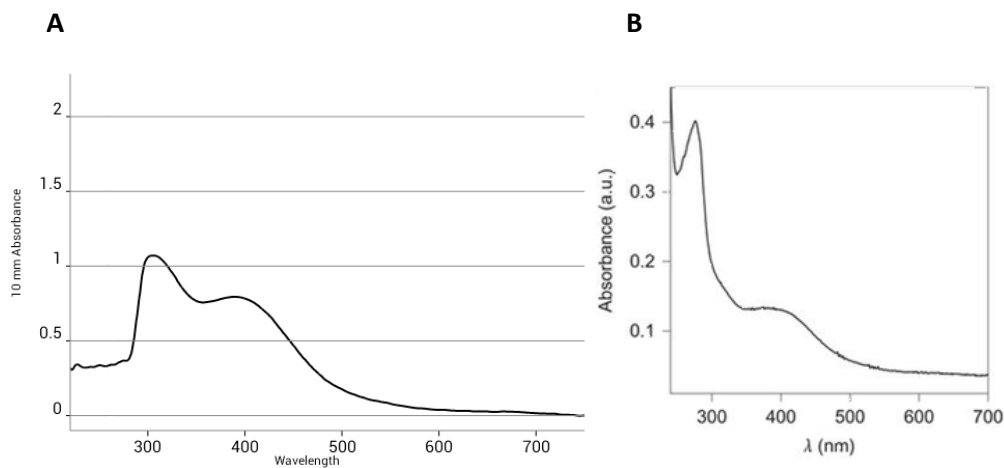


Figure 29 Absorbance spectrum of Fdx_j (A) and StrB (B). StrB contains a [4Fe-4S] cluster. The absorbance peak at 395 nm is described as a characteristic of [4Fe-4S] clusters [76][84]. Note that a [3Fe-4S] cluster cannot be excluded from these spectra.

The identity of P450_{Jα} as a cytochrome P450 enzyme and its quantification was done with CO titration [85]. The chemically reduced heme iron is able to bind CO which leads to a shift of the absorbance maximum from 420 to 450 nm. UV/VIS spectra that were recorded before and after CO gassing and the calculated difference spectrum are shown in figure 30.

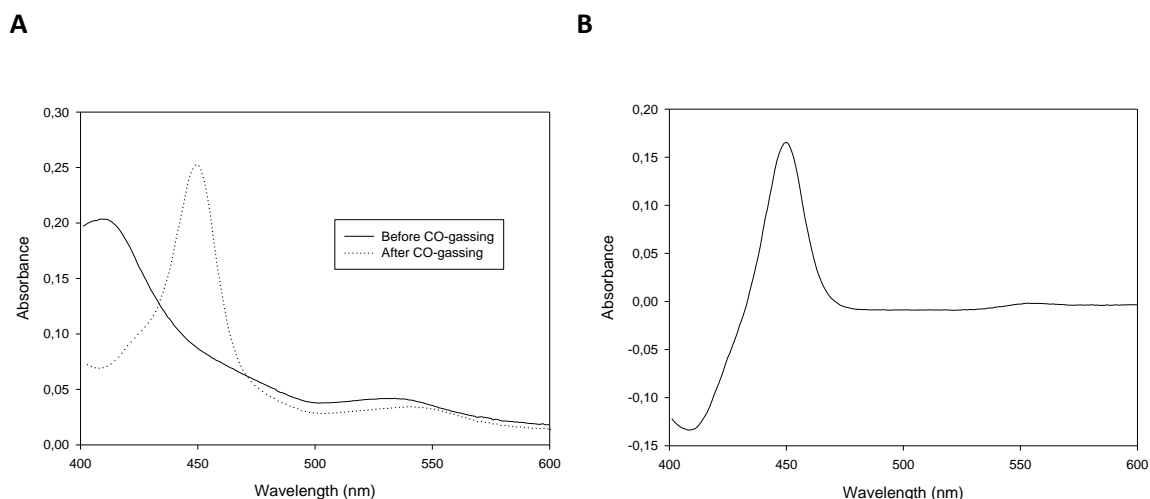
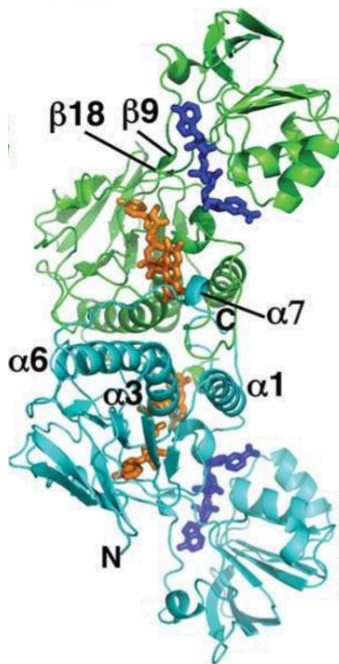


Figure 30 Absorbance spectra of P450_{Jα} before and after CO gassing are shown in A. In B, the difference spectrum between both measurements is shown. Active enzyme in this sample was obtained in a concentration of 19 μM (>95% active protein).

3.1.3 Generation homology models for FdR_{J1} and Fdx_J

Homology models were generated to get an insight into the structure of the isolated proteins. Modeling was done with the SWISS-MODEL web-based bioinformatics tool (<https://swissmodel.expasy.org/>). The used template for FdR_{J1} was the structure of ferredoxin-NADP⁺ oxidoreductase from *B. subtilis* (PDB entry 3LZW), which is a homo-dimeric protein containing several ligands: 2x FAD, 2x NADP and 4x Na⁺ [86]. Figure 31 shows the obtained model in comparison with its template. The NADP and FAD cofactors are shown in the oxidoreductase from *B. subtilis*. The sequence identity between both proteins is 55%. In general, if sequence identity is above 50% between the template and the protein that is investigated, the quality of a model is of considered to be of high accuracy. At a sequence identity of >40% between the target and template sequences, the median structure overlap between the models is >90% [87][88][89].

A



B

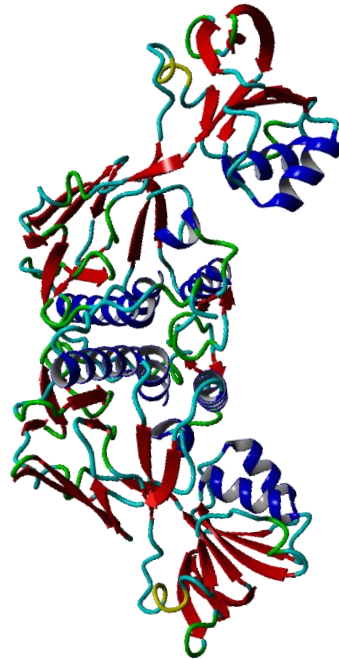


Figure 31 Model of FdR₁₁ (B) in comparison to ferredoxin-NADP⁺ oxidoreductase from *B. subtilis* (A) (PDB entry 3LZW). The figure has been taken from Komori *et al.* (2010) [86]. The dimeric structure of the template from *B. subtilis* (molecule A in green, molecule B in cyan) in complex with NADP⁺ (blue) and FAD (orange) is shown. FdR₁₁ is colored according to its structural features (α -helices in blue, β -sheets in red). The sequence identity between both proteins is 55% [86].

The ferredoxin-NADP⁺ oxidoreductase structure from *B. subtilis* shown in figure 31 contains two cofactors, NADP⁺ and FAD (flavin adenine dinucleotide). Figure 32 shows a scheme of the mechanism of electron transfer from NAD(P)H to FAD. NAD(P)H gets bound close the FAD prosthetic group inside the enzyme, which facilitates electron transfer from the cofactor to the FAD redox coenzyme.

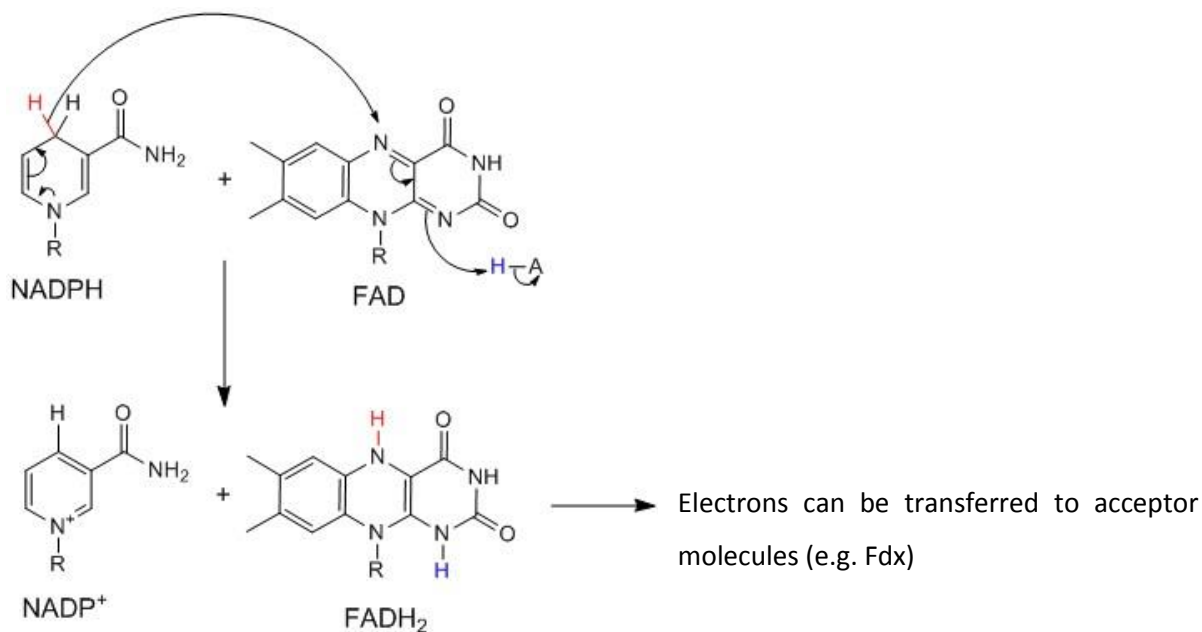


Figure 32 Electron transfer in FAD-containing ferredoxin reductases from NAD(P)H to FAD. FAD is reduced to FADH₂, which in turn can transfer electrons to a ferredoxin Fe-S cluster [90][91].

Also for Fdx, a homology model for was generated. The structure of a ferredoxin from *Bacillus thermoproteolyticus* (PDB 1IQZ) [92] was used as reference template. The *Jeotgaliococcus sp.* ATCC 8456 ferredoxin protein sequence has a 79% identity to this template. It cannot be assessed from the model and the spectrum of the molecule (figure 29), whether the ferredoxin molecule contains a [Fe3-S4] or a [Fe4-S4] cluster. In figure 33, Fdx, models with both possible cluster conformations are shown. As already mentioned before, EPR analysis would be required to identify the cluster type [76].

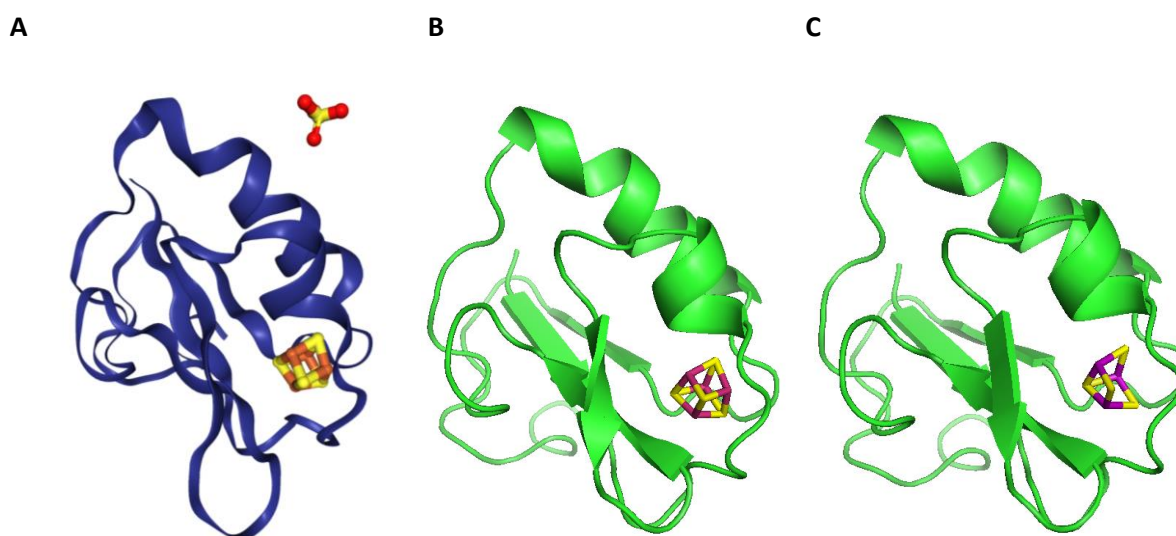


Figure 33 Models of *Jeotgaliococcus sp.* ATCC8456 ferredoxin. In the middle Fdx, containing a [Fe4-S4] cluster is shown (B), on the right side a model containing a [Fe3-S4] cluster (C). The *Bacillus thermoproteolyticus* ferredoxin (PDB ID 1IQZ) (A, left) was used to generate the model. The model was established with the web-based tool SWISS-MODEL.

3.2 Catalytic characterization of the FdR_{J1}-Fdx_J-OleT system

The *Jeotgallicoccus* sp. ATCC 8456 strain is halophilic which means it is adapted to high salt concentrations [22]. Solubility of OleT is strongly influenced by salt concentrations [22]. Therefore, all conversions and biochemical characterizations were done in a buffered system containing 300 mM KCl and 20 % (v/v) glycerol. This environment had no visible detrimental effect on the solubility of the herein characterized proteins.

3.2.1 Reductase activity determination with the small electron acceptor potassium ferricyanide

This experiment was done to determine specific activity and cofactor dependency of the purified ferredoxin reductase FdR_{J1}. Electron transfer activity of FdR_{J1} using NADH or NADPH as cofactor was analyzed using the small electron acceptor molecule potassium ferricyanide K₃[Fe(CN)₆] as final electron acceptor (figure 34). Reaction assemblies contained 1 mM K₃[Fe(CN)₆], FdR_{J1} (1 μM for NADPH oxidation or 5 μM for NADH oxidation) and 400 μM NAD(P)H. Oxidation rates of NADH and NADPH were compared.

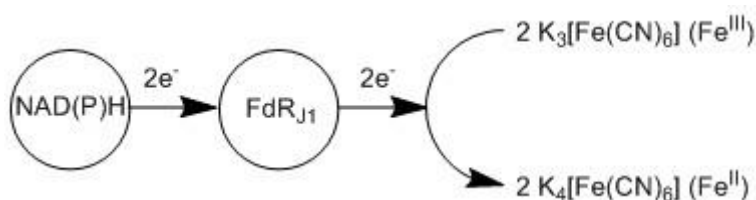


Figure 34 Reduction of K₃[Fe(CN)₆] to K₄[Fe(CN)₆] by the NAD(P)H-dependent enzyme FdR_{J1}.

Potassium ferricyanide K₃[Fe(CN)₆] (Fe^{III}), which appears yellow in aqueous solution, is reduced to colourless potassium ferrocyanide K₄[Fe(CN)₆] (Fe^{II}) by transfer of one electron from NAD(P)H via FdR_{J1}. Reduction of K₃[Fe(CN)₆] can be measured as absorbance decrease at 420 nm. Oxidation rates in the controls where ferredoxin reductase was omitted were subtracted from absorbance decrease of the three reactions containing enzyme. Blank activities of 0.13 U mg⁻¹ for NADH and 0.67 U mg⁻¹ for NADPH were recorded, respectively. Electron transfer activities of FdR_{J1} from NAD(P)H to K₃[Fe(CN)₆] are shown in table 22.

Table 22 NAD(P)H oxidation rates of FdR_{J1} using the small single electron acceptor K₃[Fe(CN)₆]³⁻.

Reductase	Cofactor	Electron acceptor	Specific activity [U mg ⁻¹]	k _{cat} [min ⁻¹]
FdR _{J1}	NADH	[Fe(CN) ₆] ³⁻	0.04 ± 0.01	1.5 ± 0.3
FdR _{J1}	NADPH	[Fe(CN) ₆] ³⁻	3.8 ± 0.8	140 ± 29

The cofactor preference proposed by the annotation of FdR_{J1} as a NADPH-dependent reductase was confirmed. For NADPH an activity of 3.8 ± 0.8 U mg⁻¹ FdR_{J1} was measured while for NADH an activity of only 0.04 ± 0.01 U mg⁻¹ was determined. In other words, FdR_{J1} activity is 93 times higher with NADPH than for NADH. The obvious preference for NADPH suggests function of the ferredoxin reductase in the secondary metabolism of *Jeotgalicoccus* sp. ATCC8456 [6][7][8].

3.2.2 Cytochrome c reduction assay

In this experiment, the compatibility of the purified electron transfer proteins FdR_{J1} and Fdx_J and ability of the system to transfer electrons to a heme group was examined. Therefore, the model acceptor protein cytochrome *c* was used instead of a P450 enzyme. Cytochrome *c* is a small protein that contains a heme group (figure 35). Due to its prosthetic group resemblance to cytochrome P450s, it is well suitable as a model protein for studies on electron transfer chains. In this experiment it was applied as single electron acceptor for reduction of Fdx_J. Reduction of the cytochrome *c* molecule can easily be determined spectrophotometrically. Another advantage of using this model molecule is that the one-electron transfer is easier to study than the more complex two-electron transfer to P450 enzymes [66][67].

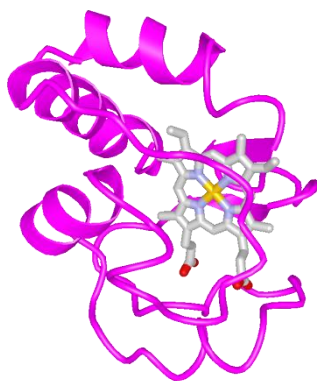


Figure 35 Cytochrome *c* from the heart from *Bos taurus* (MW = 12.23 kDa). The small protein (amino acid chain: pink) contains a heme group. This heme group can be exploited as single electron acceptor that imitates the heme group of a cytochrome P450 enzyme. (source: <https://onlinelibrary.wiley.com/doi/full/10.1002/prot.21452>)

Kinetics of electron transfer from the ferredoxin reductase (FdR_{J1}) to the ferredoxin (Fdx_J) to cyt *c* as the terminal electron acceptor were examined. As the employed system with cytochrome *c* is very robust, it was also used to study the optimal ratio between mediator and the following acceptor molecule. Therefore the concentration of both the heme-containing acceptor cyt *c* and the reductase concentration were kept constant, whereas the ferredoxin mediator concentration was varied from 0.25 to 130 μM . The electron transfer chain scheme is depicted in figure 36.

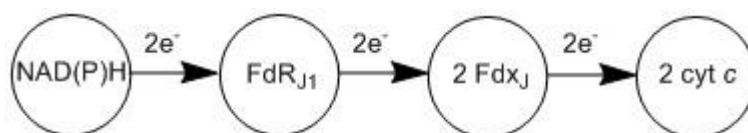


Figure 36 Scheme of electron transfer from NAD(P)H via FdR_{J1} and Fdx_J to cyt *c*. Note that NAD(P)H releases two reduction equivalents whereas cyt *c* is a one-electron acceptor.

Cyt *c* reduction was measured as increase in absorbance at a wavelength of 550 nm. Figure 37 shows the spectrophotometric measurement using Fdx_J in an exemplary concentration of 15 μM with NADPH or NADH as oxidant. Also a control measurement of a reaction where ferredoxin was omitted is shown. Using the reductant NADPH, a clear increase in absorbance at 550 nm was observed ($16.7 \text{ nmol (nmol FdR}_{J1})^{-1} \text{ min}^{-1}$), with NADH as reductant, absorbance increased only very little ($0.1 \text{ nmol (nmol FdR}_{J1})^{-1} \text{ min}^{-1}$). Without Fdx_J , absorbance increase was also marginal.

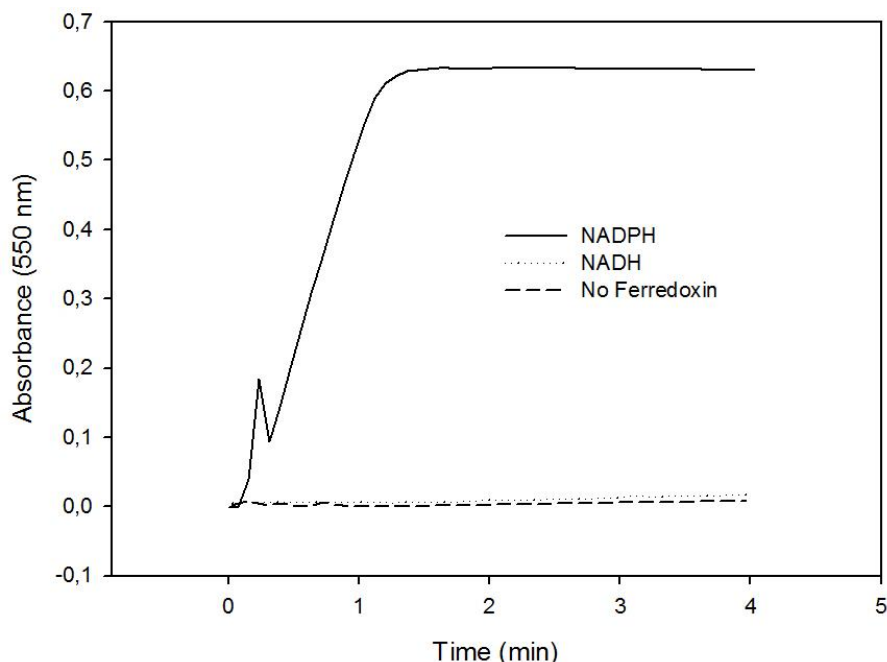


Figure 37 Cyt *c* reduction with 15 μM Fdx_J using 200 μM NADPH or NADH and 1 μM FdR_{J1} . Reduction velocity was measured with the cytochrome *c* assay as change in absorbance at 550 nm. A control without ferredoxin was measured as well (dashed line).

To ensure electron transfer works as proposed, reactions that serve as controls were prepared. Each constituent of the electron transfer chain, namely NADPH, FdR_{J1} , Fdx_J and cyt *c* was left out of one

reaction. One reaction with NADH was also prepared. Electron transfer activities with NADPH and NADH as well as activities of the controls are shown in table 23.

Table 23 Electron transfer activities from FdR_{J1} Fdx_J using cyt c as final electron acceptor. The amount of ferredoxin was 15 μM. Controls without NAD(P)H, FdR_{J1}, Fdx_J or cyt c, were prepared accordingly.

	nmol (nmol FdR_{J1})⁻¹*min⁻¹	mU mg⁻¹ FdR_{J1}
With NADH	0.1	3.6 ± 0.1
With NADPH	16.7 ± 0.9	449.6 ± 25.4
No FdR_{J1}	0.1	2.6 ± 0.1
No Fdx_J	0.1	2.8 ± 0.1
No cyt c	0	0
No reducing agent	0	0

Using 15 μM Fdx_J, electron transfer from Fdx_J to cyt c happens with an activity of 449.6 mU mg⁻¹ FdR_{J1}. Without Fdx_J, also few electrons are transferred to cyt c, indicating that direct transfer from FdR_{J1} to cyt c is possible, but much slower (160-fold slower with 2.8 mU mg⁻¹ FdR_{J1}). Omitting FdR_{J1}, cyt c is also reduced slowly (2.6 mU under the same conditions), showing that electrons can be directly transferred from NAD(P)H to Fdx_J and further to cyt c. Again oxidation of NADH (3.6 mU/mg FdR_{J1}) was much slower than of NADPH showing that NADPH is the preferred cofactor in any constellation (NADPH preferred by the factor 167 over NADH). All constituents of the transfer chain are necessary for efficient electron transfer indicating good and sufficient compatibility of both isolated proteins from *Jeotgalicoccus sp.* ATCC8456. The control reaction without cyt c was prepared to ensure absorption increase at 550 nm occurs exclusively due to cyt c reduction.

To see whether the ratio of Fdx_J to FdR_{J1} has an influence on the velocity of cyt c reduction, Fdx_J concentration was varied between 0.25 to 200 μM. Time dependent reduction was calculated as activity (ε(mM) for reduced bovine cyt c is 28.0 mM⁻¹ cm⁻¹) and plotted against Fdx_J concentration (figure 38) [93]. Reduction velocity increases hyperbolically with increasing ferredoxin amounts. At Fdx_J concentrations above 50 μM, reduction velocity reaches its maximum. The maximum velocity of cyt c reduction (v_{max}), determined by Sigma plot, is 0.043 mM/min. The calculated K_D value is 12.4 μM Fdx_J. The formula used and the calculated values for the kinetic constants are given below.

$$v = \frac{v_{max} \times [Fdx_j]}{K_m + [Fdx_j]}$$

$$v_{max} = 0.043 \pm 0.002 \text{ mM/min}$$

$$K_m = 12.44 \pm 1.81 \text{ } \mu\text{M Fdx}$$

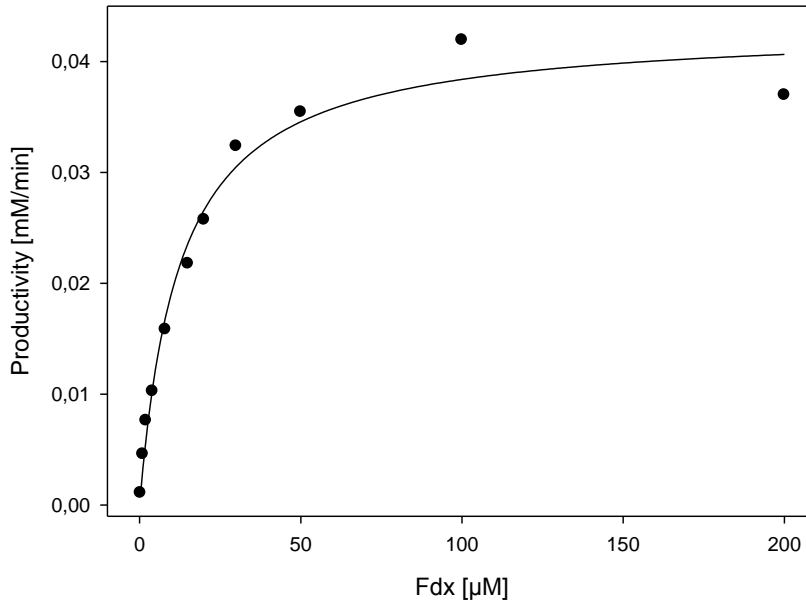


Figure 38 Michaelis-Menten kinetics of one-electron transfer from NADPH to cyt *c* via the reconstituted electron transfer chain from *Jeotgalicoccus* sp. ATCC 8456. Reduction velocity is plotted against Fdx_j concentration. Plot-point values were calculated from duplicate measurements.

Electron transfer activities were calculated for conditions at maximum reduction velocity (table 24). Activity at maximum reduction velocity is $43.2 \pm 1.8 \text{ nmol} \cdot (\text{nmol FdR}_{j1})^{-1} \text{ min}^{-1}$. K_{cat} of the electron transfer to cyt *c* is $0.72 \pm 0.03 \text{ nmol} \cdot (\text{nmol FdR}_{j1})^{-1} \text{ s}^{-1}$.

The fact that electron transfer velocity to cyt *c* increases with increasing amounts of Fdx_j has been observed before (Bell *et al.* used ratios up to 1:40 for FdR_{j1}:Fdx_j in the cyt *c* experiment) [65]. However, studies with OleT or any other 1-alkene producing monooxygenase did not take this crucial parameter into account so far [34][36][37].

Table 24 Electron transfer activities from FdR_{J1} to Fdx_J using the final electron acceptor cyt c. The activities were calculated from data obtained by Michaelis-Menten analysis at a production velocity of v_{max}. (see figure 38).

U (mg FdR _{J1}) ⁻¹	nmol*(nmol FdR _{J1}) ⁻¹ *min ⁻¹	kcat	K _D [μM]	K _{eff} (kcat k _D ⁻¹) [μM ⁻¹]
1.16 ± 0.05	43.2 ± 1.8	0.72 ± 0.03	12.4 ± 1.8	3.5

3.2.3 NADPH oxidation rates of the FdR_{J1}-Fdx_J-OleT system

As it was proven in the previous experiment that the electron transfer chain components are functional, Fdx_J and FdR_{J1} were combined with OleT to convert C14:0 FA model substrate (figure 39). At first, NAD(P)H oxidation rates when electrons are transferred over the whole chain (cofactor – FdR_{J1} – Fdx_J – OleT – O₂) were measured. In table 25, NADPH and NADH oxidation rates are shown.

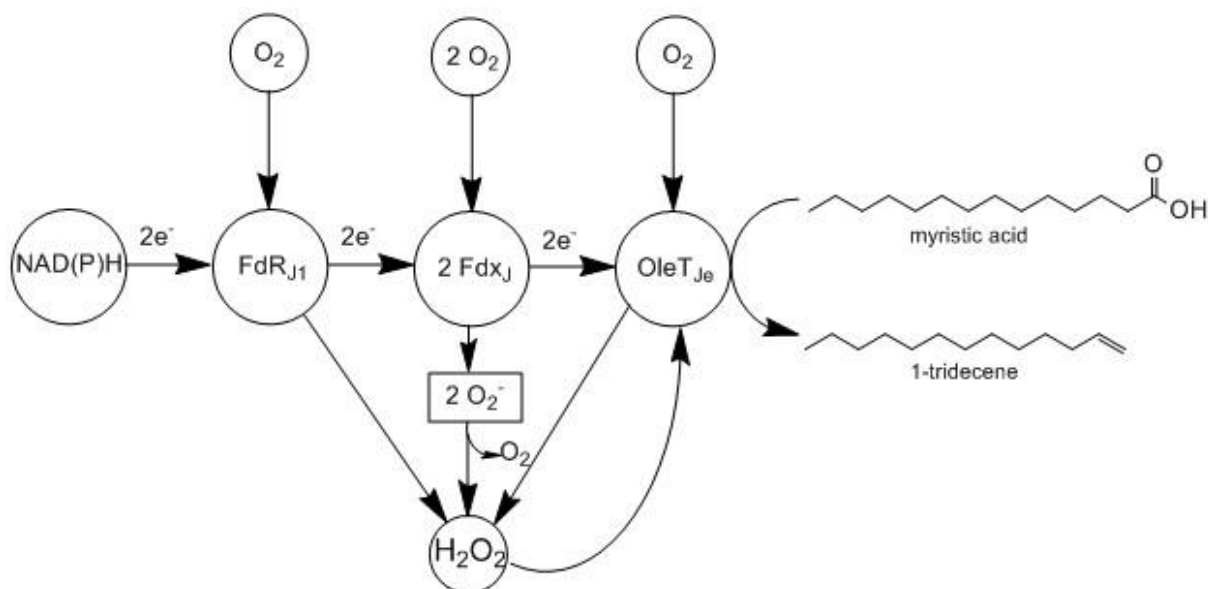


Figure 39 Scheme of possible electron transfer from NAD(P)H via FdR_{J1} and Fdx_J to OleT_{Je} for activation of O₂ in order to decarboxylate the C14:0 FA substrate. Note several exit pathways are possible to yield ROS which can trigger catalysis with OleT.

Table 25 Measurement of NAD(P)H oxidation rates. Reactions contained 200 μM NAD(P)H, 1 μM FdR₁₁, 15 μM Fdx_j, 1 μM OleT and 400 μM C14:0 FA substrate.

	Oxidation rates in $\mu\text{mol } \mu\text{mol}^{-1} \text{ min}^{-1}$	U $\text{mg}_{\text{FdR}_{11}}^{-1}$	Conversion of C14:0 (%)
all + NADPH	4.5 \pm 0.2	0.124	91
all + NADH	1.6 \pm 0.2	0.044	33
No OleT	2.0 \pm 0.0	0.055	0
No FdR₁₁	0	0	0
No Fdx_j	0.225	0.003	5
No NAD(P)H	0	0	0
No FA or EtOH	4.1 \pm 0.1	0.133	0
no FA (15 μM Ferredoxin)	4.4 \pm 0.1	0.122	0
100 μM Ferredoxin	8.6 \pm 1.4	0.238	n.d.

NADPH oxidation rates ($4.5 \mu\text{mol } \mu\text{mol}^{-1} \text{ min}^{-1}$) are about 3 times higher than NADH oxidation rates ($1.6 \mu\text{mol } \mu\text{mol}^{-1} \text{ min}^{-1}$). This confirms that NADPH remains also under these conditions the preferred cofactor. Without OleT, NADPH oxidation is still at $2.0 \mu\text{mol } \mu\text{mol}^{-1} \text{ min}^{-1}$ (45.3% of oxidation rate with OleT) and without FdR₁₁, NADPH oxidation is insignificant. This observation leads to the assumption that a significant portion of electrons leaves the transfer chain from the Fdx_j molecule, probably by reducing dissolved O₂. It has been observed before, that electrons from ferredoxin iron-sulfur clusters are able to reduce oxygen molecules to superoxide and peroxide [94][95]. From the observation that without ferredoxin still some NADPH oxidation could be measured ($0.225 \mu\text{mol } \mu\text{mol}^{-1} \text{ min}^{-1}$) the conclusion can be drawn that electrons can be either directly transferred from FdR₁₁ to OleT or that electrons leave the transfer chain so that H₂O₂ is formed by autooxidation of FdR₁₁. Reduced flavin groups have the ability to conduct a one-electron transfer to dioxygen to produce O₂⁻. A second electron transfer, coupled with proton transfer, generates an oxidized flavin and H₂O₂. Alternatively, a C(4a)-(hydro)peroxyflavin intermediate is formed which can also eliminate H₂O₂ (see figure 40). This phenomenon has been reviewed by Chaiyen *et al.* (2012) [96].

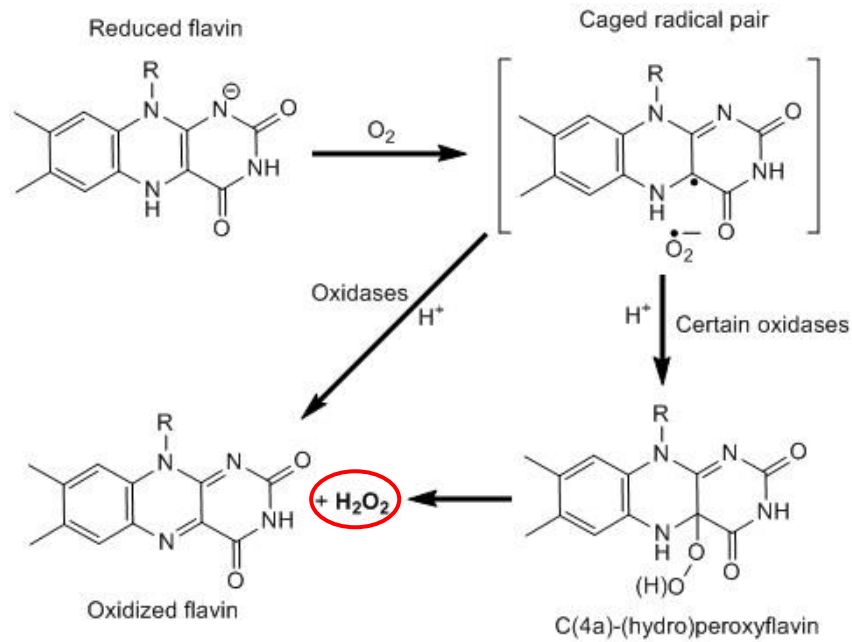


Figure 40 Autooxidation of reduced flavin to form H₂O₂. In a first reaction step, one-electron transfer from reduced flavin to dioxygen leads to the formation of a caged radical pair consisting of the flavin semiquinone and the superoxide anion. In the case of oxidases, a second electron transfer together with proton transfer oxidizes the flavin and leads to the formation of H₂O₂. In certain other oxidases, a more or less stable C(4a)-hydroperoxyflavin is formed which can also undergo H₂O₂ elimination. The figure was redrawn and adapted from Chaiyen *et al.* [96].

Figure 41 shows NADPH and NADH oxidation in comparison also with the control reaction that contained no ferredoxin. NADPH oxidation is 2.8 times faster than NADH oxidation. Without Fdx₁, cofactor oxidation is reduced by 20-fold compared to the reaction containing 15 μM Fdx₁ and NADPH.

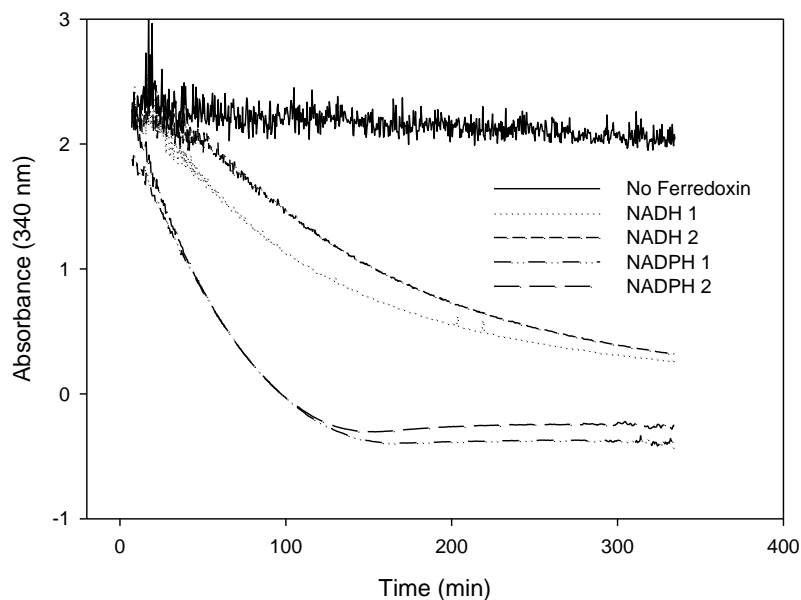


Figure 41 NADPH and NADH oxidation rates in comparison. Reactions contained all electron transfer chain components including 1 μM FdR₁₁, 15 μM Fdx₁, OleT and C14:0 FA substrate. Average oxidation rates are 4.5 μmol μmol⁻¹ min⁻¹ for NADPH and 1.6 μmol μmol⁻¹ min⁻¹ for NADH. Without Fdx₁, NADPH oxidation rate was 0.225 μmol μmol⁻¹ min⁻¹.

In table 26, NAD(P)H oxidation rates for the three electron transfer characterizing experiments that were described (potassium ferricyanide, cyt *c* or FA substrate as final electron acceptors) are summarized. It is shown that NADPH oxidation rates become slower when increasing the number of transfer chain constituents. The factor by which NADPH consumption is faster than NADH consumption is different in the three experiments that were conducted. With changing electron transfer chain length, limiting transfer steps change. OleT becomes rate limiting when present in the reaction mixture, as it is a very slow enzyme [35] with activities in the range of 0.1 – 0.3 U mg⁻¹ (table 1). Part of the electrons will not reach the end of the chain, as they will be transferred to O₂ present in the medium. Besides, also interactions between the transfer proteins might have an influence on electron transfer efficiencies [90].

Table 26 The final electron acceptor and constitution of the transfer chain influence the NAD(P)H oxidation rates.

Electron transfer chain	Final electron acceptor	NADPH oxidation rate (nmol nmol⁻¹ min⁻¹)	NADH oxidation rate (nmol nmol⁻¹ min⁻¹)
NAD(P)H-FdR_{J1}-[Fe(CN)₆]³⁻	Hexacyanoferrate(III)	140 ± 29	1.5 ± 0.3
NAD(P)H-FdR_{J1}-Fdx_J-cyt <i>c</i>	cyt <i>c</i>	16.7 ± 0.9	0.1 ± 0.0
NAD(P)H-FdR_{J1}-Fdx_J-OleT_J-O₂	C14:0 FA substrate/O ₂	4.5 ± 0.2	1.6 ± 0.2

3.2.4 Catalytic activity and selectivity of OleT dependent on mediator concentration

Rapid sequential transfer of two electrons is necessary for efficient O₂ activation in OleT. If interrupted, single electrons can uncouple from the transfer and form reactive oxygen species such as O₂⁻ (superoxide) or H₂O₂ [97]. Fdx_J potentially functions as shuttle between FdR_{J1} and OleT and in order to efficiently transfer electrons, its optimal concentration in the FdR_{J1}-Fdx_J-OleT constellation has to be determined. In the previous experiment it has been evaluated using the final electron acceptor cytochrome *c*. The influence of the Fdx_J concentration on the efficiency of electron transfer has so far not been studied for any 1-alkene forming oxygenase (see table 1). This experiment was intended to find out to what extent Fdx_J concentration influences substrate conversion and product selectivity of OleT. In order to find the optimal Fdx_J concentration, the amount of FdR_{J1} and OleT

were kept equimolar and constant at 1 μM . C14:0 FA was chosen as substrate as it has an acceptable solubility in the aqueous reaction medium and yields an industrially more relevant product (1-tridecene) compared to long chain fatty acids such as C18:0 or C20:0. With GC-MS analysis, conversions were determined in terms of substrate depletion. Determination of product increase would possibly have delivered less reliable results, due to volatility of the C13 1-alkene.

In figure 42 the conversion (in %) of C14:0 FA substrate is shown. Already at an 8-fold excess of Fdx_j over FdR_{j1} , a conversion of >96% is reached. At 100 μM Fdx_j , full conversion of C14:0 is achieved. Electrons therefore are efficiently transferred via the FdR_{j1} - Fdx_j system. Assuming electrons are able to leave ferredoxin reducing oxygen to form hydrogen peroxide, in-situ generated peroxide possibly activates OleT via the peroxide shunt [33][34].

In figure 43, selectivity for both products (1-tridecene and β -OH C14 FA) after 24 h reaction time is shown. The substrate decreases with increasing Fdx_j concentration. Accordingly, 1-alkene concentration rises. Amounts of >90% tridecene and 9.5% β -OH FA are reached, when 100 μM mediator are applied. With low Fdx_j concentrations, the selectivity for β -OH FA increases initially and reaches its maximum already at 1 μM Fdx_j (42% β -OH FA; 58% 1-alkene), but it decreases soon thereafter. At 130 μM Fdx_j no β -OH FA was formed to a detectable amount. The concentration of mediator seems to influence catalyst selectivity but one expects selectivity being influenced mainly by the direct interaction of the substrate with the catalyst. One possible explanation for this observation might be that analytical detection of low product amounts is limited. With lower Fdx_j concentrations only little amount of product can be generated. As 1-tridecene is more volatile than the β -OH FA, proportionally more C13 alkene product might disappear from the reaction headspace with lower overall product amounts. When increasing the mediator concentration to 8 μM the amount of produced β -OH FA increases in a similar way as 1-tridecene. Chemoselectivity obviously tends more towards 1-tridecene formation with increasing amounts of Fdx_j , which stabilizes at around 90% at 30-50 μM Fdx_j .

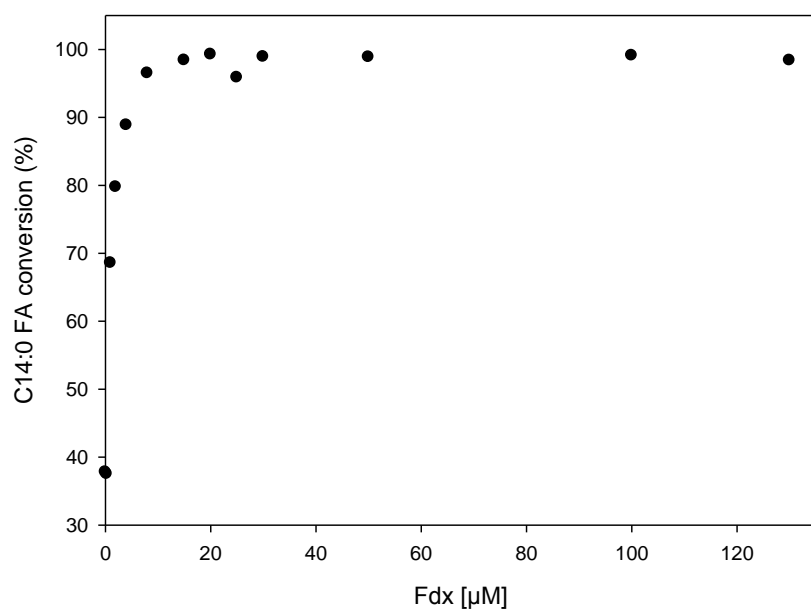


Figure 42 C14:0 FA conversion with increasing concentration of Fdx_j. 1 mL reactions in buffer C contained 1 μM FdR₁₁0 - 130 μM Fdx_j, 1 μM OleT, 400 μM NADPH and 400 μM C14:0 FA substrate in a final 2.5% EtOH concentration.

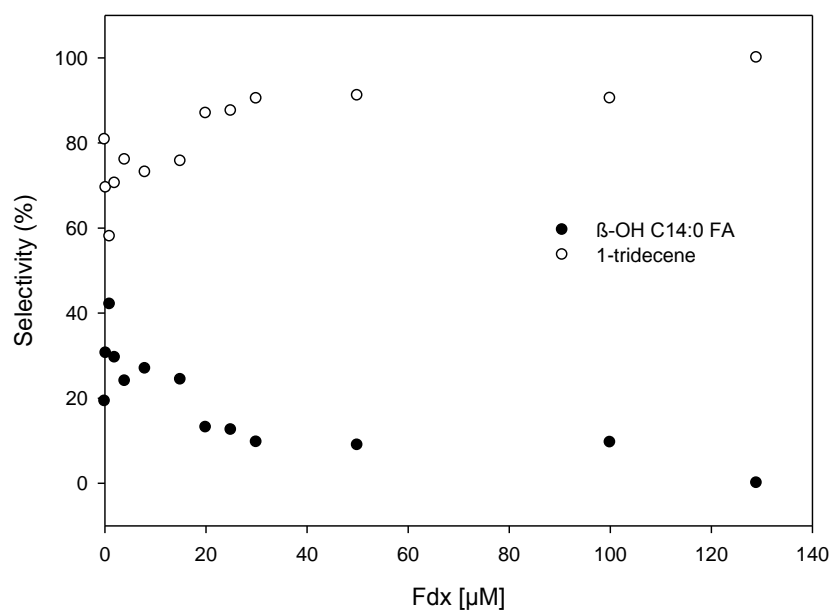


Figure 43 Selectivity of OleT at increasing amounts of Fdx_j. Products formed from C14:0 FA conversion (figure 44).

3.2.5 Quantification of H₂O₂ released by the reconstituted electron transfer chain

OleT accepts both O₂ and H₂O₂ as oxidants and uncoupling of electrons from the FdR₁₁- Fdx_j electron transport chain could potentially lead to the formation of reactive oxygen species (O₂⁻ or H₂O₂). Reaction controls for NADPH oxidation measurements done before showed cofactor oxidation in absence of Fdx_j or OleT. As already explained above, flavin groups are capable of reducing O₂ to O₂⁻

and H₂O₂ and also with ferredoxin iron-sulfur clusters O₂ oxidation to O₂⁻ and further dismutation to H₂O₂ has been observed [95][96]. The following experiment was done to prove H₂O₂ formation and to estimate how much of electrons exactly reach OleT via transfer from Fdx_j to activate O₂.

H₂O₂ concentration was determined spectrophotometrically in an assay employing end-point measurements of H₂O₂ in reactions after all NADPH was depleted (table 27). The experiment is based on the oxidation of the phenolic compound guaiacol in presence of H₂O₂ by horseradish peroxidase (HRP). Thereby, a phenyl radical is formed that reacts together with 4-aminoantipyrine (4-AAP) to form a quinoneimine dye that is strongly coloured (red) and has an absorbance peak at 509 nm [68][69]. Correlation coefficient between absorption and H₂O₂ was calculated from the calibration measurements ([abs]/H₂O₂[μM] = 0.0077). NADPH, (FdR_{J1}) and Fdx_j were assembled in reaction buffer and reacted before detection solution including HRP, guaiacol and 4-AAP was added. Table 27 shows the concentrations of detected H₂O₂ in presence/ absence of Fdx_j.

Table 27 Peroxide formation from electrons reducing dissolved O₂.

	NADPH-FdR _{J1} -Fdx _j	NADPH-FdR _{J1}
H₂O₂ concentration [μM]	53.8	2.9
% H₂O₂ formed (from NADPH-derived electrons)	13.5	0.7

It could be shown that with the FdR_{J1}-Fdx_j system 13% of electrons deriving from NADPH are transferred to O₂ for H₂O₂ formation but only 1% in case Fdx_j is absent. This result demonstrates that electrons from the electron transfer chain in fact are able to reduce O₂ to H₂O₂, which can then activate the peroxygenase OleT (as can be seen in the high coupling values). The actual numbers might be higher, as peroxide could have decomposed to some extent during the experiment due to its low stability in water and the long incubation times in this experiment [35][36].

3.2.6 Effect of catalase on catalytic activity of OleT

This experiment was carried out to evaluate the influence of peroxide on the overall substrate conversion rate. Catalase was supplemented in varying amounts (0 to 5000 U mL⁻¹) to reaction mixtures to remove produced peroxide and therefore to demonstrate (and quantify) H₂O₂ formation leading to product formation via peroxide shunt activity. Activity of OleT is about 0.1 U/mg enzyme (see table 1) and therefore an amount of 5000 U mL⁻¹ catalase (16000-fold excess specific activity compared to OleT) was considered sufficient to remove produced H₂O₂ efficiently. Conversion of substrate was determined by GC-MS. The substrate amount in the sample without OleT was taken as

100% reference value (single point calibration) and the C14:0 conversions at different catalase amounts are graphically depicted in figure 44.

The difference between conversion rate without catalase supplementation (97%) and with 5000U catalase (25%) is 72%. In the photometric H₂O₂ measurements above 13 % peroxide formation were detected. The figurative representation of the results (figure 44) shows a curve with decreasing slope, whereby the conversion at 5000 U/mL draws near a minimum value. This shows that upon consumption of (nearly) all H₂O₂ produced due to O₂ reduction presumably by FdR₁ or Fdx₁, a maximum of 25% of electrons can be transferred to OleT via the transfer chain.

Recently (2018), Wise *et al.* published a study on the mechanism of OleT. They observed an elimination of >90% of decarboxylated product if applying >1000U/mL catalase in reactions containing the CamAB system from *P. putida* (applying 10 μM of each of the redox partners). Furthermore, they have shown that OleT is unable to form the hydroperoxo-ferric intermediate that is an essential precursor for formation of compound I in the catalytic cycle of P450 enzymes [37]. This leads to the assumption that OleT is prevalently if not exclusively activated by H₂O₂. Electron transfer systems are forming controlled small amounts of H₂O₂ *in-vitro*. H₂O₂ is only available in traces and catalyst oxidation by hydrogen peroxide is limited. However, *in-vivo* limitations regarding efficient electron economy between NAD(P)H and OleT might be encountered [11][34][37].

In this study, OleT reached a TTN of 392 even under restricted amount of the electron source, which is higher than values reported for reactions catalyzed by direct addition of H₂O₂ and also higher than several of the values reached with previously tested electron transfer chains (see table 1). This provides an ideal starting point for further reaction engineering.

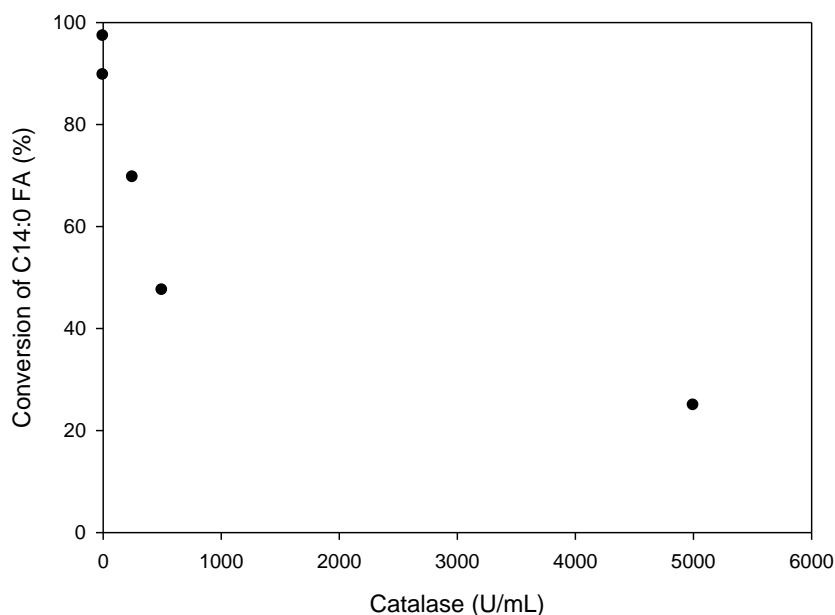


Figure 44 Influence of catalase concentration on C14:0 FA conversion. Reactions contained NADPH (400 μ M), FdR₁₁ (1 μ M), Fdx_j (30 μ M), OleT (1 μ M) and myristic acid (400 μ M) in a final EtOH concentration of 2.5% (v/v) in buffer C (KPi 100 mM; pH 7.5; 300 mM KCl; 20% (v/v) glycerol).

3.3 Influence of NADPH and substrate concentration on C14:0 FA conversion

In this experiment, concentrations of NADPH and C14:0 FA substrate were varied and thereby kept in equimolar ratio. The reactions contained 1 μ M FdR₁₁, 30 μ M Fdx_j, 1 μ M OleT and C14:0 FA substrate concentrations varying between 200 and 10000 μ M. Reaction time was calculated based on the NADPH oxidation rate at a C14:0 substrate concentration of 400 μ M. It was calculated that at a substrate concentration of 10 mM it will take 37.5 h until all NADPH is consumed. In figure 45, results are depicted graphically. It can be seen that up to a substrate concentration of 800 μ M conversion is almost complete and that at concentrations of 1 mM and higher, conversion decreases. From figure 46 it can be seen that the total amount of C14:0 FA that is converted increases linearly until a concentration of 1 mM NADPH and substrate. Then the slope decreases and at a concentration of 10 mM less total amount of substrate is converted (1736 μ M) than with 5 mM NADPH and substrate (2255 μ M). Reason for the drop between 5 and 10 mM substrate can be that the high concentration here becomes either inhibiting for enzyme activity or has a denaturing or precipitation effect on the enzyme [102][103]. Also, limited solubility can decrease availability of the substrate for conversion. Vorum *et al.* determined in 1991 the solubility of myristic acid to be around 20-30 μ M in phosphate

buffer pH 7.4 at 37°C. At higher concentrations, micellar aggregates and large liposomes are formed [104]. In this state, the fatty acids are not optimally accessible for the enzyme.

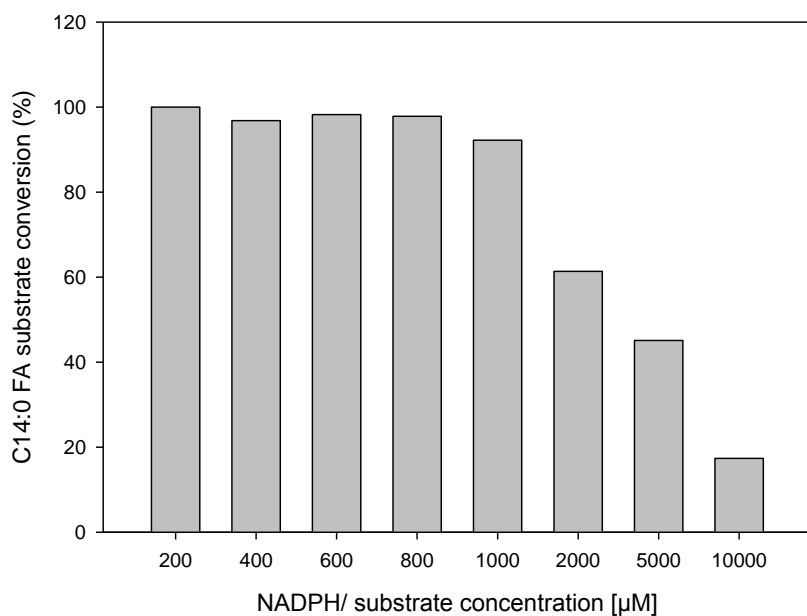


Figure 45 Influence of NADPH and substrate concentration on conversion (%). Reactions contained 1 µM FdR₁₁, 30 µM Fdx₁, 1 µM OleT and varying equimolar NADPH and C14:0 FA substrate concentrations.

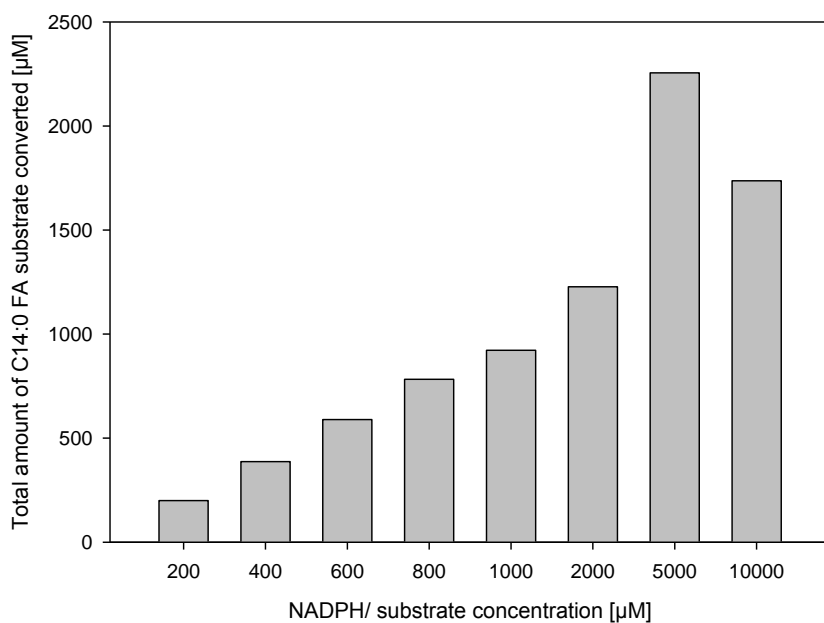


Figure 46 Total amount of C14:0 FA substrate converted at different equimolar NADPH/ substrate concentrations. Reactions contained 1 µM FdR₁₁, 30 µM Fdx₁, 1 µM OleT and varying equimolar NADPH and C14:0 FA substrate concentrations.

3.4 Biochemical characterization of P450_{Jα}

To test whether P450_{Jα} accepts fatty acids as substrates and if so, to assess the efficiency and selectivity of this newly isolated enzyme, reactions were assembled using H₂O₂ as oxidant. The reactions contained FA substrates of different chain lengths (C10:0, C12:0, C15:0 and C18:0) and H₂O₂ was added in an equimolar amount to the substrate. C10:0 FA and C12:0 FA were almost completely converted to α-OH FA (figure 47), showing that P450_{Jα} is a much more efficient peroxygenase than OleT. P450_{Jα} is highly selective towards formation of α-OH FAs. About 93.4% of C10:0 FA was converted to 98.1% α-OH FA and only 1.9% β-OH FA product was detectable.

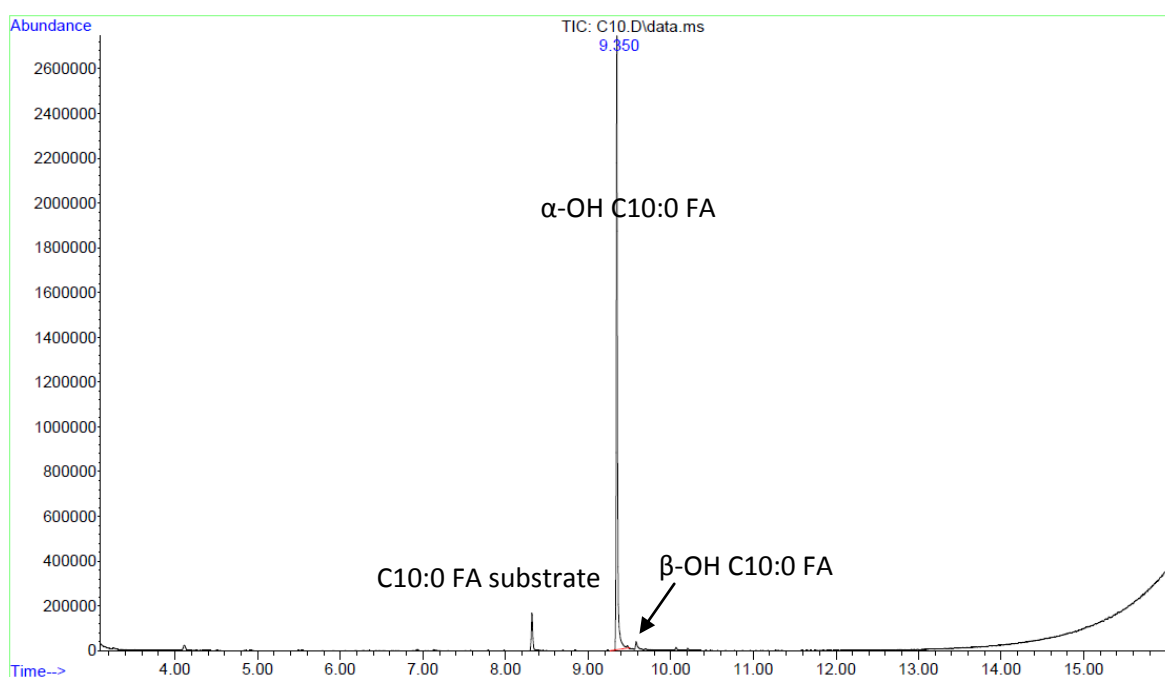


Figure 47 Conversion of C10:0 FA substrate by P450_{Jα}. 93.4% of C10:0 FA were converted to 98.1% α-OH FA and 1.9% β-OH FA.

To test feasibility of the new electron transfer system consisting of FdR₁ and Fdx₁ with P450_{Jα}, it was assembled *in-vitro* and oxidation rates of NADH and NADPH were measured. The results of these measurements are shown in figure 48. Oxidation of NADPH employing the new cytochrome P450 enzyme is comparable to the oxidation observed with OleT. In table 28, the values of initial NAD(P)H consumption rates of OleT and P450_{Jα} are shown.

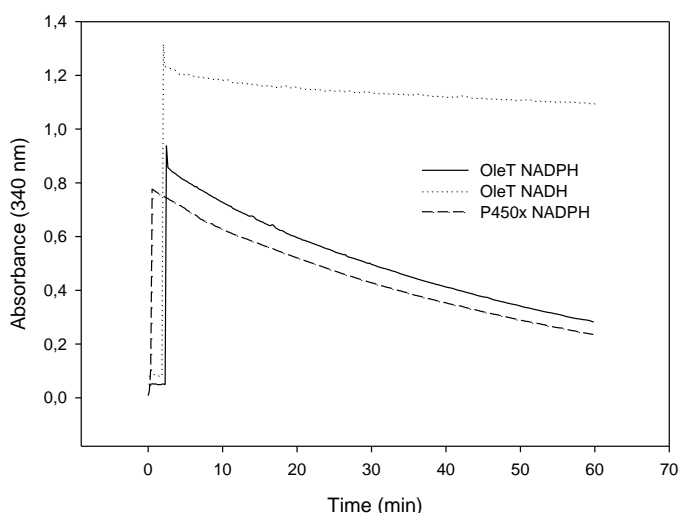


Figure 48 Oxidation rates of NADH or NADPH when employing the FdR_{J1}-Fdx_J system and OleT or P450_{Jα} were determined spectrophotometrically (at 340 nm). The substrate that was used was C12:0 FA. Standard 1 mL reactions were carried out in 100 mM KPi buffer (pH 7.5, 20% Glycerol, 300 mM KCl) containing 200 μM NAD(P)H and C12:0 in a final EtOH concentration of 2.5%, 1 μM FdR_{J1}, 2 μM Fdx_J and 1 μM P450.

Table 28 NAD(P)H consumption rates [mM h⁻¹] employing the FdR_{J1}-Fdx_J system and OleT or P450_{Jα}.

Enzyme/reductant	Initial NAD(P)H oxidation rate [mM h ⁻¹]
P450 _{Jα} /NADPH	0.154
OleT/NADPH	0.183
OleT/NADH	0.043

The fact that NADPH oxidation rates are in the same range when applying P450_{Jα} or OleT leads to the assumption that the electron transport chain can be applied efficiently for both enzymes. Due to the findings that H₂O₂ can be formed by the electron transfer chain proteins, the oxidation rates indicate also that the P450 enzymes do not work as monooxygenases but as peroxygenases. To find evidence for this assumption, the system was applied to convert FA substrates. For this electron transfer experiment, 1 mM NAD(P)H, 1 μM FdR_{J1}, 2 μM Fdx_J, 1 μM P450_{Jα} and 1 mM substrate in a final EtOH concentration of 2.5% in buffer C were used. FA substrates of varying chain length were tested (table 29).

Table 29 Conversions (%) of FA substrate to α -OH FAs using NADH or NADPH as reductants and the FdR_{1j}-Fdx_j-P450_{J α} electron transfer system. Reactions contained 1 mM NAD(P)H, 1 μ M FdR_{1j}, 2 μ M Fdx_j and 1 mM substrate in a final EtOH concentration of 2.5% (v/v) in buffer C.

Substrate (FA)	(%) of substrate converted to α -OH FA	
	NADH	NADPH
C10:0	0.16	2.29
C12:0	1.91	7.86
C13:0	1.00	7.81
C15:0	0.00	5.26
C16:0	0.00	1.28
C18:0	0.00	0.11

Fatty acid conversions were significantly higher if NADPH was used as oxidant (4-14 times higher, depending on the substrate chain length). Fatty acids of chain lengths >C14:0 were not converted at all using NADH. The substrates C12:0 and C13:0 were best converted in the applied constellation of the redox chain with P450_{J α} . FA conversion as found in this experiment are lower than with OleT (with 2 μ M Fdx_j already 53% of substrate could be converted). As it was found out by the previously described experiments with OleT, a higher ratio of Fdx_j to FdR_{1j} would possibly lead to higher conversion of FA to α -OH FA.

4 Summary and Conclusion

A new native electron transfer system for the cytochrome P450 fatty acid decarboxylase OleT has been isolated from *Jeotgalicoccus sp.* ATCC8456. The class I electron transfer system was identified by applying protein-BLAST and manual search in the host genome. After its production in *E. coli* host cells and His-tag-purification, the system comprised of the ferredoxin Fdx_j and the ferredoxin reductase FdR_{j1} was characterized.

In a first experiment to characterize electron transfer, the inorganic electron acceptor K₃[Fe(CN)₆] was applied to measure its reduction by FdR_{j1}. FdR_{j1} was found to be NADPH-dependent as electron transfer to the small acceptor molecule K₃[Fe(CN)₆] with this cofactor (3.8 U mg⁻¹ FdR_{j1}) was 93-fold higher than with NADH.

In a further approach, electron transfer from NAD(P)H via FdR_{j1} and Fdx_j to the small protein cytochrome *c* was examined. This electron acceptor contains a heme prosthetic group analogous to P450 enzymes. The influence of Fdx_j concentration on overall electron transfer kinetics was tested. Maximum activity measured with the system employing NADPH as reducing agent was 1.16 U mg⁻¹ FdR_{j1} at a Fdx_j concentration of >50 μM. This experiment has shown that electrons can be transferred from the FdR_{j1}-Fdx_j system to a heme group and that an increased Fdx_j concentration has positive influence on the measured cyt *c* reduction velocity.

When testing transfer through the FdR_{j1}-Fdx_j-OleT system, again Fdx_j concentrations were varied and a sharp increase of conversion (%) was observed until a maximum of >95 % was reached at a >15-fold excess of Fdx_j over FdR_{j1}. In comparison, the highest coupling efficiency reported to date was 61% (Lu *et al.*, 2018) [4]. Increased Fdx_j concentrations were also shown to have a beneficial influence on selectivity towards 1-tridecene formation. From this experiment it can be concluded, that the Fdx_j concentration has a crucial influence on the coupling efficiency, which reached >95%.

Fatty acid decarboxylation still occurred if Fdx_j was left out of the reaction (0.003 U mg⁻¹), leading to the assumption that electron transfer can occur directly from FdR_{j1} to OleT or that electrons will reduce O₂ from the reaction medium to H₂O₂ [96]. H₂O₂ in turn can activate OleT via the peroxide-shunt. Coupling efficiencies are defined by the amount of product that is formed from a certain amount of cofactor. Therefore, coupling efficiencies determined without addition of catalase do not reflect the actual quality of electron transport via all constituents of the FdR_{j1}-Fdx_j-OleT system.

To measure the amount of H₂O₂ that is formed by electrons deriving from NAD(P)H, a photometric assay was performed in which H₂O₂ oxidizes guaiacol to a phenyl radical that is coupled with with 4-

AAP to form a red quinoneimine dye. About 14% (54 μM) of electrons deriving from NADPH were found as H_2O_2 in the reaction solution.

To have a more precise result of the extent to which electrons from the transfer chain reduce O_2 to H_2O_2 , a C14:0 FA conversion experiment applying different concentrations of catalase was conducted. Catalase decomposes H_2O_2 which is formed by O_2 reduction to H_2O and O_2 and thereby prevents it from being involved in the peroxide-shunt. Substrate conversion decreased from 97% without catalase to 25% with 5000 U/mL catalase. This result indicates that OleT works mainly as a peroxygenase and confirms what has recently been published by Wise *et al.* (2018) [37]. They stated that formation of the hydroperoxo-ferric adduct in the P450 catalytic cycle is not possible in OleT. From this they draw the conclusion that OleT is mainly if not exclusively working as a peroxygenase [37]. However, controlled production of very low H_2O_2 concentrations is beneficial for catalyst stability and catalysis is extremely efficient with the new electron transfer system.

Also, C14:0 substrate concentrations were increased (and thereby kept equimolar to NADPH concentration). The maximum TTN achieved with this experiment was 2255 (5 mM C14:0 FA). The highest TTN reported before with OleT was 2096, applying 5 mM C18:0 FA and the CamAB-FDH redox system [35].

Besides of this new electron transfer system, the gene for a second cytochrome P450 enzyme ($\text{P450}_{\text{I}\alpha}$) was isolated from *Jeotgalicoccus sp.* ATCC8456 and expressed in *E. coli* BL21(DE3) cells. It has been discovered that $\text{P450}_{\text{I}\alpha}$ is an extremely efficient peroxygenase with synthetic potential for fatty acid α -hydroxylation. About 93% of C10:0 FA substrate were converted when using an equimolar amount of H_2O_2 and reaction selectivity towards α -hydroxylation is very high (>98%).

5 Additional Data and Information

5.1 DNA and protein sequences

Fdx_J (BASYS00361); Ferredoxin

DNA sequence:

ATGTGCGCTAAGAAATACACAATCGTTGACCAAGATACTTGTATCGCATGCGGCGCCTGC
GGAGCAGCAGCACCCGGATATTTATGATTATGATGATGACGGTATTGCTTATGTTATCTTA
GATGACAATAAAGGCATTACTGCTGTACCAGAAGATCTTCTGGAAGATATGGAAGATGCA
TTTGATGGCTGTCCGACAGATTCAATTAAGTTGAAGAAGAACCATTTGATGGTGATCCA
TTGAAGTATGAATAG

Amino acid sequence:

MCAKKYTIVDQDTCIACGACGAAAPDIYDYDDDGIAYVILDDNKGITAVPEDLLEDMEDA
FDGCPTDSIKVEEPPFDGDPLKYE

FdR_{J1} (BASYS01288); Ferredoxin-NADP-reductase, trxB

DNA sequence:

ATGAAAGATGAAATTACAGATATAACAATTATTGGCGGTGGACCAACAGGTCTATTCTCT
ACATTCTATGCTGGAATGAGACAGATGTCTGTACGCTTAATCGATAGCTTACCTGAATTA
GGTGGACAGTTAACTGAACTTTATCCGGATAAATATATTTATGATGTCGGCGGATTCCA
AAAATCCTCGCCAAAGATCTTGTAATAATTTAGTGAACAGGGCGAAATACGCTGAACCT
GATTTTCATTTAGGTGAACTGTTCAATCATATAGAAAAGAAGATGATCACTTTGTCCTA
ACAACGGACAAAGGTGAATATTTAACACGTACAATTTTGATTACAGCTGGTGTGCGCGCT
TTCCAACCTAGAAACTTGGTCTAGAAAATGAAGTAGAATTCGAAGGCGCTTCCCTACAA
TATGCTGTTTCGTGATTTAGAAAAATTCAAAGATAAAGATGTCGTCGTTCTTGGCGGCGGT
GACTCAGCACTTGACTGGGCACTCATGTTAGAAAACTTGCTAAATCAGTCACACTTGTG
CACAGACGTGAACGTTTTACAGCACATGAAACGACAGTCCAACAAGTTAAAGACTCCAGT
GTAACAGTTAAAACATCTCTTAATGTAACAGAAATTAAGGGTGATGCAGGTCAGATTGAA
GAATTAGTTTTAACGGCTAAAGATGGTAGCGAAGAAGTAATTCAAGCAGACCAACTTATC
GTTAACTTTGGTAACATTTCTTCACTAGGACCACTTAAAGATTGGGGTCTAAAGCTGGAT
AAAAACTCAATCGAAGTAGATGCTCACATGCAGACAAACATCGAAGGTATCTTCGCAGCA
GGAGATGTCACTACCTTTGAAGGTAAAGTTAAACTAATTGCCACTGGATTCCGGTGAGGCA
CCAGTCGCAATTTCATAACGCTAAATCTTCATACGATGCTAAGTCTCGTATCCAACCAAAA
CACTCTACAAGTGTCTTCAAACAAAATTA

Amino acid sequence:

MKDEITDITIIGGGPTGLFSTFYAGMRQMSVRLIDSLPELGGQLTELYPDKYIYDVGGFP
KILAKDLVNNLVEQAKYAEPDFHLGETVQSYRKEDDHFVLTDDKGEYLTRTILITAGVGA
FQPRKLGLENEVEFEGASLQYAVRDLEKFKDKDVVVLGGGDSALDWALMLEKLAKSVTLV
HRRERFTAHETTVQQVKDSSVTVKTSLNVTIIEKGDAGQIEELVLTAKDGSSEVIQADQLI
VNFNGNISSLGPLKDWGLKLDKNSIEVDAHMQTNIIEGIFAAGDVTTFEGKVKLIATGFGEA
PVAISYAKSSYDAKSRIQPKHSTSVFKQN

OleT (BASYS00724); CYP152L1

DNA sequence:

TTGGCATTGGCTTTACTGTTTATATATAATGGTAGAGTACATTCTGAATTGGAGGAATGAA
ATTATGGCAACACTTAAGAGGGATAAGGGCTTAGATAATACTTTGAAAGTATTAAGCAA
GGTTATCTTTACACAACAAATCAGAGAAATCGTCTAAACACATCAGTTTTCCAACTAAA
GCACTCGGTGGTAAACCATTCTGAGTTGTGACTGGTAAGGAAGGCGCTGAAATGTTCTAC
AACAATGATGTTGTTCAACGTGAAGGCATGTTACCAAACGTATCGTTAATACGCTTTTT
GGTAAAGGTGCAATCCATACGGTAGATGGTAAAAACACGTAGACAGAAAAGCATTGTTC
ATGAGCTTGATGACTGAAGGTAACCTGAATTATGTACGAGAATTAACGCGTACATTATGG
CATGCGAACACACAACGTATGGAAAGTATGGATGAGGTAATATTTACCGTGAATCTATC
GTACTACTTACAAAAGTAGGAACACGTTGGGCAGGCGTTCAAGCACCACTGAAGATATC
GAAAGAATCGCAACAGACATGGACATCATGATCGATTCAATTTAGAGCACTTGGTGGTGCC
TTTAAAGGTTACAAGGCATCAAAGAAGCACGTCGTCGTGTTGAAGATTGGTTAGAAGAA
CAAATTATTGAGACTCGTAAAGGGAATATTCATCCACCAGAAGGTACAGCACTTTACGAA
TTTGACATTGGGAAGACTACTTAGGTAACCAATGGACTCAAGAACTTGTGCGATTGAC
TTAATGAACACATTCCGCCATTAATCGCAATCAACAGATTCTTTTATTCCGTTTACAC
GCGATGAACGAAAACCAATCACACGTGAAAAAATTAATCAGAACCTGACTATGCATAT
AAATTCGCTCAAGAAGTTCGTCGTTACTATCCATTCTGTTCCATTCTTCCAGGTAAAGCG
AAAGTAGACATCGACTTCCAAGGCGTTACAATCCTGCAGGTGTAGGTCTTGCATTAGAT
GTTTATGGTACAACGCATGATGAATCACTTTGGGACGATCCAAATGAATTCGCCCAGAA
AGATTGAAACTTGGGACGGATCACCAATTTGACCTTATTCCACAAGGTGGTGGAGATTAC
TGGACAAATCACCGTTGTGCAGGTGAATGGATCACAGTAATCATCATGGAAGAAACAATG
AAATACTTTGCAGAAAAAATAACTTATGATGTTCCAGAACAAGATTTAGAAGTGGACTTA
AACAGTATCCCAGGATACGTTAAGAGTGGCTTTGTAATCAAAAATGTTTCGCGAAGTTGTA
GACAGAACATAA

Amino acid sequence:

MALALLFIYNGRVHSNWRNEIMATLKRDKGLDNTLKVLRKQGYLYTTNQRNRLNTSVFQTK
ALGGKPFVVVTGKEGAEMFYNNVQREGMLPKRIVNTLFGKGAIHTVDGKKHVDRKALF
MSLMTEGNLNYVRELTRTLWHANTQRMESMDEVNIYRESIVLLTKVGRWAGVQAPPEDI
ERATDMDIMIDSFRALGGAFKGYKASKEARRRVEDWLEEQIETRKGNIHHPPEGTALYE
FAHWEDYLGPNMDSRTCAIDLMTFRPLIAINRFVSFGLHAMNENPITREKIKSEPDYAY
KFAQEVRRYYPFVPLPGKAKVDIDFQGV TIPAGVGLALDVYGTTHDESLWDDPNEFRPE
RFETWDGSPFDLIPQGGGDYWTNHRCAGEWITVII MEETMKYFAEKITYDVPEQDLEVDL
NSIPGYVKSGFVIKNVREVVDR

P450_{Jα} (BASYS00261)

DNA sequence:

ATGAATTCAAATATGCCAAATGATTCTGGTTTCGACAAGACTTTAAGCGTCTTAAAGAG
GGTTATGAATTCGTCATGAACCGTGACAAGGAAATGCATACAAACATTTTCGAAACACGT
ATCCTCGTTGAAAAGACAATCTGCCTCACAGGTAGTGAGCTCGCTGAACTATTTTACGAC
AACACCCGCTTCAGCCGCACTGATGCTGCACCTGCCAGAGTACAAAAACACTTTTCGGT
GAAGGTGGCGTACAAGGTCTCGATGGTGATGAACACAAAAACCGTAAAGCGATGTTTCATG
TCTTAATGGATAACAAAGCGATGGATGAAATAGAAGATTTAACACAGAAATATTGGCAC
GAATACTTTGAAGAAATTGATTGGAACGACACCGTAGAGTTATATGAAGCAGCGAAAGTT
GTATTTCTCAAAGTCGCTTGTGACTGGGTTGGAGTGTCTCTAGAAGATGAAGACATCGAA
ACTCGTGCCAGTCAGATTGCCGATTTATACGAATCACCTGCAGCACTCGGAATCCAACAC
TGGAAGGGACGTAAATCTAGATCAGAAGCAGAAGACTGGATTGAGCGACTTATTGAAGGT
GTTAGAAACGGTGAGCTTGAAGCAGACAAAGATAGAGCACTCTATAAGTTCGCTATGCAC
AAAGATTTAAATGATGAACTCTGGATGCTCAAGTTGCTACAGTTGAGCTTTTAAACCTC
ATTCGTCCAATTAATGCTATCAGTGTATGGGTTGCAATGATTGGTCTCGCTATTCATGAA
CACCCAGACGCTGCAGAGAAATTGAAAGATGCCAATCAACAACAATTAGAGTGGTTCATT
CAAGAAGTCAGACGTTATTATCCCTTCTTCCATTTCGAGTGGCACGAGTGAAACTCGAT
TTCGAATGGCAAGGTTATGAGTTTAAAGAAGGCACTTTAACACTATTAGACTTATACGGT
ACCAACCGTCATCCAGACGACTGGGTAGACCCTGATGAATTTAAACCCGAAAGATTTGAA
GGTTGGCAAGAGACACCACTTCACTTTATACCACAAGGTGGTGGATCTTACGACTTCGGT
CACCGCTGTGCAGGGGAGTTTATCACAATCGTCATGATGAGAACAACACTCGACTTTTAA
GTCAATCACCTAGAATTCAAAGTACCAGAACAAGATTTTGGCTTTGAATTTAACGATATT
CCAGCTGTTCTAATGACAAAGTGAAGATTAAGCCAACACGTATCAAATAA

Amino acid sequence:

MNSNMPNDSGFDKTLVSLKEGYEFVMNRDKEMHTNIFETRILVEKTICTLGSELAELFYD
NTRFSRTDAAPARVQKTLFEGGGVQGLDGDEHKNRKAMFMSLMDNKAMDEIEDLTQKYWH
EYFEEIDWNDTVELYEAAKVVFLKVACDWVGVSLLEDEDIETRASQIADLYESPAALGIQH
WKGRKRSRSEAEDWIERLIEGVRNGELEADKDRALYKFAMHKDLNDELDAQVATVELLNL
IRPINAISVWVAMIGLAIHEHPDAAEKLKDANQQQLEWFIQEVRRYYPFFPFAVARVKLD
FEWQGYEFKEGTLTLLDLYGTNRHPDDWVDPDEFKPERFEGWQETPFNFIPQGGGSYDFG
HRCAGEFITIVMMRTTLDLFLVNHLEFKVPEQDFGFEFNDIPAVPNDKVKIKPTRIK

5.2 Positions of all used enzymes in the *Jeotgalicoccus sp.* ATCC 8456 genome

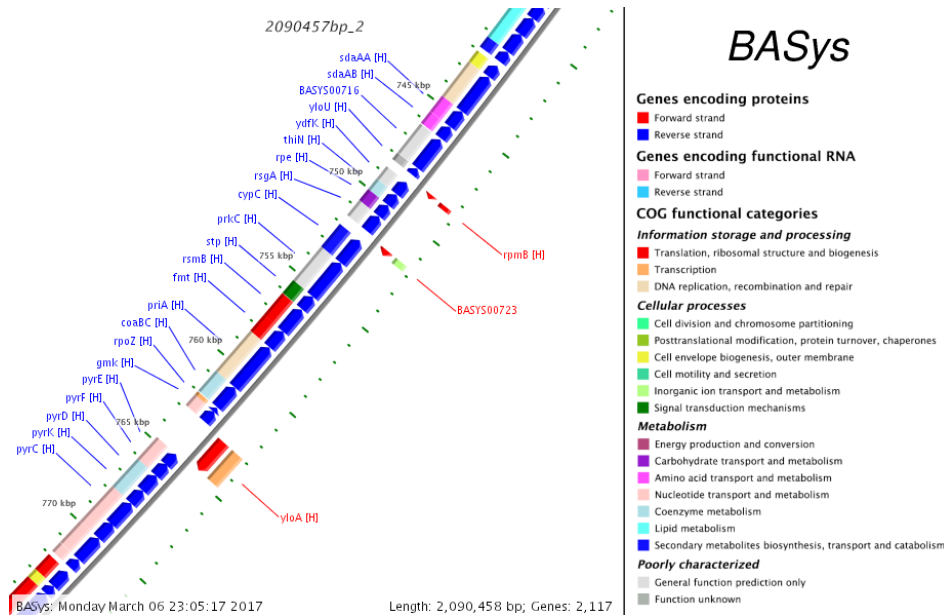


Figure 49 Position of the gene for OleT (BASYS00724 *cypC*) in the *Jeotgalicoccus sp.* ATCC8456 genome.

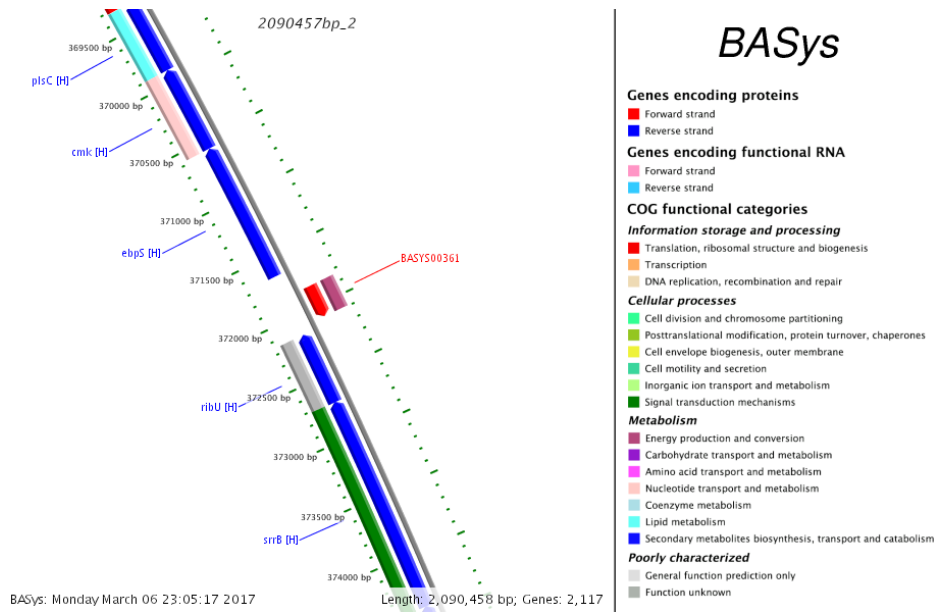


Figure 50 Position of the gene for Fdx₁ (BASYS00361) in the *Jeotgalicoccus sp.* ATCC8456 genome.

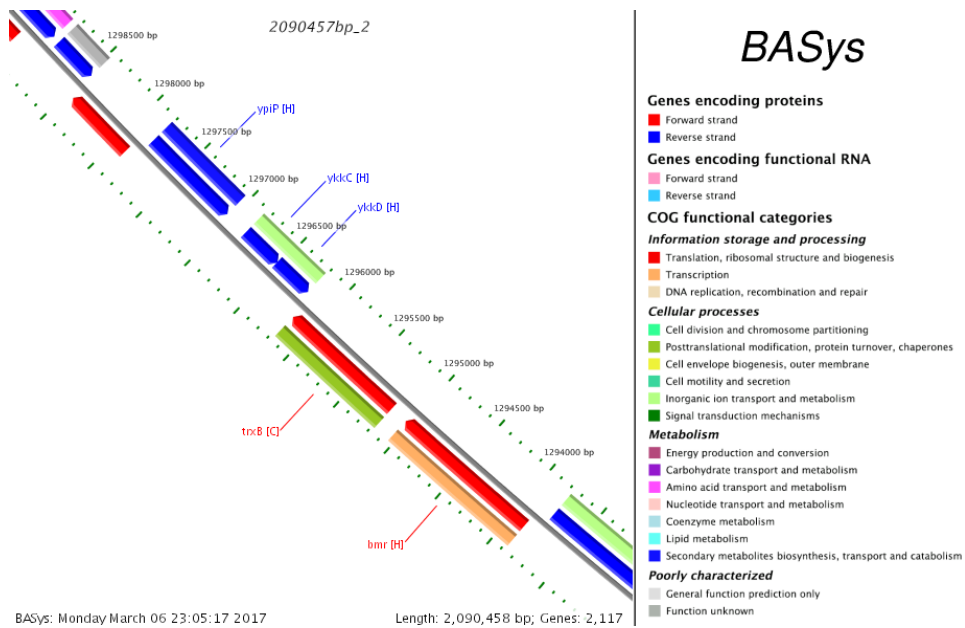


Figure 51 Position of the gene for FdR₁₁ (BASYS01288 trxB) in the *Jeotgalicoccus sp.* ATCC8456 genome.

P450_{Jα} BASYS00261

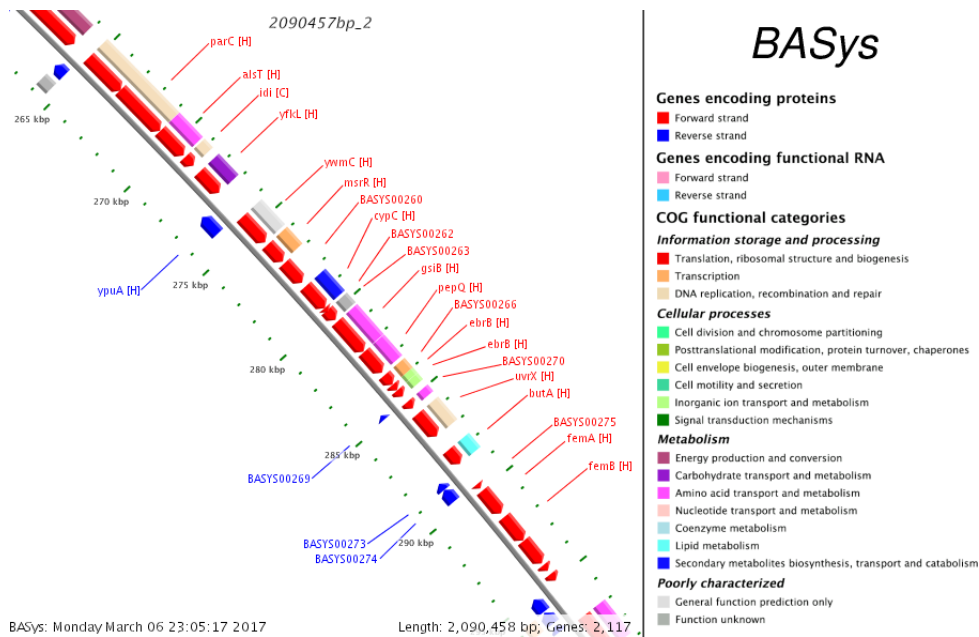


Figure 52 Position of the gene for P450_{Jα} (BASYS00261) in the *Jeotgalicoccus sp.* ATCC8456 genome.

5.3 Supplementary information regarding LC-MS/MS analysis

SDS gel bands were digested with a standard-protocol and analyzed with LC-MS/MS:

LC-MS/MS analysis was done in a 120 minutes run (CID, Top20) using nanoHPLC (Ultimate 3000 RSLCnano system - Dionex) in combination with Orbitrap Velos Pro. Data-evaluation was carried out with the software proteome discoverer, including the following search criteria: used data banks: whole proteome of the original strain according to .fasta file & general lab contaminations, enzyme: semiTrypsin, max. missed cleavage sites: 2; Cys modification: carbamidomethylation (static modification); variable Met modification: oxidation; MS/MS ion search with decoy database search included; precursor mass tolerance +/- 10 ppm; product mass tolerance +/- 0.7 Da; acceptance parameters: peptide mass deviation:10ppm; peptide confidence: high; minimum 2 peptides; ion score cut off: 20 and a maximum peptide rank:1.

Analysis of the 15 kDa band obtained by repeating the OleT purification protocol by *Rude et al.* (2011) led to 72 protein-hits, among them several proteins with a size of about 15 kDa [11].

Analysis of the ~18 kDa band obtained from purification of heterologously produced Fdx_J resulted in 7 hits (including mainly human proteins and BASYS00361) (table 32).

Table 30 LC-MS/MS protein analysis hits. Heterologous expressed Fdx_j (highlighted in grey) was excised from SDS gel and submitted to LC-MS/MS analysis because band height did not correspond to the theoretical weight of the protein.

Accession	Description	Score	Coverage	# Proteins	# Unique Peptides	# Peptides	# PS Ms	# AAs	MW [kDa]	calc. pI
P35527	Keratin, type I cytoskeletal 9 OS=Homo sapiens GN=KRT9 PE=1 SV=3 - [K1C9_HUMAN]	1665.48	51.69	1	26	26	39	623	62.0	5.24
P04264	Keratin, type II cytoskeletal 1 OS=Homo sapiens GN=KRT1 PE=1 SV=6 - [K2C1_HUMAN]	1542.73	36.49	1	24	27	35	644	66.0	8.12
P13645	Keratin, type I cytoskeletal 10 OS=Homo sapiens GN=KRT10 PE=1 SV=6 - [K1C10_HUMAN]	1460.00	30.48	1	21	21	31	584	58.8	5.21
P00766	Chymotrypsinogen A OS=Bos taurus PE=1 SV=1 - [CTRA_BOVIN]	817.25	34.29	1	12	12	22	245	25.6	8.16
P35908	Keratin, type II cytoskeletal 2 epidermal OS=Homo sapiens GN=KRT2 PE=1 SV=2 - [K22E_HUMAN]	833.01	23.00	1	15	18	18	639	65.4	8.00
P00002	BASYS00361 BASYS00361, 371840-372094 (Clockwise) Ferredoxin [H]	528.41	76.19	1	9	9	13	84	9.1	3.88
B7L4L6	30S ribosomal protein S7 OS=Escherichia coli (strain 55989 / EAEC) OX=585055 GN=rpsG PE=3 SV=1 - [RS7_ECO55]	233.66	19.23	2	3	3	5	156	17.6	10.30

5.4 Cyt c reduction experiment - output SigmaPlot

Nonlinear Regression

Data Source: Data 1 in Notebook1

Equation: Hyperbola; Single Rectangular, 2 Parameter

$$f = a * x / (b + x)$$

R	Rsqr	Adj Rsqr	Standard Error of Estimate
0,9901	0,9803	0,9782	0,0021

	Coefficient	Std. Error	t	P	VIF
a	0.0432	0.0018	23.8916	<0.0001	2.7365
b	12.4396	1.8119	6.8657	<0.0001	2.7365

5.5 GC-MS spectra

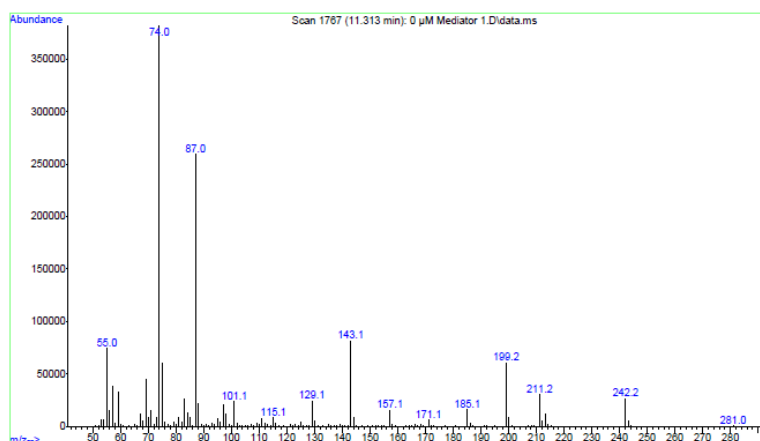


Figure 53 GC-MS spectrum of myristic acid methyl ester (C14:0 FA substrate).

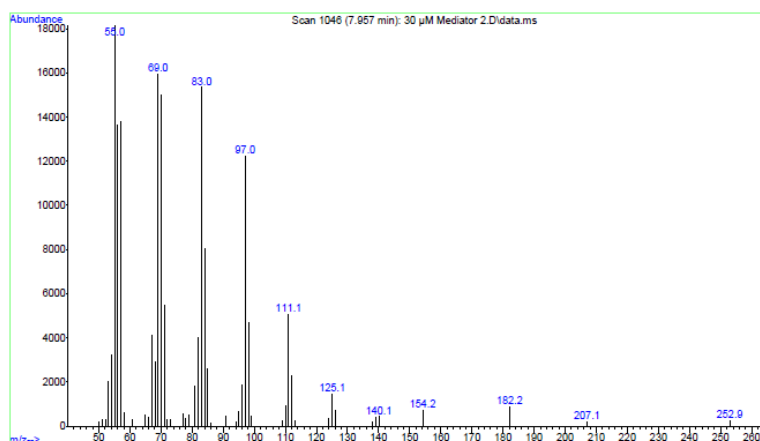


Figure 54 GC-MS spectrum of 1-tridecene produced from C14:0 FA conversion with OleT (main product) [35].

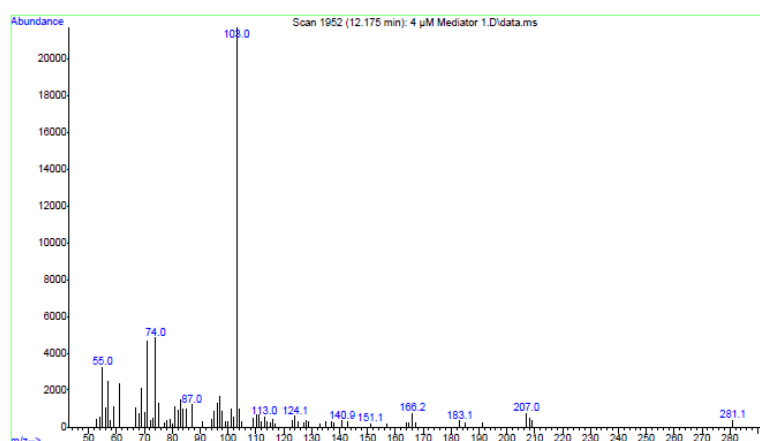


Figure 55 GC-MS spectrum of β -hydroxy myristic acid methyl ester produced from C14:0 FA conversion with OleT (side product) [35].

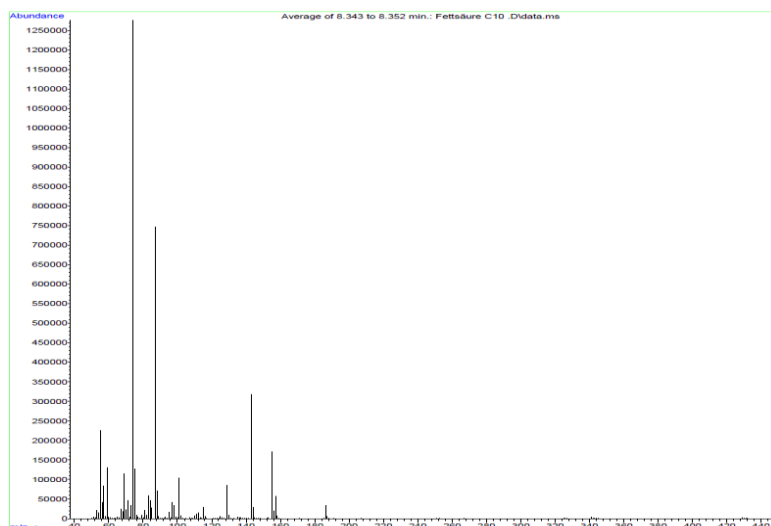


Figure 56 GC-MS spectrum of decanoic acid methyl ester.

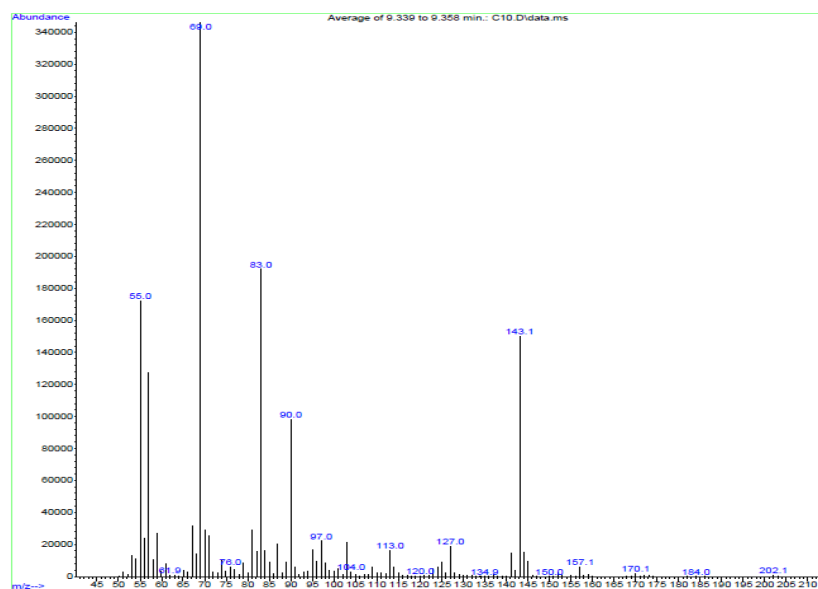


Figure 57 GC-MS spectrum of α -hydroxy decanoic acid methyl ester produced from C10:0 FA conversion with P450_{J α} .

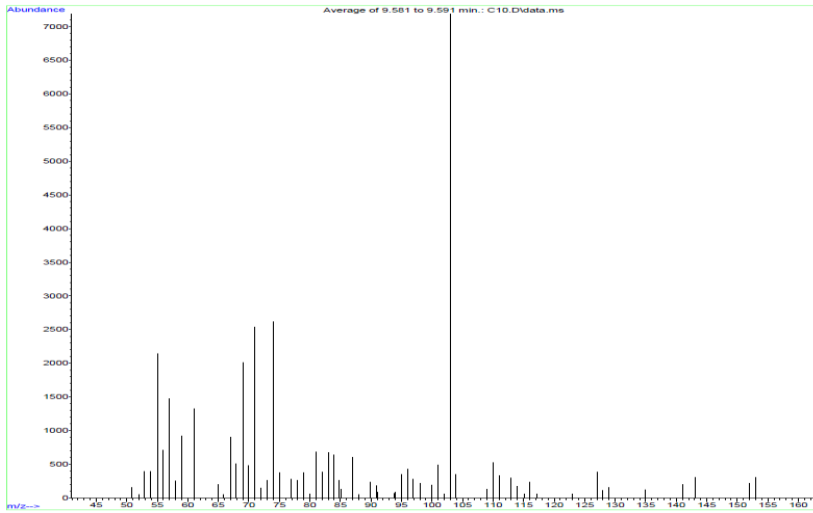


Figure 58 GC-MS spectrum of β -hydroxy decanoic acid methyl ester produced from C10:0 FA conversion.

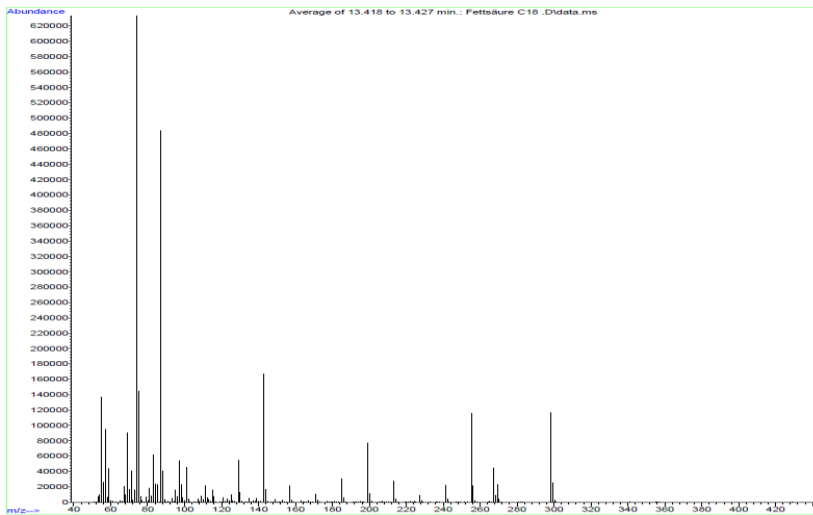
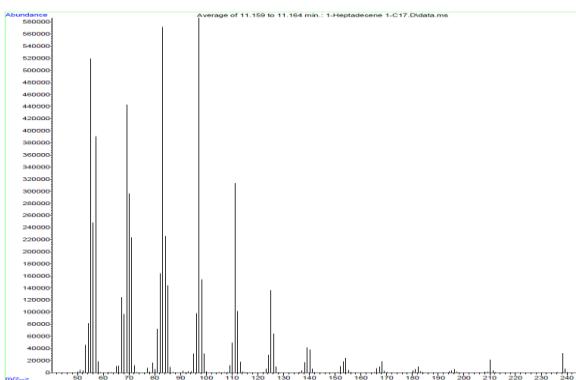


Figure 59 GC-MS spectrum of stearic acid methyl ester.

A



B

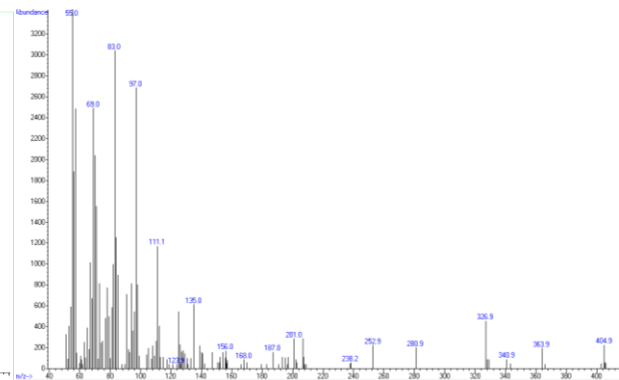


Figure 60 GC-MS spectrum of 1-heptadecene. A) analytical standard. B) obtained by C18:0 FA conversion from the putative OleT containing fraction (3.1 figure 17B).

5.6 GC-MS traces of fatty acid conversions

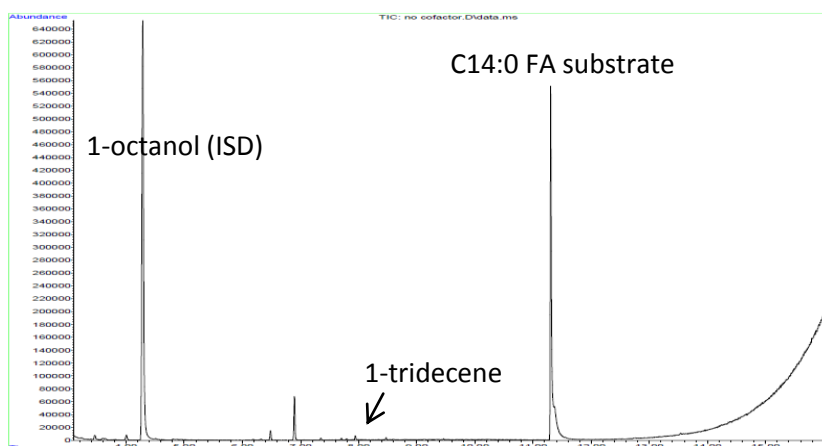


Figure 61 Conversion of C14:0 FA. Control reaction without NAD(P)H. Reactions contained 1 μM FdR_{J1}, 30 μM Fdx_J, 1 μM OleT and 400 μM C14:0 FA substrate.

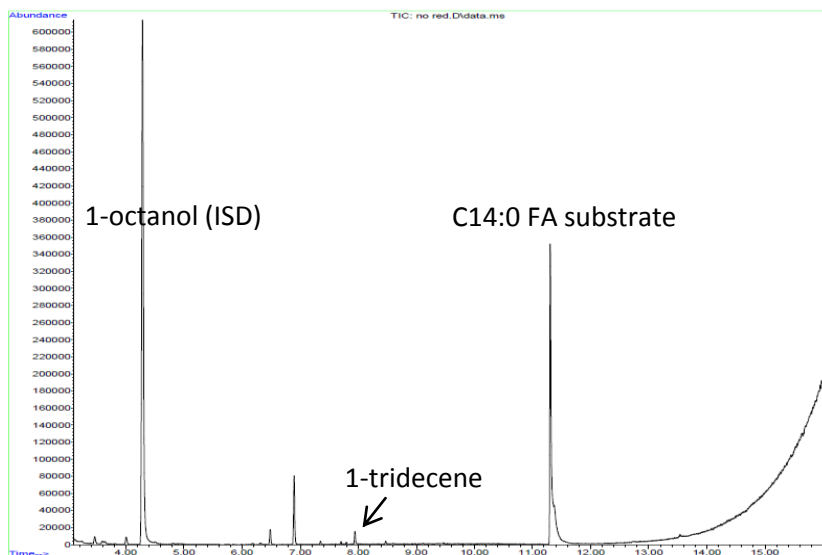


Figure 62 Conversion of C14:0 FA. Control reaction without FdR_{J1}. Reactions contained 30 μM Fdx_J, 1 μM OleT_{Je}, 400 μM NADPH and 400 μM C14:0 FA substrate.

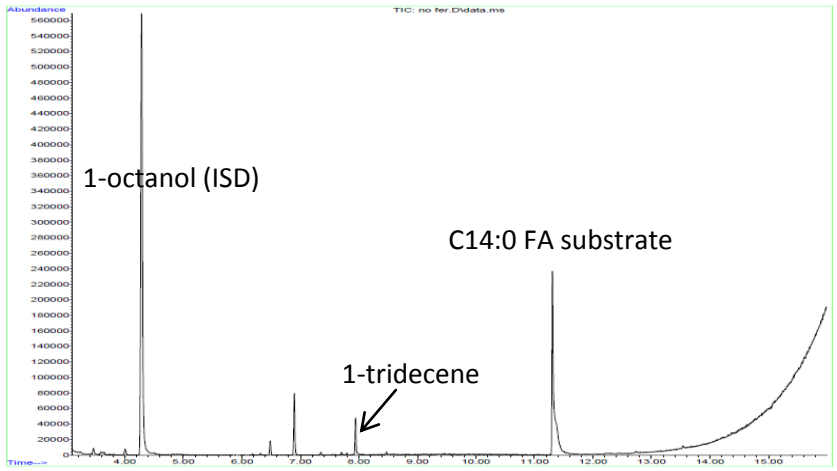


Figure 63 Conversion of C14:0 FA. Control reaction without Fdx_J. Reactions contained 1 μM FdR_{J1}, 1 μM OleT_{Je}, 400 μM NADPH and 400 μM C14:0 FA substrate.

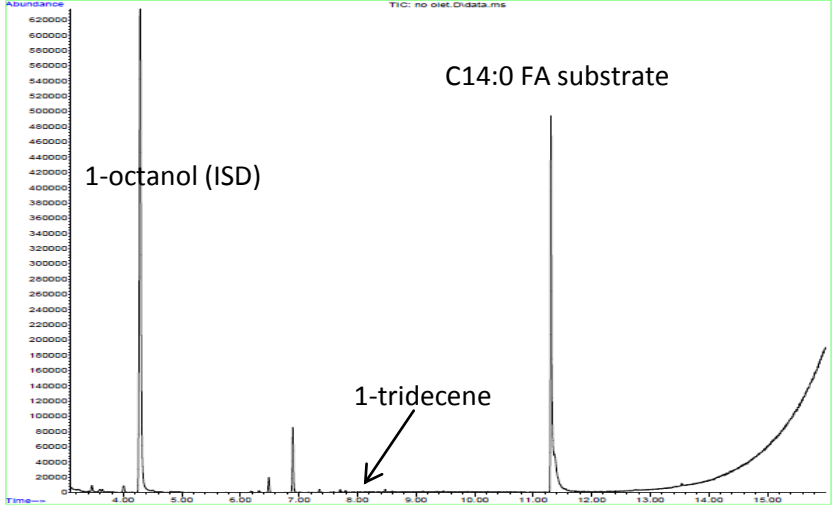


Figure 64 Conversion of C14:0 FA. Control reaction without OleT_{Je}. Reactions contained 1 μM FdR_{J1}, 30 μM Fdx_J, 400 μM NADPH and 400 μM C14:0 FA substrate.

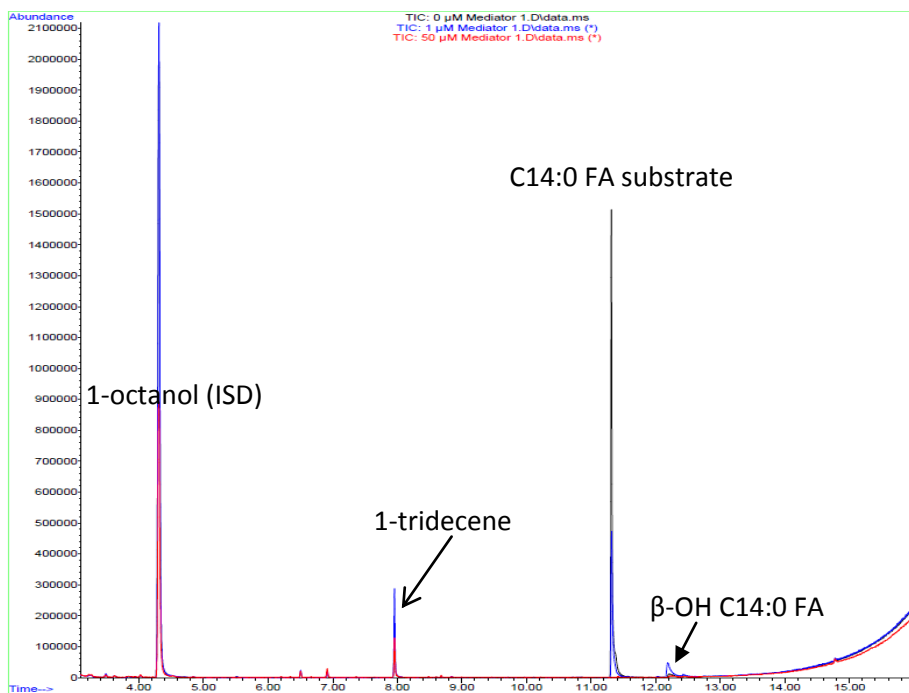


Figure 65 Overlay of GC-MS chromatograms of reactions containing different amounts of Fdx_J (0 μM, 1 μM or 50 μM). Reactions contained 1 μM FdR_{J1}, 1 μM OleT_{Je}, 400 μM NADPH and 400 μM C14:0 FA substrate.

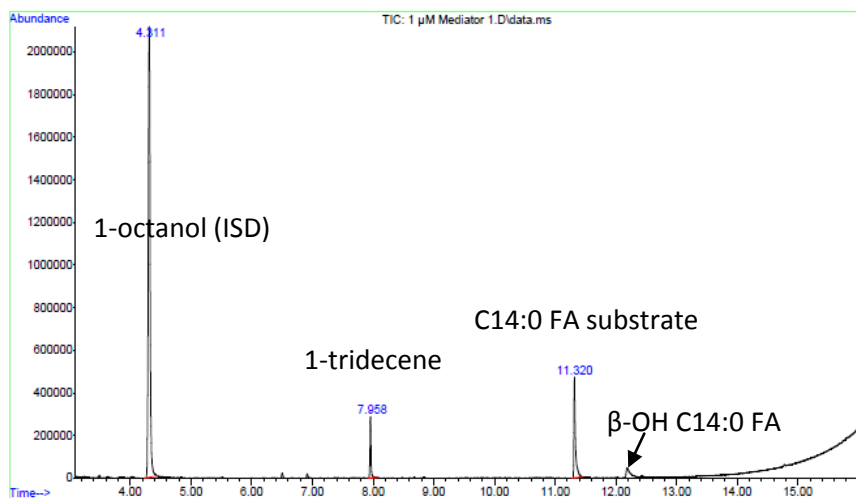


Figure 66 GC-MS chromatogram of reaction containing 1 μM of Fdx_J. Reactions contained 1 μM FdR_{J1}, 1 μM OleT, 400 μM NADPH and 400 μM C14:0 FA substrate.

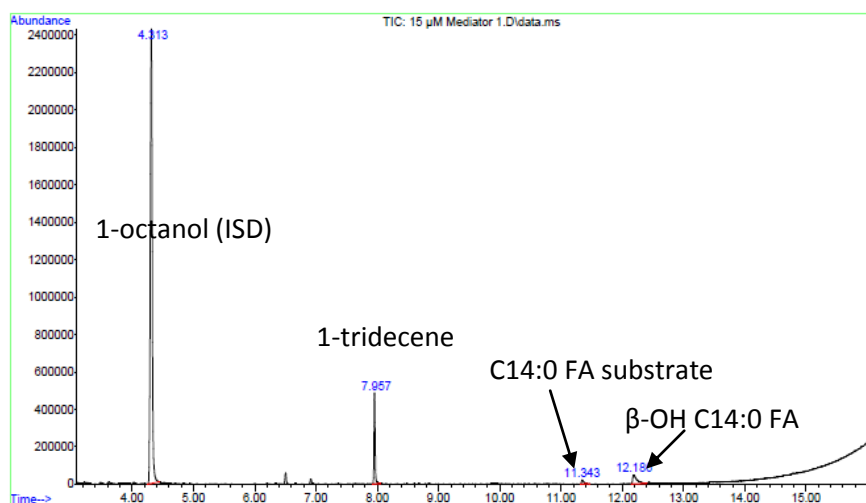


Figure 67 GC-MS chromatogram of reaction containing 15 μM of Fdx_j. Reactions contained 1 μM FdR_{j1}, 1 μM OleT_{je}, 400 μM NADPH and 400 μM C14:0 FA substrate.

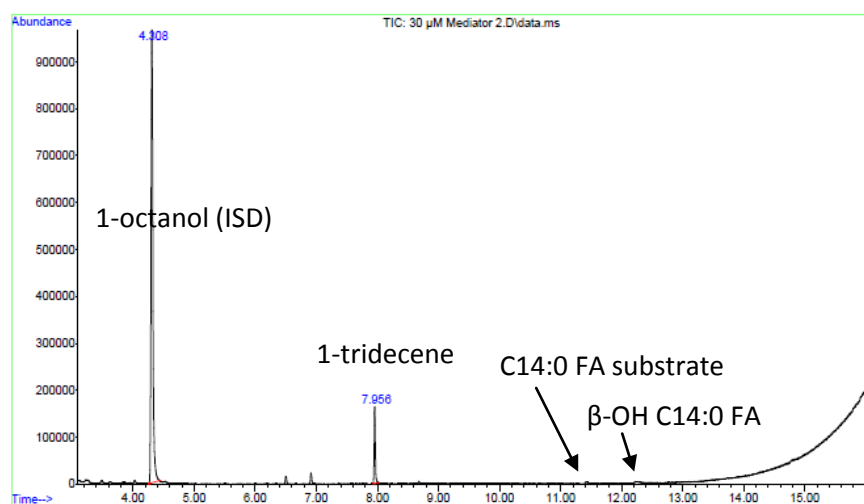


Figure 68 GC-MS chromatogram of reaction containing 30 μM of Fdx_j. Reactions contained 1 μM FdR_{j1}, 1 μM OleT_{je}, 400 μM NADPH and 400 μM C14:0 FA substrate.

5.7 Impact of catalase addition on fatty acid conversion

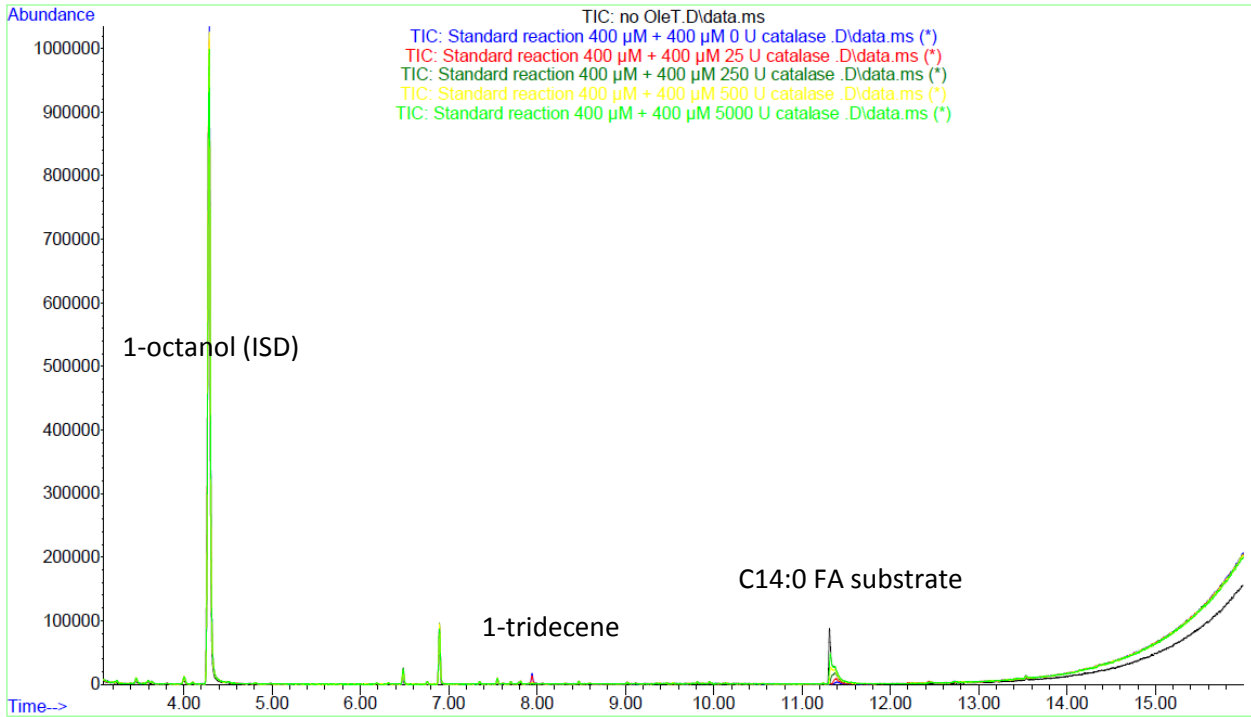


Figure 69 GC/MS spectra of catalase study reactions.

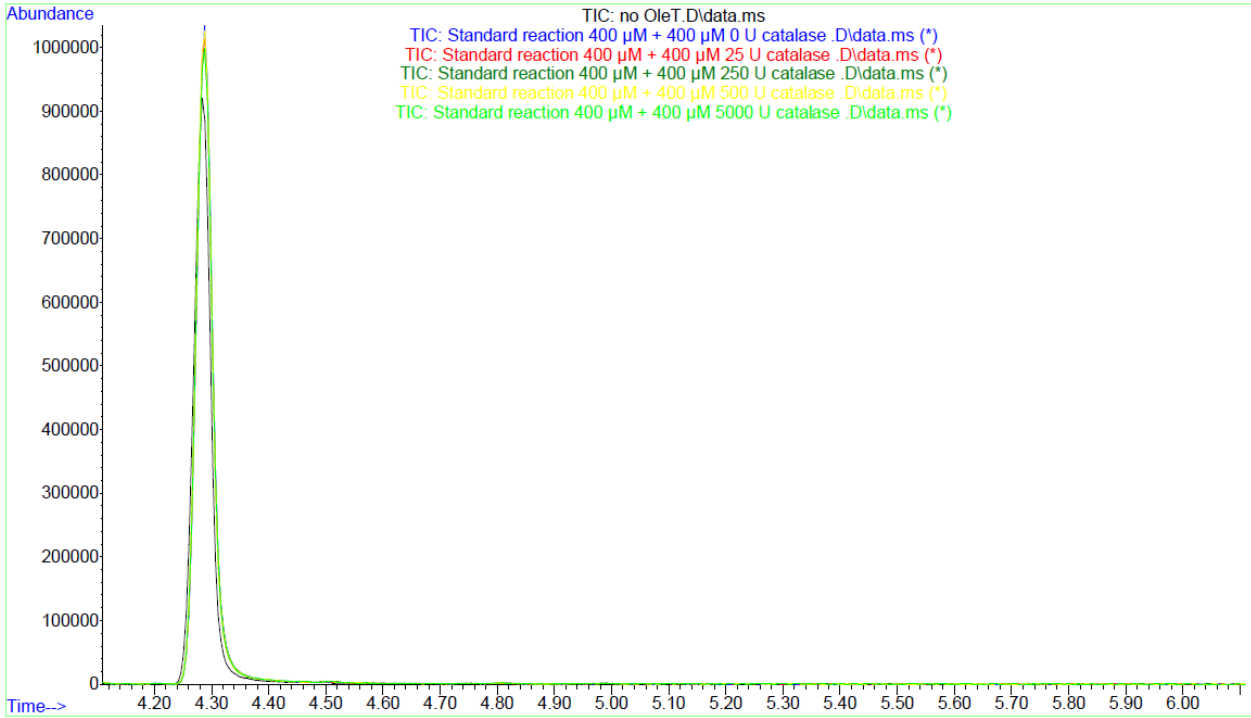


Figure 70 Catalase study 1-octanol (ISD).

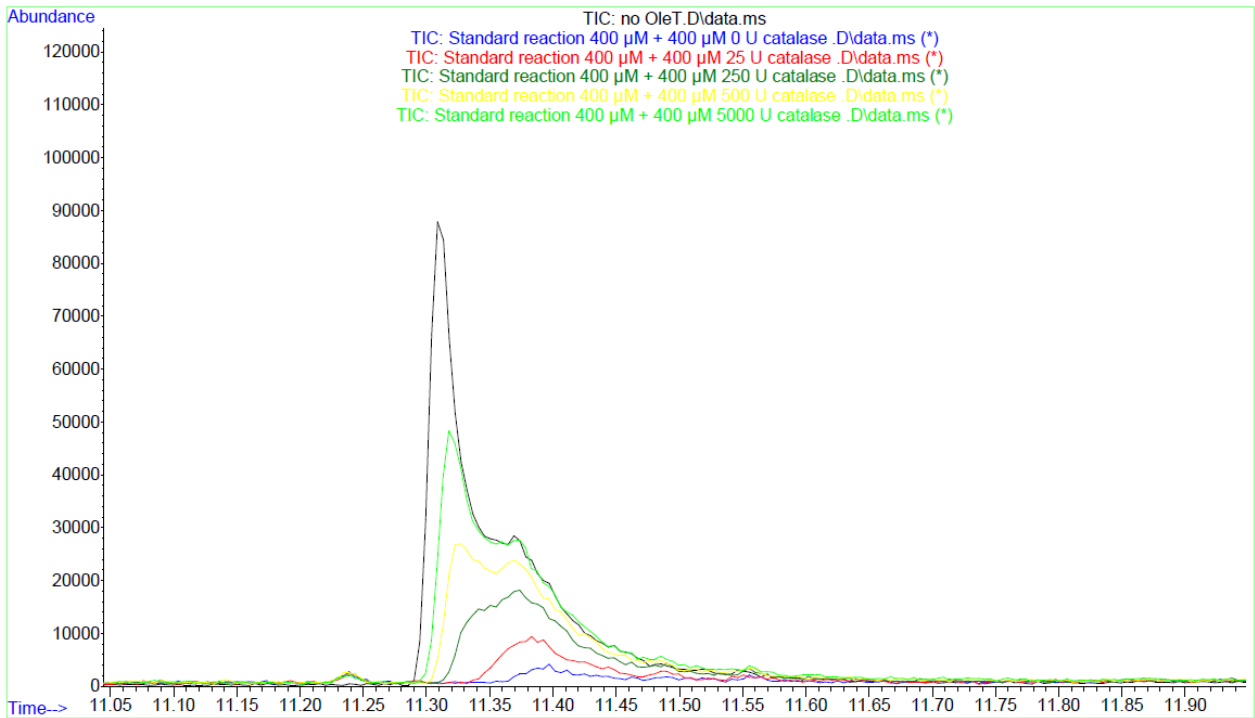


Figure 71 Catalase study substrate peak overlay. Increasing amounts of catalase (0 to 5000 U ml⁻¹) were applied. With increasing concentration of catalase, less substrate is converted. Black: Control without OleT (100% standard).

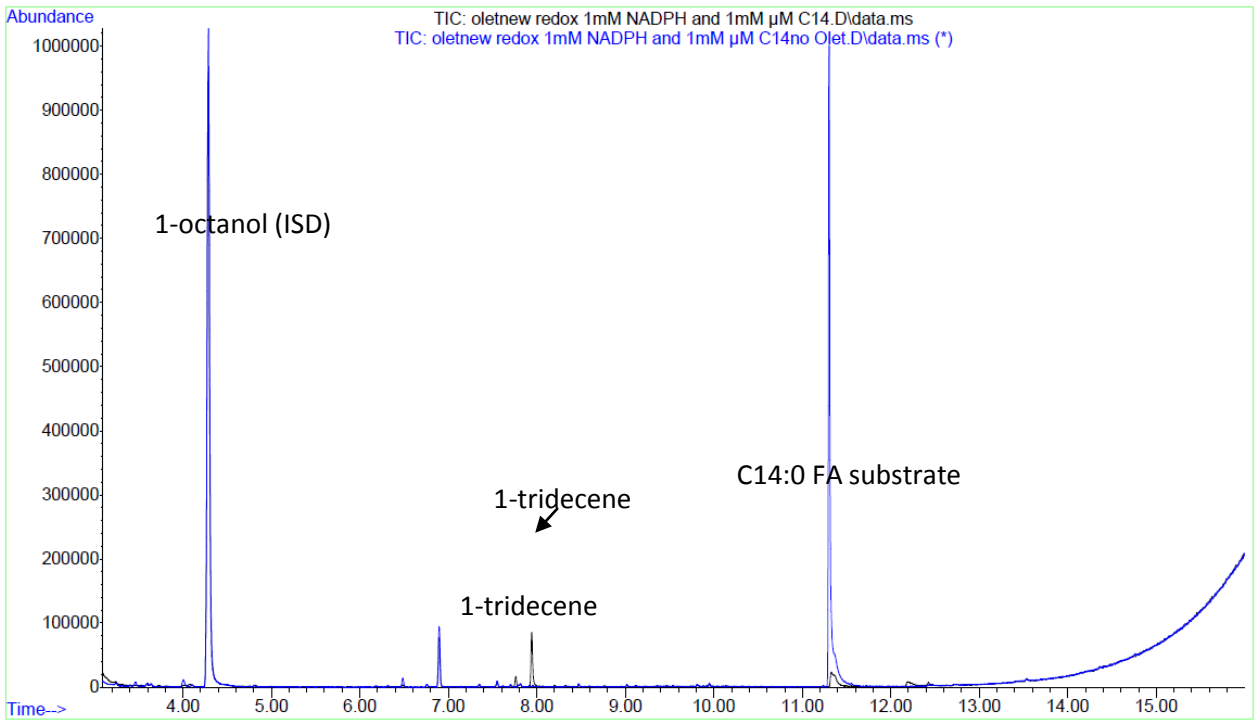


Figure 72 NADPH/ substrate concentration study. 1 mM FA was converted using 1 mM NADPH (black lane). Also a control reaction without OleT is shown (blue lane).

6 References

- [1] M. A. Rude and A. Schirmer, "New microbial fuels: a biotech perspective," *Curr. Opin. Microbiol.*, vol. 12, no. 3, pp. 274–281, Jun. 2009.
- [2] S. Ray, P. V. C. Rao, and N. V Choudary, "Poly- α -olefin-based synthetic lubricants: a short review on various synthetic routes," *Lubr. Sci.*, vol. 24, no. 1, pp. 23–44, Sep. 2011.
- [3] P. P. Peralta-Yahya, F. Zhang, S. B. del Cardayre, and J. D. Keasling, "Microbial engineering for the production of advanced biofuels," *Nature*, vol. 488, p. 320, Aug. 2012.
- [4] C. Lu *et al.*, "An Engineered Self-Sufficient Biocatalyst Enables Scalable Production of Linear α -Olefins from Carboxylic Acids," *ACS Catal.*, vol. 8, no. 7, pp. 5794–5798, Jul. 2018.
- [5] M. Eramo, "Ethylene Forum," *Ethyl. Mark. Outlook*, 2013.
- [6] G. J. Blomquist and L. L. Jackson, "Chemistry and biochemistry of insect waxes," *Prog. Lipid Res.*, vol. 17, no. 4, pp. 319–345, 1979.
- [7] J. A. McIntosh, M. S. Donia, and E. W. Schmidt, "Ribosomal Peptide Natural Products: Bridging the Ribosomal and Nonribosomal Worlds," *Nat. Prod. Rep.*, vol. 26, no. 4, pp. 537–559, Apr. 2009.
- [8] H. Fukuda, T. Fujii, and T. Ogawa, "Microbial production of c3- and c4-hydrocarbons under aerobic conditions," *Agric. Biol. Chem.*, vol. 48, no. 6, pp. 1679–1682, 1984.
- [9] A. Dennig, A. Thiessenhusen, S. Gilch, T. Haas, and M. Hall, "Biotechnologische Herstellung terminaler Alkene und Diene," *BIOspektrum*, vol. 22, no. 6, pp. 614–616, Oct. 2016.
- [10] Y. Liu, K. E. Kim, M. B. Herbert, A. Fedorov, R. H. Grubbs, and B. M. Stoltz, "Palladium-Catalyzed Decarbonylative Dehydration of Fatty Acids for the Production of Linear Alpha Olefins," *Adv. Synth. Catal.*, vol. 356, no. 1, pp. 130–136, Jan. 2014.
- [11] M. A. Rude, T. S. Baron, S. Brubaker, M. Alibhai, S. B. Del Cardayre, and A. Schirmer, "Terminal Olefin (1-Alkene) Biosynthesis by a Novel P450 Fatty Acid Decarboxylase from *Jeotgalicoccus* Species," *Appl. Environ. Microbiol.*, vol. 77, no. 5, pp. 1718–1727, Mar. 2011.
- [12] R. A. Kerr, "The looming oil crisis could arrive uncomfortably soon," *Science*. 2007.
- [13] OGI editors, "IEA: EXCESS OIL INVENTORIES WILL PERSIST INTO 2018," *Oil Gas J.*, vol. 115, no. 6b, p. 26, 2017.
- [14] Y.-S. Jang *et al.*, "Engineering of microorganisms for the production of biofuels and perspectives based on systems metabolic engineering approaches," *Biotechnol. Adv.*, vol. 30, no. 5, pp. 989–1000, Sep. 2012.
- [15] A. W. Munro, H. M. Girvan, and K. J. McLean, "Variations on a (t)heme—novel mechanisms, redox partners and catalytic functions in the cytochrome P450 superfamily," *Nat. Prod. Rep.*, vol. 24, no. 3, pp. 585–609, 2007.
- [16] G. I. Lepesheva and M. R. Waterman, "CYP51—the omnipotent P450," *Mol. Cell. Endocrinol.*, vol. 215, no. 1–2, pp. 165–170, Feb. 2004.
- [17] M. A. Butler, M. Iwasaki, F. P. Guengerich, and F. F. Kadlubar, "Human cytochrome P-450PA (P-450IA2), the phenacetin O-deethylase, is primarily responsible for the hepatic 3-demethylation of caffeine and N-oxidation of carcinogenic arylamines," *Proc. Natl. Acad. Sci.*, vol. 86, no. 20, p. 7696 LP-7700, Oct. 1989.
- [18] F. Hannemann, A. Bichet, K. M. Ewen, and R. Bernhardt, "Cytochrome P450 systems—

- biological variations of electron transport chains," *Biochim. Biophys. Acta - Gen. Subj.*, vol. 1770, no. 3, pp. 330–344, Mar. 2007.
- [19] R. Bernhardt, "Cytochrome P450: Structure, function, and generation of reactive oxygen species BT - Reviews of Physiology Biochemistry and Pharmacology, Volume 127," Berlin, Heidelberg: Springer Berlin Heidelberg, pp. 137–221, 1996.
- [20] B. Meunier, S. P. de Visser, and S. Shaik, "Mechanism of Oxidation Reactions Catalyzed by Cytochrome P450 Enzymes," *Chem. Rev.*, vol. 104, no. 9, pp. 3947–3980, Sep. 2004.
- [21] R. Bernhardt and V. B. Urlacher, "Cytochromes P450 as promising catalysts for biotechnological application: chances and limitations," *Appl. Microbiol. Biotechnol.*, vol. 98, no. 14, pp. 6185–6203, 2014.
- [22] J. Belcher *et al.*, "Structure and Biochemical Properties of the Alkene Producing Cytochrome P450 OleTJE (CYP152L1) from the *Jeotgalicoccus* sp. 8456 Bacterium," *J. Biol. Chem.*, vol. 289, no. 10, pp. 6535–6550, Mar. 2014.
- [23] H. Xu *et al.*, "In vitro oxidative decarboxylation of free fatty acids to terminal alkenes by two new P450 peroxygenases," *Biotechnol. Biofuels*, 2017.
- [24] Z. Rui *et al.*, "Microbial biosynthesis of medium-chain 1-alkenes by a nonheme iron oxidase," *Proc. Natl. Acad. Sci.*, vol. 111, no. 51, pp. 18237–18242, Dec. 2014.
- [25] A. Dennig, S. Kurakin, M. Kuhn, A. Dordic, M. Hall, and K. Faber, "Enzymatic Oxidative Tandem Decarboxylation of Dioic Acids to Terminal Dienes," *European J. Org. Chem.*, vol. 2016, no. 21, pp. 3473–3477, Jul. 2016.
- [26] R. Bernhardt, "Cytochromes P450 as versatile biocatalysts," *J. Biotechnol.*, vol. 124, no. 1, pp. 128–145, Jun. 2006.
- [27] M. K. Trower, R. Lenstra, C. Omer, S. E. Buchholz, and F. S. Sariaslani, "Cloning, nucleotide sequence determination and expression of the genes encoding cytochrome P-450soy and ferredoxinsoy (soyB) from *Streptomyces griseus*," *Mol. Microbiol.*, vol. 6, no. 15, pp. 2125–2134, Sep. 2018.
- [28] M. K. Trower, M. H. Emptage, and F. S. Sariaslani, "Purification and characterization of a 7Fe ferredoxin from *Streptomyces griseus*," *Biochim. Biophys. Acta - Protein Struct. Mol. Enzymol.*, vol. 1037, no. 3, pp. 281–289, 1990.
- [29] M. Ramachandra, R. Seetharam, M. H. Emptage, and F. S. Sariaslani, "Purification and characterization of a soybean flour-inducible ferredoxin reductase of *Streptomyces griseus*," *J. Bacteriol.*, vol. 173, no. 22, p. 7106 LP-7112, Nov. 1991.
- [30] A. J. Green, A. W. Munro, M. R. Cheesman, G. A. Reid, C. von Wachenfeldt, and S. K. Chapman, "Expression, purification and characterisation of a *Bacillus subtilis* ferredoxin: a potential electron transfer donor to cytochrome P450 Biol," *J. Inorg. Biochem.*, vol. 93, no. 1, pp. 92–99, 2003.
- [31] S. Kadkhodayan, E. D. Coulter, D. M. Maryniak, T. A. Bryson, and J. H. Dawson, "Uncoupling Oxygen Transfer and Electron Transfer in the Oxygenation of Camphor Analogues by Cytochrome P450-CAM: DIRECT OBSERVATION OF AN INTERMOLECULAR ISOTOPE EFFECT FOR SUBSTRATE C-H ACTIVATION," *J. Biol. Chem.*, vol. 270, no. 47, pp. 28042–28048, Nov. 1995.
- [32] P. W. Roome, J. C. Phillely, and J. A. Peterson, "Purification and properties of putidaredoxin reductase," *J. Biol. Chem.*, vol. 258, no. 4, pp. 2593–2598, Feb. 1983.
- [33] K. Faber, *Biotransformations in Organic Chemistry*, 6th ed. Springer-Verlag Berlin Heidelberg, 2011.

- [34] Y. Liu *et al.*, "Hydrogen peroxide-independent production of α -alkenes by OleTJE P450 fatty acid decarboxylase," *Biotechnol. Biofuels*, vol. 7, no. 1, p. 28, 2014.
- [35] A. Dennig *et al.*, "Oxidative Decarboxylation of Short-Chain Fatty Acids to 1-Alkenes," *Angew. Chemie Int. Ed.*, vol. 54, no. 30, pp. 8819–8822, Jun. 2015.
- [36] B. Fang *et al.*, "Mutagenesis and redox partners analysis of the P450 fatty acid decarboxylase OleTJE," *Sci. Rep.*, vol. 7, p. 44258, Mar. 2017.
- [37] C. E. Wise, C. H. Hsieh, N. L. Poplin, and T. M. Makris, "Dioxygen Activation by the Biofuel-Generating Cytochrome P450 OleT," *ACS Catal.*, pp. 9342–9352, Aug. 2018.
- [38] J. L. Grant, C. H. Hsieh, and T. M. Makris, "Decarboxylation of Fatty Acids to Terminal Alkenes by Cytochrome P450 Compound I," *J. Am. Chem. Soc.*, vol. 137, no. 15, pp. 4940–4943, Apr. 2015.
- [39] L. Hammerer, C. K. Winkler, and W. Kroutil, "Regioselective Biocatalytic Hydroxylation of Fatty Acids by Cytochrome P450s," *Catal. Letters*, vol. 148, no. 3, pp. 787–812, 2018.
- [40] M. Sarah *et al.*, "Production of alkenes and novel secondary products by P450 OleTJE using novel H₂O₂-generating fusion protein systems," *FEBS Lett.*, vol. 591, no. 5, pp. 737–750, Feb. 2017.
- [41] A. Luthra, I. G. Denisov, and S. G. Sligar, "Spectroscopic features of cytochrome P450 reaction intermediates," *Arch. Biochem. Biophys.*, vol. 507, no. 1, pp. 26–35, Mar. 2011.
- [42] S. G. Sligar and I. C. Gunsalus, "Proton coupling in the cytochrome P-450 spin and redox equilibria," *Biochemistry*, vol. 18, no. 11, pp. 2290–2295, May 1979.
- [43] J. Rittle and M. T. Green, "Cytochrome P450 Compound I: Capture, Characterization, and C-H Bond Activation Kinetics." *Science*, vol. 330, no. 6006, pp. 933–937, Nov. 2010.
- [44] I. G. Denisov, T. M. Makris, S. G. Sligar, and I. Schlichting, "Structure and chemistry of cytochrome P450," *Chemical Reviews*, 105 (6), pp. 2253–2278, April 2005.
- [45] C. H. Hsieh *et al.*, "The Enigmatic P450 Decarboxylase OleT Is Capable of, but Evolved To Frustrate, Oxygen Rebound Chemistry," *Biochemistry*, vol. 56, no. 26, pp. 3347–3357, Jul. 2017.
- [46] I. Matsunaga, T. Sumimoto, A. Ueda, E. Kusunose, and K. Ichihara, "Fatty acid-specific, regiospecific, and stereospecific hydroxylation by cytochrome P450 (CYP152B1) from *Sphingomonas paucimobilis*: Substrate structure required for α -hydroxylation," *Lipids*, vol. 35, no. 4, pp. 365–371, Apr. 2000.
- [47] A. Weckbecker and W. Hummel, "Glucose Dehydrogenase for the Regeneration of NADPH and NADH," in *Microbial Enzymes and Biotransformations*, J. L. Barredo, Ed. Totowa, NJ: Humana Press, 2005, pp. 225–238., 2005.
- [48] A. Weckbecker, H. Gröger, and W. Hummel, "Regeneration of Nicotinamide Coenzymes: Principles and Applications for the Synthesis of Chiral Compounds," in *Biosystems Engineering I: Creating Superior Biocatalysts*, C. Wittmann and R. Krull, Eds. Berlin, Heidelberg: Springer Berlin Heidelberg, 2010, pp. 195–242., Feb. 2010.
- [49] S. J. Berry and R. Rivera, G. N. Bennett, and K.-Y. San, "Metabolic Engineering of *Escherichia coli*: Increase of NADH Availability by Overexpressing an NAD⁺-Dependent Formate Dehydrogenase," *Metab. Eng.*, vol. 4, no. 3, pp. 217–229, Jul. 2002.
- [50] J. Kuper, T. S. Wong, D. Roccatano, M. Wilmanns, and U. Schwaneberg, "Understanding a Mechanism of Organic Cosolvent Inactivation in Heme Monooxygenase P450 BM-3," *J. Am. Chem. Soc.*, vol. 129, no. 18, pp. 5786–5787, May 2007.
- [51] M. K. Julsing, S. Cornelissen, B. Bühler, and A. Schmid, "Heme-iron oxygenases: powerful

- industrial biocatalysts?," *Curr. Opin. Chem. Biol.*, vol. 12, no. 2, pp. 177–186, Apr. 2008.
- [52] E. O'Reilly, V. Köhler, S. L. Flitsch, and N. J. Turner, "Cytochromes P450 as useful biocatalysts: addressing the limitations," *Chem. Commun.*, vol. 47, no. 9, pp. 2490–2501, 2011.
- [53] V. B. Urlacher and S. Eiben, "Cytochrome P450 monooxygenases: perspectives for synthetic application," *Trends Biotechnol.*, vol. 24, no. 7, pp. 324–330, Jul. 2006.
- [54] L. C. Seaver and J. A. Imlay, "Hydrogen Peroxide Fluxes and Compartmentalization inside Growing *Escherichia coli*," *J. Bacteriol.*, vol. 183, no. 24, pp. 7182–7189, Dec. 2001.
- [55] J. P. N. Ribeiro, M. A. Segundo, S. Reis, and J. L. F. C. Lima, "Spectrophotometric FIA methods for determination of hydrogen peroxide: Application to evaluation of scavenging capacity," *Talanta*, vol. 79, no. 4, pp. 1169–1176, Sep. 2009.
- [56] M. G. Tabka *et al.*, "pET System Manual," *pET Syst. Man.*, vol. 78, pp. 1–16, January 2012.
- [57] D. Hanahan, J. Jessee, and F. R. Bloom, "[4] Plasmid transformation of *Escherichia coli* and other bacteria," *Methods Enzymol.*, vol. 204, pp. 63–113, Jan. 1991.
- [58] J. A. Bornhorst and J. J. Falke, "[16] Purification of Proteins Using Polyhistidine Affinity Tags," *Methods Enzymol.*, vol. 326, pp. 245–254, 2000.
- [59] T. Omura and R. Sato, "The Carbon Monoxide-binding Pigment of Liver Microsomes I. EVIDENCE FOR ITS HEMOPROTEIN NATURE," *J. Biol. Chem.*, vol. 239, no. 7, 1964.
- [60] S. C. Gill and P. H. von Hippel, "Calculation of protein extinction coefficients from amino acid sequence data," *Anal. Biochem.*, vol. 182, no. 2, pp. 319–326, Nov. 1989.
- [61] R. H. HOLM, "TRINUCLEAR CUBOIDAL AND HETEROMETALLIC STRUCTURAL AND REACTIVITY THEMES IN CHEMISTRY AND BIOLOGY CUBANE-TYPE IRON-SULFUR CLUSTERS," in *Advances in Inorganic Chemistry*, 38th ed., Richard Cammack and A. G. Sykes, Eds. Harvard University, Cambridge, Massachusetts: Academic Press Inc. Harcourt Brace Jovanovich Publishers, pp. 1–71, 1992.
- [62] D. Prat, J. Hayler, and A. Wells, "A survey of solvent selection guides," *Green Chem.*, vol. 16, pp. 4546–4551, July 2014.
- [63] N. HASHIMOTO, T. AOYAMA, and T. SHIOIRI, "New Methods and Reagents in Organic Synthesis. 14. A Simple Efficient Preparation of Methyl Esters with Trimethylsilyldiazomethane (TMSCHN₂) and Its Application to Gas Chromatographic Analysis of Fatty Acids," *Chem. Pharm. Bull. (Tokyo)*, vol. 29, no. 5, pp. 1475–1478, 1981.
- [64] Z. ; Zheng, Y. ; Xiao, R. ; Wu, H. E. M. Christensen, F. ; Zhao, and J. Zhang, "Bacterial Electrocatalysis of K₄[Fe(CN)₆] Oxidation," *APA*, pp. 1-2, 2018.
- [65] S. G. Bell, A. B. H. Tan, E. O. D. Johnson, and L. L. Wong, "Selective oxidative demethylation of veratric acid to vanillic acid by CYP199A4 from *Rhodospseudomonas palustris* HaA2," *Mol. Biosyst.* 6, pp. 206-214, Sept. 2009.
- [66] T. Lacour, T. Achstetter, and B. Dumas, "Characterization of Recombinant Adrenodoxin Reductase Homologue (Arh1p) from Yeast: IMPLICATION IN IN VITRO CYTOCHROME P450_{11β} MONOOXYGENASE SYSTEM," *J. Biol. Chem.*, vol. 273, no. 37, pp. 23984–23992, Sep. 1998.
- [67] A. Schallmeyer, G. den Besten, I. G. P. Teune, R. F. Kembaren, and D. B. Janssen, "Characterization of cytochrome P450 monooxygenase CYP154H1 from the thermophilic soil bacterium *Thermobifida fusca*," *Appl. Microbiol. Biotechnol.*, vol. 89, no. 5, pp. 1475–1485, 2011.
- [68] P. Trinder and D. Webster, "Determination of HDL-Cholesterol Using 2,4,6-Tribromo-3-Hydroxybenzoic Acid with a Commercial CHOD—PAP Reagent," *Ann. Clin. Biochem.*, vol. 21, no. 5, pp. 430–433, Sep. 1984.

- [69] V. Vojinović, R. H. Carvalho, F. Lemos, J. M. S. Cabral, L. P. Fonseca, and B. S. Ferreira, "Kinetics of soluble and immobilized horseradish peroxidase-mediated oxidation of phenolic compounds," *Biochem. Eng. J.*, vol. 35, no. 2, pp. 126–135, Jul. 2007.
- [70] A. Córdoba, N. Alasino, M. Asteasuain, I. Magario, and M. L. Ferreira, "Mechanistic evaluation of hematin action as a horseradish peroxidase biomimetic on the 4-aminoantipyrine/phenol oxidation reaction," *Chem. Eng. Sci.*, vol. 129, pp. 249–259, Jun. 2015.
- [71] B. Meyer, D. G. Papisotiriou, and M. Karas, "100% protein sequence coverage: a modern form of surrealism in proteomics," *Amino Acids*, vol. 41, no. 2, pp. 291–310, 2011.
- [72] M. Katagiri, B. N. Ganguli, and I. C. Gunsalus, "A Soluble Cytochrome P-450 Functional in Methylene Hydroxylation," *J. Biol. Chem.*, vol. 243, no. 12, pp. 3543–3546, Jun. 1968.
- [73] B. P. Unger, I. C. Gunsalus, and S. G. Sligar, "Nucleotide sequence of the *Pseudomonas putida* cytochrome P-450cam gene and its expression in *Escherichia coli*," *J. Biol. Chem.*, vol. 261, no. 3, pp. 1158–1163, Jan. 1986.
- [74] H. Koga, E. Yamaguchi, K. Matsunaga, H. Aramaki, and T. Horiuchi, "Cloning and Nucleotide Sequences of NADH-Putidaredoxin Reductase Gene ($camA$) and Putidaredoxin Gene ($camB$) Involved in Cytochrome P-450cam Hydroxylase of $Pseudomonas putida$," *J. Biochem.*, vol. 106, no. 5, pp. 831–836, 1989.
- [75] W. Ying, "NAD⁺/NADH and NADP⁺/NADPH in Cellular Functions and Cell Death: Regulation and Biological Consequences," *Antioxid. Redox Signal.*, vol. 10, no. 2, pp. 179–206, Nov. 2007.
- [76] T. Shirakawa *et al.*, "Identification of Variant Molecules of *Bacillus thermoproteolyticus* Ferredoxin: Crystal Structure Reveals Bound Coenzyme A and an Unexpected [3Fe–4S] Cluster Associated with a Canonical [4Fe–4S] Ligand Motif," *Biochemistry*, vol. 44, no. 37, pp. 12402–12410, Sep. 2005.
- [77] I. Gudim, M. Hammerstad, M. Lofstad, and H.-P. Hersleth, "The Characterization of Different Flavodoxin Reductase-Flavodoxin (FNR-Fld) Interactions Reveals an Efficient FNR-Fld Redox Pair and Identifies a Novel FNR Subclass," *Biochemistry*, vol. 57, no. 37, pp. 5427–5436, Sep. 2018.
- [78] H. Onoda, O. Shoji, K. Suzuki, H. Sugimoto, Y. Shiro, and Y. Watanabe, "α-Oxidative decarboxylation of fatty acids catalysed by cytochrome P450 peroxygenases yielding shorter-alkyl-chain fatty acids," *Catal. Sci. Technol.*, vol. 8, no. 2, pp. 434–442, 2018.
- [79] M. Scott, C. W. Gunderson, E. M. Mateescu, Z. Zhang, and T. Hwa, "Interdependence of Cell Growth and Gene Expression: Origins and Consequences," *Science (80-.)*, vol. 330, no. 6007, p. 1099 LP-1102, Nov. 2010.
- [80] S. Jaganaman, A. Pinto, M. Tarasev, and D. P. Ballou, "High levels of expression of the iron-sulfur proteins phthalate dioxygenase and phthalate dioxygenase reductase in *Escherichia coli*," *Protein Expr. Purif.*, vol. 52, no. 2, pp. 273–279, Apr. 2007.
- [81] L. Nachin, L. Loiseau, D. Expert, and F. Barras, "SufC: an unorthodox cytoplasmic ABC/ATPase required for [Fe–S] biogenesis under oxidative stress," *EMBO J.*, vol. 22, no. 3, p. 427 LP-437, Feb. 2003.
- [82] H. M.N, H. P.L, and H. W.R, " *Pyrococcus furiosus* ferredoxin is a functional dimer," *FEBS Lett.*, vol. 531, no. 2, pp. 335–338.
- [83] H. Huang *et al.*, "Heterologous overproduction of [4Fe4S]- and [2Fe2S]-type clostridial ferredoxins and [2Fe2S]-type agrobacterial ferredoxin," *Protein Expr. Purif.*, vol. 121, pp. 1–8, May 2016.
- [84] K. R. Schramma, L. B. Bushin, and M. R. Seyedsayamdost, "Structure and biosynthesis of a macrocyclic peptide containing an unprecedented lysine-to-tryptophan crosslink," *Nat.*

1484, no. 2, pp. 278–286, 2000.

- [103] P. Tortora, G. M. Hanozet, A. Guerritore, M. T. Vincenzini, and P. Vanni, “Selective denaturation of several yeast enzymes by free fatty acids,” *Biochim. Biophys. Acta - Enzymol.*, vol. 525, no. 2, pp. 297–306, 1978.
- [104] H. Vorum, R. Brodersen, U. Kragh-Hansen, and A. O. Pedersen, “Solubility of long-chain fatty acids in phosphate buffer at pH 7.4,” *Biochim. Biophys. Acta - Lipids Lipid Metab.*, vol. 1126, no. 2, pp. 135–142, 1992.